JIMMA INSTITUTE OF TECHNOLOGY
SCHOOL OF CHEMICAL ENGINEERING

Synthesis and Characterization of Bagasse Based Cellulose Hydrogel for Methylene Blue Dye Removal from Textile Industry Wastewater

By

Lidiya Abdisa Ejjeta

A Thesis to be Submitted to Jimma University, Jimma Institute of Technology, School of Chemical Engineering in Partial Fulfillment for the Requirement of Masters of Science Degree in Chemical Engineering (Process Engineering)

January 2021

Jimma, Ethiopia

JIMMA UNIVERSITY

JIMMA INSTITUTE OF TECHNOLOGY

SCHOOL OF CHEMICAL ENGINEERING

This is to certify that the thesis prepared by **Lidiya Abdisa Ejjeta** entitled **"Synthesis and Characterization of Bagasse Based Cellulose Hydrogel for Methylene Blue Dye Removal from Textile Industry Wastewater"** and submitted in partial fulfillment of the requirements for the award of the Degree of Master of Science in Chemical Engineering (Process Engineering) complies with the regulations of the University and meets the accepted standard with respect to originality and quality.

Approved By Examining Board

Shimelis Kebede (PhD)
_____

External Examiner   Signature   Date
                                        05/02/21

Abrha Gebremeskel (MSc)
_____

Internal Examiner   Signature   Date

Samuel Gesesse (MSc)
_____

 Chair Person   Signature   Date

Ermias Girma (MSc)
_____

School Dean   Signature   Date
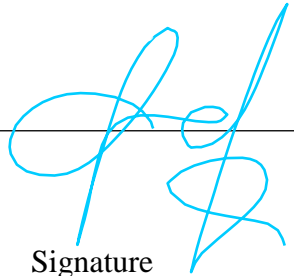
DECLARATION

I declare that this thesis work entitled "Synthesis and Characterization of Bagasse Based Cellulose Hydrogel for Methylene Blue Dye Removal from Textile Industry Wastewater" is my own work in agreement with internationally accepted practices, and has not been presented for degree program in Jimma University and any other university. I duly acknowledged and referred all the materials used in this work.

Name of researcher	Signature	Date
Lidiya Abdisa Ejjeta	_____	_____

Submission date _____

This thesis has been submitted for examination with our approval as university advisor and co- advisor.

Hundessa Dessaleng (PhD)   28/1/2021

Advisor   Signature   Date

Samuel Gesesse (MSc)   _____   _____

Co-advisor   Signature   Date

ACKNOWLEDGMENTS

First I would like to thank almighty GOD for his endless support; Next, I am most grateful to my advisor, Dr. Eng. Hundessa Dessaleng, for his constructive ideas, and continuous guidance from the start to completion of this thesis work. I am also much indebted to my co-advisor Mr. Samuel Gesese for his willingness, patience, and constructive guidance as co-advisor as well as School chair. I am also much indebted to all my family for your patience and support. I am so grateful for Adama science and Technology University, Addis Ababa Science and Technology University School of Chemical and Bio-Engineering and Central laboratory staffs. Especially I would like to thank Mr. Abraham and Mr. Yeshaneh for your help during product characterization. I pay my deep sense of gratitude to Jimma Institute of Technology School of Chemical Engineering, Faculty of Material Science and Engineering, School of Environmental Engineering, friends, relatives, and all people who contributed to this thesis work directly or indirectly with willing heart.

ABSTRACT

Textile industry wastewater comprises a number of toxic pollutants capable of causing serious health and environmental problems. The inevitable impact of these pollutants necessitates removal/treatment before being released to the environment. Although several wastewater treatment approaches have been devised, removal of cation dyes like methylene blue dye – a highly toxic and harmful component of the effluent – remained challenging. To address this, we synthesized a highly efficient and cost-effective sugarcane bagasse based cellulose hydrogel capable of removing methylene blue dye from textile industry wastewater. The hydrogel was synthesized by cross-linking cellulose with the non-toxic citric acid (CA) through esterification reaction and showed good swelling ratio (75.44 g/g), gel content (86.81%), thermal stability and porosity structures, less crystallinity index (66.46%) than cellulose (77.61%) with (50-150) nm particle size, 101.15 nm z-average particle size and low PDI (0.05)—indicators of good uniformity and uni-modal graph of nanomaterial. A predicted removal efficiency of 98.76% at an optimized condition of the input variables 4.97 g/L adsorbent dosage, 10.32 mg/L initial concentration of the dye and 51.97 minute, contact time). Further adsorption isotherm and kinetics modeling indicated that Langmuir adsorption isotherm and pseudo-first-order fit the experimental data. Performance of the hydrogel was assessed using methylene blue dye bearing synthetic wastewater and real textile wastewater collected from Arbaminch Textile industry, Ethiopia. When using the synthetic wastewater in triplicates, the hydrogel showed an average of 98.65% removal efficiency and small deviation between two result (0.1%) show high concordances with the predicted value. When applied on the real textile wastewater, it reduced the color (dyes) from (2459 to 1044) Pt-Co and achieved the safety standard for water quality parameters. Further, we assessed reusability of the hydrogel for five successive cycles and observed a declining tendency of the removal efficiency down to 70.63% at the last cycle. Generally, these results demonstrate the superior efficiency of the hydrogel and its feasibility of for methylene blue dye removal.

Keywords: *Hydrogel, Methylene Blue Dye, Bagasse, Wastewater.*

TABLE OF CONTENTS

Contents   **Page N<u>o</u>**

LIST OF TABLES

LIST OF FIGURES

ABBERVIATIONS AND ACRONYMS

AEPA	Addis Ababa Environmental Protection Authority
AOP	Advanced Oxidation Process
BOD	Biological Oxygen Demand
CA	Citric Acid
COD	Chemical Oxygen Demand
CMC	Carboxyl Methylene Cellulose
CV	Crystal Violet
DS	Dissolved Solid
DVS	Divinylsulfone
ECH	Epichlorohydrin
ECM	Extracellular Matrix
EPA	Ethiopian Environmental Protection Authority
FRP	Free Radical Polymerization
HGB	Hydrophilic Gels for Biological Use
ISPCH	Industrial Safety and Pollution Control Hand Book
MBD	Methylene Blue Dye
PHEMA	poly (hydroxyethyl methacrylate)
PVA	Polyvinyl Alcohol
SAP	Supper Adsorbent Hydrogel
SB	Sugarcane Bagasse
SEM	Scanning Electron Microscope
TDS	Total Dissolved Solid
TGA	Thermogravimetric Analysis
TS	Total Solid
TSS	Total Suspended Solid

1. INTRODUCTION

1.1. Background of the Study

Industrialization has become a key factor for a quality life by fulfilling gaps in socio-economy of the world. The industrial sectors are growing on a continuous scale with production of hazardous wastewater (Kurecic & Smole, 2016). They have a proficiency to produce more than million tons of occupied toxic dyes (about 7×10^5 tones annually) while coloring their finished products. This results in a release of enormous amounts of colored wastewater and other harmful toxic pollutants from various factories like textile, rubber, plastic, pulp, paper, etc with a toxicity potential to the environment and health in many countries (Ramesh, 2013). In a textile industry, a finishing stage of the product, which passes through multi-steps (bleaching, dying, finishing and printing steps), require various chemicals, dyes and huge amount of water resulting in generation of high amount of toxic and harmful effluents including dyes, heavy metals, degradable organic and inorganic salts (Mostafa, 2016).

A recent report estimated that textile industry has a potential to release 51% of toxic and harmful wastewater in which greater than half is discharged from a dying process. These industrial wastes are depicted by large amount of biological oxygen demand (BOD), chemical oxygen demand (COD), total suspended solid (TSS), total dissolved solid (TDS), total solid (TS), dissolved oxygen (DO), highly fluctuating pH and strong colors which are a primary concern for human health and aquatic life (Henze & Comeau, 2008). The inevitable impact of such pollutants on economic development and quality life standard necessitates removal/treatment of the wastes before being released. Million tons of cation dyes like methylene blue dye (which can causes cancers, cardiovascular disease, gastrointestinal disease and other common diseases,) are produced annually (Liu et al., 2011). To achieve this, many researchers have devised several waste treatment approaches.

The widely practiced approaches are broadly classified into physical, chemical and biological methods. In the physical method, the dye is removed physically by equalization, membrane filtration, ion exchange, irradiation, titanium dioxide treatment, homogenization, flotation, flocculation, coagulation, adsorption, etc. (Joshi et al., 2004).

The chemical dye removal method includes oxidation process, ozonation, photochemical, ultraviolet (UV) irradiation, Fenton's treatment, electrochemical destruction, and H_2O_2 and NaOCl treatment. This approach has been used over long period of time (Katheresan et al., 2018). Whereas the biological method including decolorization by white-rot fungi or other microbial cultures (mixed bacteria), adsorption by living or dead microbial biomass and anaerobic textile dye bioremediation system is cheap and performed before the effluent pollutes the environment (Katheresan et al., 2018). Among the dye removal approaches mentioned above, adsorption technique is more eloquent and realistic than other treatment techniques due its low cost, ability to remove a wide range of compounds within a short period of time, high surface area that permit adsorption. Activated carbon was one of the adsorption techniques widely applied in textile industry over a long period of time. But it has been limited recently by a virtue of its lower efficiency for removing of pollutant that are not attracted to carbon, high cost and energy intensiveness (Dargo et al., 2014).

More recently, many advanced low-cost adsorbents including natural materials, bio-sorbents, and non-conventional adsorption techniques have been employed (Kurecic & Smole, 2016). Given its economic feasibility, biocompatibility and adsorption efficiency, a non-conventional adsorption material called hydrogel – a three-dimensional matrix of hydrophilic gel polymer that can able to absorb huge amount of water, swell but does not affect nearby dissolution appeared from cross linking between matrix chains (Okay, 2009) – has got attention nowadays (Van et al., 2018). Although the first poly (hydroxyethyl methacrylate) (PHEMA) based hydrogel was used as soft contact lenses, later studies have been focused on synthesizing modern hydrogel with wide functionality including adsorption of toxic effluents (Sannino et al., 2009).

Based on their shape and physiochemical properties, hydrogel beads, film and nano composites are the widely employed hydrogel types in wastewater treatment (Garg et al., 2017). Hydrogel is mainly synthesized via esterification, free radical polymerization, graft polymerization, cross-linking and ionization radiation (Hakam et al., 2015). Cross-linking agents play a big role in enhancing equilibrium swelling degree and mechanical properties of the hydrogel in such a way that nature of the agent has ability to fluctuate properties of the adsorbent.

The hydrophilic group attached to the polymer backbone allows the hydrogel molecule to hold water (Bahram et al., 2016). Traditionally, removal of cation dyes from wastewater is challenging and became a common problem. Million tons of cation dyes like methylene blue dye (which can causes cancers, cardiovascular disease, gastrointestinal disease and other common diseases,) are produced annually (Liu et al., 2011). However, hydrogel has demonstrated to be an excellent dye adsorbent material with extremely high level of methylene blue dye adsorption (Garg et al., 2017). Synthesis of bagasse based cellulose hydrogel for dye removal has been taken special consideration due to its abundance, renewability, biodegradability and biocompatibility (Zhou et al., 2011). Bagasse offers advantage of being low cost, eco-friendly and yielding great quantity. It is also a suitable polysaccharide for synthesis of adsorbent hydrogel which commonly consists of cellulose, hemicellulose, lignin and extractive composition (Maitra & Shukla, 2014).

Cellulose is the first plentiful renewable polymer raw material originated from its unbranched chain of 3-Hydroxyl group (OH) on each monomer that provides ability to form hydrogen bond (Klemm et al., 2010). The ability of cellulose to form intra- and inter-molecular hydrogen bonds by hydroxyl group makes linear cellulose chain straight and supports to bring together into a crystalline and morphological structures (Aye et al., 2018). Furthermore, cellulose based hydrogel is suitable adsorbent for removal of cation dyes (Yang et al., 2010).

1.2. Statement of the Problem

Although numerous treatment options have been described, all the approaches have their own limitations in terms of environmental remediation, cost-effectiveness and applicability for removal of non-biodegradable dyes like methylene blue dye (Scholz, 2018). Chemical treatment method is expensive due to the use of excess chemicals during processing steps and disposal of removed dye as a sludge. The sludge is difficult to be recycled due to breaking down of the dyes into simple pieces and destroying the presence of atom in the color compound (Bhargava, 2016). Biological treatment method is not widely practiced due to its complex process and difficulty to apply for removal of all type of dyes. Application of adsorption technique which is the most effective physical method, such as activated carbon is limited by virtue of its less efficiency for removal of chemicals that are not attracted to carbon and high cost due to energy intensiveness (Dargo et al., 2014 ; Shendge, 2017).

Moreover, all these approaches are inefficient for removal of all type of dye, especially its application toward non-biodegradable dye (eg. methylene blue dye) which has a serious socio-economic and health impacts. Although recent numerous studies have shown improved Methylene blue dye adsorption capability of hydrogel (Hakam et al., 2015; Zendehdel et al., 2010; Zhou et al., 2011). Choosing appropriate raw material and cross-linking agent remained challenging.

Raw materials like carbon nanotubes material, laboratory based cellulose powder and petrochemical based polymers employed in previous studies are expensive, non-renewable and toxic (Kabir et al., 2018). Other studies used sugarcane bagasse (a cost-effective and renewable agricultural waste)-based polymer hydrogel that have a virtue of high matrix or hydrophilic network, but employed costly and toxic cross-linking agents such as acrylic acid, Succinic anhydride, Epichlorohydrin (ECH), Divinylsulfone (DVS) and etc (Maitra & Shukla, 2019). In addition, they lead hydrogel with lower adsorption surface and equilibrium swelling – resulting in low methylene blue dye removal inefficiency (Pitrod, 2016 ; Vuono, 2014). Consequently, lack of efficient and cost-effective treatment method causes release of the harmful wastewater to the environment in many countries (Kurecic & Smole, 2016).

For example, there are more than 100 firms engaged in manufacturing textile and apparel in Ethiopia (Assefa & Sahu, 2016). Almost all are located very near to fresh water body, and directly discharge untreated and toxic effluent into the nearby canals, rivers, farm lands, lakes and streams due to lack of treatment plant. Several reports have shown that the values of water quality parameter such as BOD, COD, pH, TS, TDS, DS and color of textile wastewater discharged has considerably higher than the safe limits set by Ethiopian Environmental Protection Authority (EPA) (Gemeda et al., 2020; Dadi et al., 2017).

Considering these challenges, we hypothesized to synthesize a highly efficient and cost-effective bagasse based cellulose hydrogel with enhanced swelling ratio for physical adsorption of methylene blue dye effluents from textile industry and reuse the treated water. The bagasse based cellulose hydrogel was thought to be synthesized by cross-linking method via esterification reaction using a renewable sugarcane bagasse as a raw material. To achieve this, we set the following objectives.

1.3. Objectives

1.3.1. General objective

❖ To synthesize bagasse based cellulose hydrogel for removal of methylene blue dye from textile industry wastewater.

1.3.2. Specific objectives

✓ Specific objectives of the study were to:

❖ Characterize component of sugarcane bagasse such as lignin, hemicellulose, cellulose and extractives

❖ Extract cellulose from sugarcane bagasse and carry out its physico-chemical characterization such as functional group, crystallinity and morphological analysis.

❖ Synthesize bagasse based cellulose hydrogel for of methylene blue dye removal

❖ Carry out thermal, physical and chemical characterization of bagasse based cellulose hydrogel such as functional group, crystallinity, thermal stability, and morphological analysis, particle size, swelling ratio, gel content and degradability in a soil.

❖ Assess effect of process variables such as adsorbent dosage (mg/L), initial concentrations of methylene blue dye (mg/L) and contact time (minute) on removal efficiency of hydrogel.

❖ Characterize water quality parameters in wastewater such as- chemical oxygen demand (COD, mg/L), total dissolved solid (TDS, mg/L), total suspended solid (TSS, mg/L), Total solid, color (%), pH, turbidity (NTU) and temperature (℃).

1.4. Significance of the Study

Textile industry is one of the production sectors that use various chemicals, dyes and huge amount of water at multi-finishing steps, generating enormous amounts of toxic and harmful effluent wastes. This necessitates removal/treatment of the wastes before being released to the environment. Although different wastewater treatment approaches have been devised, efficient removal of such wastes, particularly cations like methylene blue dye, remained challenging due to environmental impacts, cost and non-biodegradability characteristics of the dye. Here, we report an alternative biodegradable, economical, non-toxic and simple adsorption hydrogel for wastewater treatment. The hydrogel can replace convectional dye removal techniques and prepared from cellulose extracted from sugarcane bagasse (agricultural wastes).

The bagasse based cellulose hydrogel can efficiently remove methylene blue dye from textile industry wastewater and the treated water can be reused for different purposes such as irrigation. In general, the present finding provides an alternative removal approach of methylene blue dye and other cation dyes in wastewater and solves water scarcity.

1.5. Scope of the Study

This research study mainly covered: collection and preparation of sugarcane bagasse, extraction of cellulose from sugarcane bagasse and its characterization, synthesize and characterization of hydrogel. Synthesized hydrogel was applied for removal of methylene blue dye from textile industry wastewater. Effects of operating parameter such as initial concentration of methylene blue dye adsorbent dosage and contact time and on removal efficiency of hydrogel were also investigated.

2. LITERATURE REVIEW

2.1. Textile industry wastewater

Textile industry is one of the largest industry sectors that consumes huge amount of water. Fresh water is used at each manufacturing stages and, in turn, about 200 – 350 L wastewater per Kg of finished products is generated, resulting in an average pollution of 100 Kg per ton of fabrics (Ahmed, 2015). Wet processing operations during textile chemical processing – i.e. desizing, scouring, bleaching dyeing, printing and finishing – are the major causes of wastewater pollution. Specifically, dyeing and finishing processes are the main stages for production of enormous amount of pollutant wastes since a wide range of chemicals and dyestuffs are used to color final products. For example, most of the dyes are exhausted on the fiber of the finished products during dyeing, but the unfixed ones go into wastewater causing deep color. Even as much as 50% of the dyes might be discharged as an effluent (Joshi et al., 2004). Table 2.1 summarizes the sources, composition and characteristics of wastewater discharged from textile industries.

Table 2.1. Sources, characteristics and composition of wastewater in textile industry

Source	Composition	Characteristics
Sizing	Carboxymethylene cellulose (CMC) and Polyvinyl Alcohol (PVA)	High in BOD and COD
Desizing	Mineral acid, fat, wax, pectin, PVA	High in BOD, COD, TSS &DS
Scouring	Caustic soda, detergent, soda ash	High pH
Bleaching	Sodium hypochlorite, H_2O_2, acid, surfant, sodium phosphate raw material fiber	High alkalinity and acidity
Mercizing	Caustic soda solution, wax	High pH and DS, Low BOD
Dying	Dyestuff, reducing agent, oxidizing agent, urea, Acetic acid, detergent	Strongly colored, High BOD, DS, Low SS, heavy metal
Printing	Paste, urea starch, gum, oil, binders, acid, reducing agent, alkali	Highly colored, High BOD, oily appearance

Source: (Henze & Comeau, 2008).

Textile wastewater has been increasing over years and becoming a major cause of pollution in the world. Several chemicals used in the textile industry are considered as major toxic pollutants and cause undesirable aesthetic impact. A considerable amount of dye-bearing wastewater is discharged to natural streams, rivers and farmers land without proper treatment, thus, posing severe problems to agriculture-based life-style, aquatic life, food web and aesthetic nature of the environment (Sivri & Toroz, 2007; Kurecic & Smole, 2009; Ramesh, 2013; Mondal et al, 2017).

Such effluents drastically decrease oxygen concentration due to the presence of hydrosulfides and blocks the passage of light through water body, resulting in detrimental effects to the territorial and aquatic ecosystem (Ramesh, 2013). The toxic dyes in the effluent also contain substances capable of decreasing photosynthesis – a process by which plants get their nutrient. Further, some of these dyes degrade into a highly toxic products with a potential of causing carcinogenic, mutagenic, and allergen effects to human being even at low concentration (<1 ppm) (Kurecic & Smole, 2009). About 40% of globally used colorant contains organically bound chlorine – a well-known carcinogenic substance (Sivri & Toroz, 2007).

Dyes are widely used in a number of industries including textile industry to color their products. These industries require more than 100,000 engaged dyes in commerce, of which an estimated 2% of the produced dyes are discharged into effluents from the associated industries. For example, the total dye consumption of a textile industry is in excess of 107 Kg/day worldwide, resulting in a discharge of 1,000 tons per day or more into waste streams (Ramesh, 2013). Treatment of wastewater containing dyes is very difficult since the dyes are recalcitrant organic molecules, resistant to biological degradation and stable to light (Dargo et al., 2014). The toxic cationic methylene blue dye is one of the dyes that become a challenging in wastewater treatment and discussed below.

2.2. Methylene blue dye

Methylene blue dye (Fig. 2.1), with a chemical name of tetramethylthionine chloride, is one of most common cation dye manufactured by Caro in 1876 as aniline. It is a commonly applied dye in textile industry for dying of finishing product (Neethu et al., 2017). Methylene blue dye is easily recognized due to its appearance as deep blue (at its oxidized state) (Fig. 2.2) with a maximum absorption at 609 - 665 nm (Hakam et al., 2015). The physical and chemical properties of methylene blue dye are shown in Table 2.2.
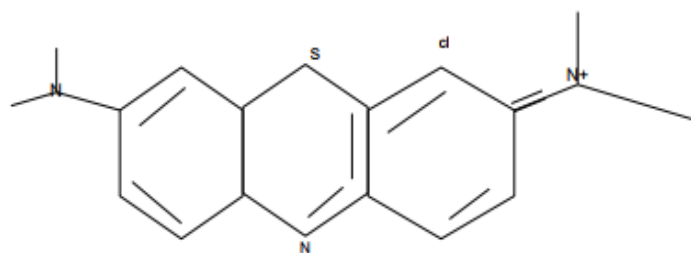
Figure 2.1. Structure of methylene blue dye**. Source:** (Zendehdel et al., 2010)

Table 2.2. Chemical and physical properties of methylene blue dye

Chemical and physical properties	Value
Melting temperature	$180^{o}C$
Solubility in water	1g/25ml
pH value	3(10 g/L H_2O)
Molecular weight	319.85 g/mol
Color	Dark blue
Chemical formula	$C_{16}H_{18}ClN_3S$

Source: (Koch., 2013)

In contrary to its benefits, this stable compound is very toxic and almost non-biodegradable in environment which lasts for many years. Several literatures reported the effect of methylene blue dye on human being like increased heartbeat, cyanosis, vomiting, shocking, headache, tissue neurosis, bluish stained skin, anemia, dyspnea, depression, respiratory stimulation and increased blood pressure and other chronic diseases. It has also been reported to cause bluish discoloration of the urine and stool, Heinz body formation in dogs and cats and conjunctive injury in rabbits (Koch et al., 2013; Sheet et al., 2019).

Furthermore, methylene blue dye is not only pollutes the environment but also depletes the oxygen content and inhibits sunlight from reaching the water source (Hakam et al., 2015), affecting other terrestrial- and aqua-life.

Figure 2.2. Textile effluent directly discharged to the environment

Source: (science direct.com)

2.3. Textile westewater treatment approach

Broadly, three textile wastewater treatment approaches (chemical, physical and biological) have been devised. All the approaches have their own advantages and limitations (Table 2.3). Therefore, more effective textile wastewater handling seems to be a blend of different methods. Physicochemical methods have been extensively used in textile treatment plants, which give good removal efficiency of suspended materials. Chemical treatment is a method of removing dyes from discharged effluent by breaking down into small and simplest pieces and destroying atom presence for the color of the compound. The method has been further classified into many categories including chemical precipitation, convectional oxidation by oxidizing agent (ozone), irradiation (electrochemical processing) and advanced oxidation process. Recently these methods are restricted due to collection of concentrated sludge causing disposal problem. There is also the prospect that derivate contaminant will appear because of excessive chemical used during process (Joshi et al., 2004).

Biological treatment approach relies on small organisms like bacteria, nematodes, etc for breaking down of organic wastes using aerobic and anaerobic mechanisms. The method is cheap and performed before the effluent pollute the environment (Katheresan et al., 2018).

Both mechanisms have given good result when applied to removal of organic pollutant while color removal in field application by using aerobic method did not show expected results (Siddique et al., 2017). The conventional biological treatment is the most economically used methods compared to other physical and chemical processes. However, biological treatment is incapable of obtaining satisfactory color elimination for concentrated wastes (Dargo et al., 2014). Physical method removes color physically by equalization, homogenization, and flotation, various adsorption technique, coagulation flocculation, ion exchange and membrane separation (Joshi et al,, 2004), and membrane filtration (Siddique et al., 2017). Among these, dye removal by adsorption technique is absolutely eloquent and more realistic in terms of cost and time effectiveness than other treatment technique. Hence, adsorption technique and its application in removal of methylene blue dye from textile wastewater are described.

Adsorption is a phase transfer process that is widely used in practice to remove substances from fluid phases (gases or liquids). The solid material that provides the surface for adsorption is referred as adsorbent. The species that will be adsorbed are named adsorbate. In wastewater treatment, adsorption has been proved as an efficient removal process for a multiple solutes. Here, molecules or ions are removed from the aqueous solution by adsorption onto solid surfaces. This reverse process is referred to as desorption (Neethu et al., 2017).

Chemisorption and physisorption are the two most common categories of adsorption technique. Chemisorption, also called chemical adsorption, includes formation of chemical bond between adsorbate and adsorbent by irreversible system. Physisorption or physical adsorption occurs through physical interaction like hydrogen bonding, van der Waals, and hydrophilic interactions between adsorbate and adsorbent, and acts in a reversible manner (Chirani et al., 2015; Haque & Mondal, 2016). Of the two, the physical adsorption method is eloquently recommended by numerous researchers.

Table 2.3. Summary of treatment options

Method	Advantage	Disadvantage
Chemical method		
Oxidation process	Simplicity of application	H_2O_2 agent needs to be activated by some means
Fenton's agent	Fenton's reagent is suitable chemical means	Sludge generation
Photochemical	No sludge is produced and less foul odours	Formation of by products
NaOCl	Initiates and accelerates azo-bond cleavages	Release of aromatic amines
Electrochemical destruction	No consumption of chemical and no sludge build up	Relatively high flow rates cause direct decrease in dye removal
Physical Method		
Adsorption by activated carbon	Good removal of wide variety of dyes	Cost of activated carbon
Membrane filtration	Removes all dye types	Concentrated sludge
Ion exchange	No adsorbent loss during regeneration	Not effective for all types dyes
Irradiation	Effective oxidation at lab scale	Requires a lot of dissolved O_2
Titanium dioxide	Low price	Insoluble in water toxicity
Electro-coagulation	Economically feasible	High sludge production
Biological Method		
Decolorization by white-rot fungi	White-rot fungi can degrade dyes using enzymes	Enzyme production has been shown to be unreliable
Adsorption by living or dead microbial biomass	Certain dyes have a particular affinity for binding with microbial species	Not effective for all types of dyes
An aerobic textile dye bioremediation system.	Allows azo and other water-soluble dye to be decolorized	Anaerobic breakdown yields methane and hydrogen sulphate

Source: (Crini & Lichtfouse, 2019)

2.4. Methylene blue dye Removal approach from textile wastewater

Removal of cationic dyes from industrial effluents is still an important but challenging subject in the field of environmental remediation. Many techniques have been developed and applied to overcome the unresolved dye problems. Although all techniques offered some solutions, major disadvantages such as low decolorization rate and producing secondary pollution of adsorbing materials could also occur. Moreover, they are costly, not portable and complicated. Now, the commonly used technique for removing dyes by adsorption is a promising approach because of its low performance cost and ease of technical access (Liu et al., 2011). Studies conducted on the adsorption of methylene blue dye using activated carbon synthesized from sugarcane bagasse demonstrated that the maximum adsorption capacity was found to be 136.84 mg/g for the powdered adsorbent which is lower than the standard activated carbon (236 mg/g) (Das, 2013).

Hence, dye removal using functional polymers became a new approach for environmental applications. Different polymeric adsorbents, particularly hydrogels comprising different functional groups and ability to trap the molecules of dyes, has gained much attentions (Hakam et al., 2015). For example, a semi-interpenetrating hydrogel composed of copolymer of acrylamide and acrylicacid with poly vinyl alcohol as linear polymer for removal of methylene blue from aqueous solutions showed good dye adsorption capacity. Hence, the composites can be used as good membranes for removal of cationic dyes from aqueous solutions while they do not release harmful materials into water (Zendehdel et al., 2010).

Another study showed the feasibility of cotton cellulose hydrogel for removal of methylene blue dye from textile wastewater and aqua solutions. Adsorbent cotton cellulose hydrogel with good swelling properties and methylene blue dye adsorption capacity has been observed (Hao liu et al., 2011). Zhou et al. (Zhou et al., 2006) investigated modified polysaccharide (gum arabic) based hydrogel for removal of methylene blue dye from aqua solution and the hydrogel removed cation dye from textile toxic pollutant. Further, cellulose based hydrogel derived from low cost and locally available materials like sugarcane bagasse for removal the dye from textile industry wastewater may provide more robust efficiency and investigated in this study.

2.5. Over-views on hydrogel

Hydrogel is the first cross-linked network material described by its typical properties in literature. Since then, the number of studies on considerable applications of the hydrogel began to rise including application for wastewater treatment (Haque & Mondal, 2016). Hydrogel can be defined as water-swollen cross-linked polymeric networks or as hydrophilic polymers that swell in water, but does not dissolve (Chirani et al., 2015). The hydrophylicity of these polymers is supported by hydrophilic functional groups attached to the polymer backbone like hydroxyl, carboxyl, sulfonate or amide groups (Fig. 2.2) which develop ability to resist dissolution.
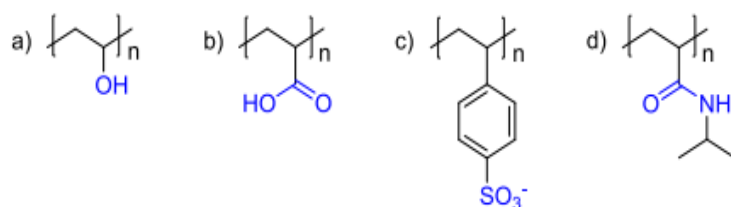
Figure 2.3. Chemical structure found in hydrophilic group of hydrogels

Source : (Chirani et al., 2015)

The swelling of hydrogels can be depends on the monomers used for the cross-linking, type of the crosslinking, homopolymeric and polymeric interpenetrating networks. Usually the water content of a swollen hydrogel is larger than the amount of the dry gel itself. Their physical structure may be crystalline, semi crystalline or amorphous. The gel is a state that is neither completely liquid nor completely solid. This half liquid-like and half solid-like properties cause many interesting relaxation behaviors that are not found in either a pure solid or a pure liquid (Garg et al., 2017).

2.5.1. Classification of hydrogel

2.5.1.1. Natural hydrogel

Natural hydrogel can be derived from different polysaccharides including, chitosan, matrigel, collagen, fibrin and other natural material derivatives. Natural hydrogel is good in accordance with its biocompatibility and biodegradability nature. In contrary to its benefit those natural hydrogel has two most common drawbacks.

The first one is their final microstructures (fine detail of their mechanical properties) and their dependency on gelation situation as well as polymerization conditions are challenging to interpret simply. Second one is their composition may varies at each single batch due to their natural origin which is difficult to understood their exact composition (Catoira et al., 2019).

2.5.1.2. Synthetic hydrogel

Synthetic hydrogels are homo-polymer or copolymer covalently cross-linked with three dimensional water swollen networks. Their final structure is fine and depends on polymerization condition and operating parameter including temperature, environmental control, even though, synthetic polymer such as poly (ethylene glycol), poly (lactic acid), poly (2-hydroxypropyl metharcylimide), poly (acryl amide), and poly (vinyl alcohol) are great and versatile in controlling chemical structure of the hydrogel and its structure is clearly understood, synthetic hydrogel is more flexible for tuning chemical composition and mechanical properties (Chieng et al., 2014).

2.6. Current study on hydrogel

The available hydrogels are completely petroleum-based carbon nanotubes material and polyelectrolytes gels, which have large impact on environment. Studies were carried out on synthesis of the poly (N-isopropyl acrylamide) (PNIPAm) hydrogel nano composites containing graphene oxide (GO) and GO plus carbon nanotubes (CNT) in order to apply for tissue delivery. They observed that the composites with GO and GO-CNT enhance the hydrogel mechanical and electrical properties, and also increase the capacity to incorporate tetracycline antibiotic molecules (tet) that allow to inhibit bacterial growth (Pereyra et al., 2017; Atya et al., 2019). Even though the swelling of these composite materials is smaller than the pure hydrogel due to law degree of substitution of GO, recent trend showed that non-biodegradability of polymeric materials so that they will be harmless for the health and environment. In this regard, scientists have gained enough success by incorporating cellulose (Chirani et al., 2015), chitosan (Li et al., 2009; Venkatesham et al., 2018), proteins and starch in polymeric chains (Haque & Mondal, 2016).

Further, hydrogels have recently drawn great attention for use in a wide variety of biomedical applications such as cell therapeutics, wound healing, cartilage/bone regeneration and the sustained release of drugs.

This is due to their biocompatibility and the similarity of their physical properties to natural tissue (Sivri & Toroz, 2007). Recently, hydrogel got superior attention for removal of industrial and pharmaceutical effluent (Luqman et al., 2019). According to Zhou et al. (Zhou et al., 2011), hydrogel synthesized from cotton cellulose show high adsorption capacity of methylene blue dye with good swelling capacity. The result also showed the highly porous structure and elastic behavior of the synthesized hydrogel that enable to adsorb the cation dye into active site of the adsorbent.

2.6.1. Cellulose and cellulose hydrogel

2.6.1.1. Cellulose

Cellulose is the most abundant naturally occurring polymer of glucose (Fig. 2.4) found as the main constituent of plants and natural fibers such as cotton and linen. Some bacteria (e.g., *Acetobacter xylinum*) are also able to synthesize cellulose. The biodegradation of cellulose progressively leads to decreased molecular weight, lower mechanical strength and increased solubility. Moreover, higher biodegradation rates of cellulose are likely yielded by lower degrees of crystallinity and improved water solubility (Sivri & Toroz, 2007). The primary occurrence of cellulose is the existing lignocellulose material in forests, with wood as the most important source. Other cellulose-containing materials include agriculture residues, water plants, grasses and other plant substances. Besides cellulose, they contain hemicelluloses, lignin, and a comparably small amount of extractives. Commercial cellulose production concentrates on harvested sources such as wood or naturally highly pure sources such as bagasse (Klemm & Schmauder, 2010). The ability of cellulose to form intra- and inter-molecular hydrogen bonds by hydroxyl group enables to make linear cellulose chain straight, support to bring together into crystalline structure, and give cellulose a large number of crystalline fiber structures and morphologies (Aye et al., 2018).

Cellulose positive effect is that it is characterized by its low density, good mechanical properties as well as biodegradability. In other words, due to its strong inter- and intra-molecular hydrogen bonding, cellulose neither melts nor dissolves readily in common solvents. Chemical modification reactions continue to play a dominant role in improving the overall utilization of cellulose to produce water-soluble derivatives for various applications.

$$nC_6H_{12}O_6 \longrightarrow (C_6H_{10}O_5)_n + nH_2O$$

glucose   cellulose
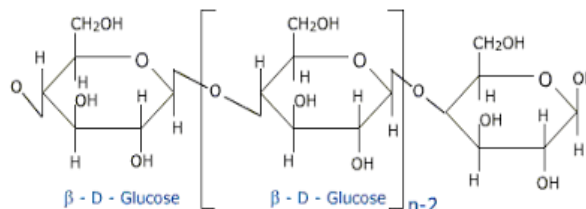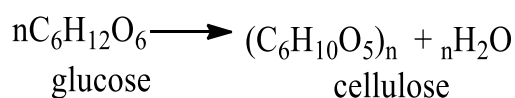
(A) Formation of cellulose   (B) Structure of cellulose

Figure 2.4. Formation and structure of cellulose. **Source:** (Researchgate.net)

2.6.1.2. Cellulose hydrogel

Hydrogels based on cellulose comprising many organic biopolymers including cellulose, chitin, and chitosan are hydrophilic materials, which can absorb and retain a huge proportion of water in the interstitial sites of their structures. These polymers feature many amazing properties such as responsiveness to pH, time, temperature, chemical species and biological conditions besides a very high-water absorption capacity (Kabir et al., 2018). Cellulose and cellulose derivatives can be polymerized in producing green hydrogels for improving the absorption performance of many adsorbent products (Haque & Mondal, 2016). This sustainable material in plants has numerous functional possibilities and expected with the demand for environmentally biocompatible products (Aye et al., 2018).

Hence, in recent years, cellulose hydrogels became the most attractive one for wastewater treatment due to its biodegradable and biocompatible nature as well as cheap and toxic free (Karunakaran, 2016). According to Haque & Mondal (Haque & Mondal, 2016) study, cellulose hydrogel synthesized from cotton ensures that the characteristic of prepared hydrogel can be effectively used in personal absorbent products, tissue engineering, biomedical application and water purification. Even though the study demonstrated that synthesized hydrogel show excellent efficiency as adsorbent of methylene blue dye in polluted textile wastewater, adsorption amount increases much higher than the previously reported by (Zhou et al., 2011, 2006). Investigation of polymer on bacterial cellulose hydrogels also shows excellent biocompatibility of the biomaterial and less latent toxic effect for methylene blue dye removal when compare to the synthetic one (Hakam et al., 2015).

2.7. Cross-linking strategy

Behavior of converting liquid polymer into solid gel by limiting its capability to move individually in accordance with linking one polymer chain to another is called cross-linking method. Cross-linked polymers are mechanically strong, show polymers insolubility in solvent and excellent stability (Maitra & Shukla, 2014). Venkatesham (Venkatesham et al., 2018) synthesized hydrogel with and without cross-linking, and applied both for pollutant removal from wastewater. According to researchers finding, the hydrogel in the absence of cross-linking agent shows disintegration behavior in acidic medium, while cross-linked hydrogel showed insolubility in acidic solution (pH 1-7) and improved mechanical properties. Cross-linking process gains good network structures for hydrogels. Moreover, adsorption experiment using the cross-linked hydrogel also shows excellent removal efficiency and better mechanical properties (disintegration behavior is not observed). Cross-linking not only improve mechanical properties of the polymer network, but also demonstrate no toxicity (Thakur & Singh, 2018). Further, Golor et al. (Golor et al., 2020) has shown significance of citric acid (CA) for cross-linking of cellulose hydrogel.

Cross-linking is performed through a physical or chemical bond that links the functional groups of polymer chain to that of another one through covalent bonding or supramolecular interaction such as hydrogen bonding.

Chemical cross linking method is due to strong primary forces like covalent bonding including esterification reaction, chain growth polymerization, addition and condensation polymerization (cation/anionic), gamma and electron beam polymerization. Chemical cross-linking method results in strong mechanical properties such as stable toward external stimuli (Maitra & Shukla, 2014). Physical cross-linking method is due to secondary forces including hydrogen bonding. Physical cross-linking method has been criticized its heterogeneous behavior due to free chain ends, mechanically weak and change in the environmental parameters (such as pH and temperature) or lack of stability towards external stimuli (ionic strength may disrupt network structure of the hydrogel(Maitra & Shukla, 2014).

Biological method is another cross-linking strategy which has not developed for industrial scale till date. Stability of cross-linking and improvement in polymer properties depends on the type and degree of cross-linking (Mane et al., 2016). On the basis of the cross-linking method, the hydrogels can be divided into chemical and physical gels. Physical gels are formed by molecular self-assembly through hydrogen bonds, while chemical gels are formed by covalent bonds (Chang & Zhang, 2011).

2.7.1. Cross linking via esterification reaction

It is well known that the effective swelling of bagasse cellulose-based hydrogels require a chemically cross-linked network that can be obtained via different paths. Chemical cross-linking via esterification is one of them using either formaldehydes compounds which are toxic or other alternative but not dangerous esterification reagents (Demitri et al., 2008). Esterification is the process of combining an organic acid (RCOOH) with an alcohol (ROH) to form an ester (RCOOR) and water or a chemical reaction resulting in a formation of at least one ester product. Carboxylic acid is a main organic acid forming ester with alcohol. According to Demitri et al. (Demitri et al., 2008), the two main stages of reaction between poly functional carboxylic acid with cellulose are due to attachment of the poly functional carboxylic acids via esterification with cellulosic hydroxyl group and its further reaction with another cellulosic hydroxyl group producing a cross-linking between cellulose chains.

Attachment of poly functional carboxylic acids to cellulose hydroxyl group via esterification reaction of first cyclic anhydride would expose a new carboxylic group unit which has proper chemical connectivity to form new intra-molecular anhydride moiety with adjacent carboxylic acid unit. Further reaction with cellulose hydroxyl of another chain can then lead to cross-linking (Chang & Zhang, 2011). Cellulose hydrogel synthesized via esterification reaction has good mechanical properties. Furthermore, it has more porous structures than the non-cross-linked one but esterification reagent are reported as toxic for long period of time. In order to fulfill gap through this, CA are engaged as green cross-linking agent (Chang & Zhang, 2011). According to Yang et al. (Yang et al., 2010), CA can be successfully used as a cross-linking agent for synthesis of hydrogel from carboxyl methylene cellulose (CMCNa). The issues of toxicity and reagent costs can be overcome with CA.

2.7.1.1. Reaction mechanism between cellulose and citric acid

During preparation of CA solution, CA is dissolved with water which leads to cyclic unhdride, dissociation of hydrogen ion from citric acid yield hydronium ion formation. When CA is heated, it dehydrates to yield the cyclic anhydride that reacts with extracted cellulose successively (Yang et al., 2010). Fig. 2.5 shows structure and formation of cyclic anhydride during dissolution of citric acid into water in the presence of heat. An optimal degree of swelling for practical applications has been achieved using low CA concentration. The first reaction mechanism in esterification reaction is formation of cyclic anhydride at high temperature.
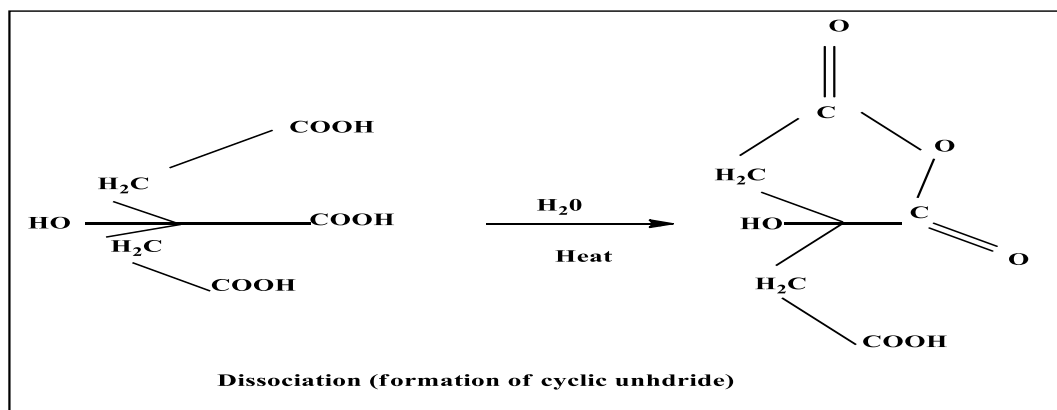
Figure 2.5. Dissociation (Formation of cyclic anhydride)

Cyclic anhydride formed can be esterifying the hydroxyl group present on the adjacent of cellulose chain, which leads to formation of ester bonds. In other words, when carboxylic acid attached to cellulose carboxyl groups via esterification reaction of first cyclic anhydride, new carboxylic acid group unit having proper chemical connectivity to form new intra-molecular anhydride moiety with adjacent carboxylic acid unit can be exposed. Further, reaction with a cellulose hydroxyl of another chain can then leads cross-linking of cellulose chains which gain hydrogel with network structures (Thakur & Singh, 2018). Figure 2.6 shows ester bond formation between cellulose and cyclic acid and further esterification reaction (cross-linking between cellulose chains).
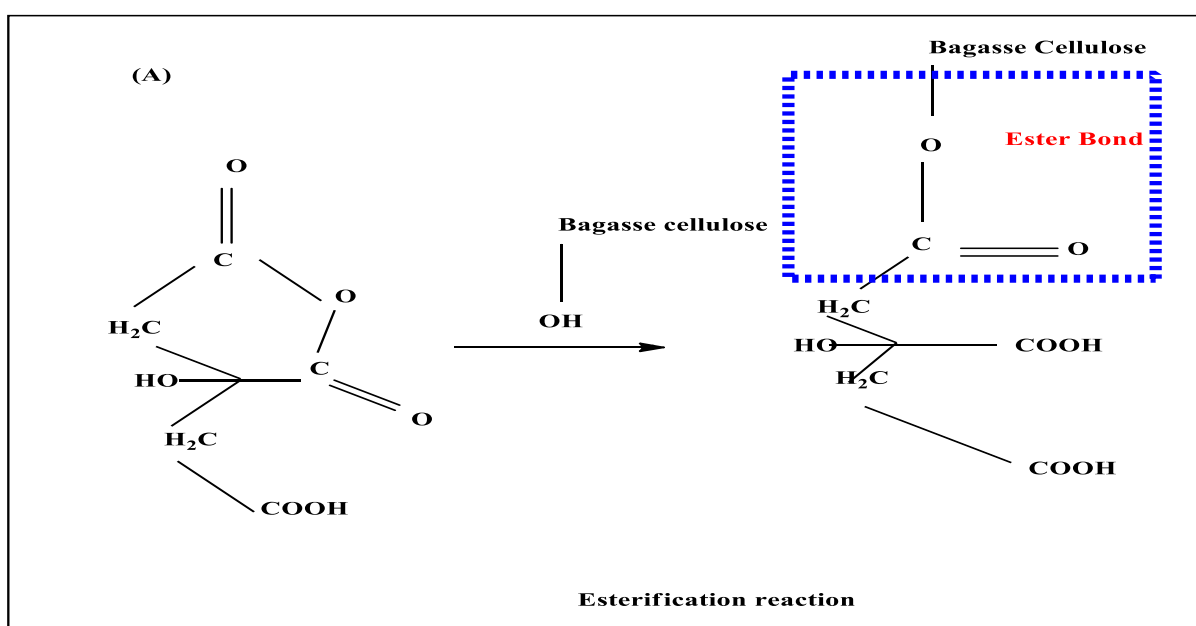
Figure 2.6. Cross-linking mechanism via esterification reaction
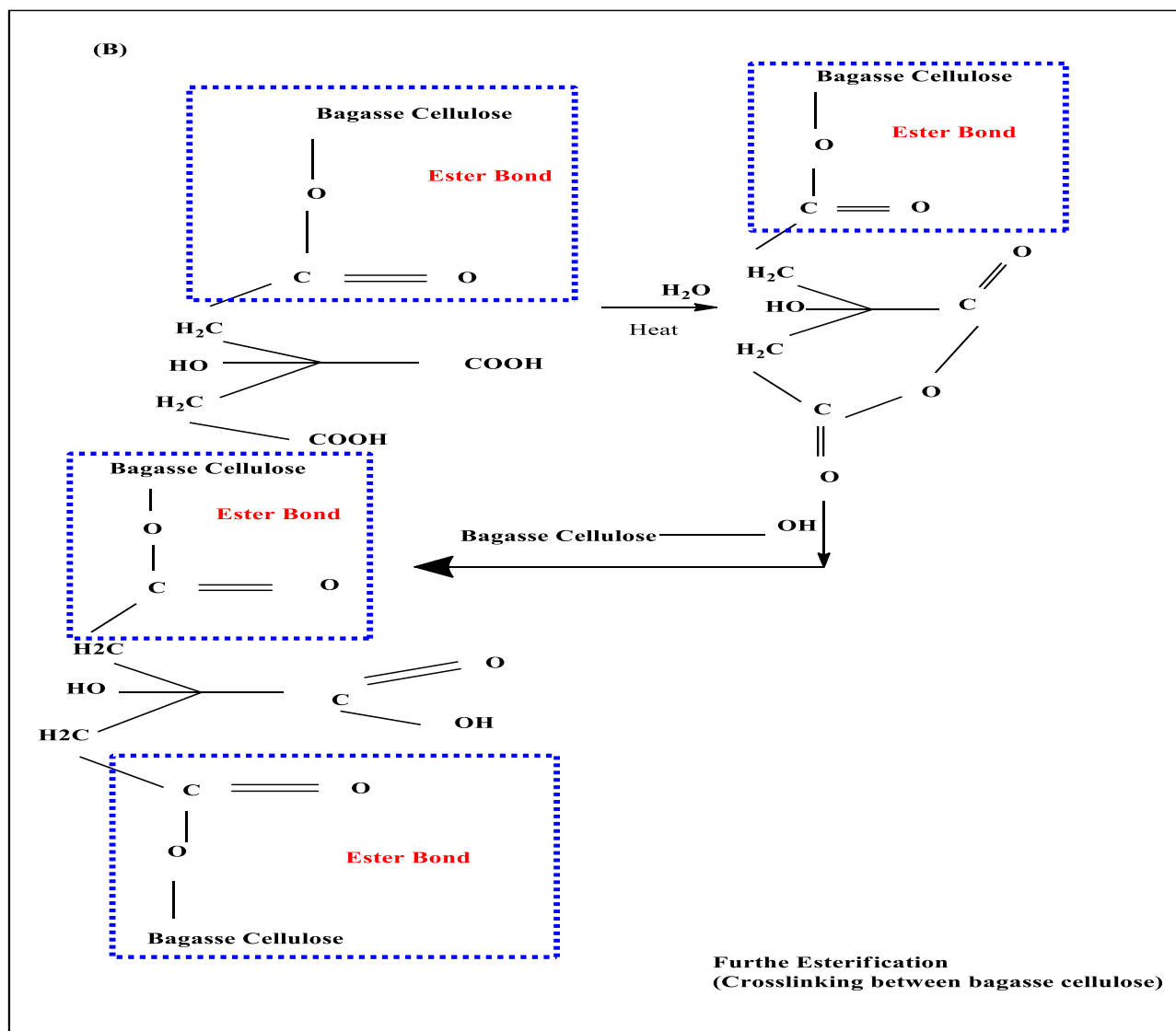
Figure 2.6. Continued

2.8. Physical and chemical properties of cellulose hydrogel

2.8.1. Swelling and elasticity

The term swelling in hydrogel is expanding of polymer chain volume due to interaction between liquid molecules and polymer network which absorbs huge amount of water than dry one. Hydrogels are special materials capable of absorbing huge amount of water when swelling, usually more than 100 or even 1000 times of their dry weight, reaching much higher water content than conventional hydrogels. It is a valuable variable to evaluate in the area of pollutant adsorption study as it affects surface properties of hydrogel itself (Sivri & Toroz, 2007).

Swelling degree at equilibrium and its elastic modulus can be influenced based on type of cross-linking agent and its concentration used, density of polymer network, temperature, pH values and salt in the swelling medium (Ganji et al., 2010). Adsorption capacity of hydrogel and swelling ratio have direct proportion, high swelling capacities means higher number of ionic groups in the surface of hydrogel which will enhance the adsorption capacity of the hydrogel (Yang et al., 2010). Swelling ratio of hydrogel can be determined according to Equation (2.1) below.

$$\text{Swelling ratio (g/g))} = \frac{W_{sg} - W_{ns}}{w_{ns}} \ldots\ldots\ldots\ldots\ldots\ldots\ldots\ldots\ldots\ldots\ldots\ldots\ldots\ldots (2.1)$$

Where: W_{sg} = Weight of swollen gel

W_{ns} = Weight of non-swollen gel

2.8.2. Biocompatibility and degradability of hydrogel

Biocompatibility (non-toxicity) of polymer is the capability of material to function with a suitable host feedback in a particular application. It's better for any polymer if it passes cytotoxicity and in vivo toxicity – especially if the product is synthesized from petrochemical based material, it is strongly advised to test and improving its toxicity (Kaczmarek et al., 2019). Basically, hydrogels synthesized from agricultural wastes including cellulose are green and biocompatible due to its primary occurrence of naturally toxic free even though type of cross-linking agent, chemicals and other additives during synthesize may lead to toxicity behavior. Research must be directed toward finding alternative cross-linking approaches and using green chemicals during production (Garg et al., 2017).

Biodegradable polymer materials can be metabolized by living organism or degraded under certain conditions. Most of petrochemical based polymer materials have a property that make them resistance to microorganisms and other natural degradation forces and lead them to remain in the environment after disposal. This causes series problems worldwide that leads to the environmental pollution, waste management and land shortage issues for solid waste management. To overcome these challenges, there is increasing demand of biodegradable polymeric materials (Saruchi et al., 2016).

Despite the fact that cellulose and cellulose derivatives can be biodegradable and simply metabolized by microorganism in the soil, one study has shown okara cellulose hydrogel lost up to 97% of weight in 14 days and complete degradation in 28 days (Cui et al., 2019). The beauty of cellulose based hydrogel is that it can degraded in the soil without any addition of enzyme, while other polysaccharides such as starch need enzyme like α-amylase for degradation.

2.8.3. Mechanical Properties

Mechanical properties of hydrogel can be different based on the purpose of materials. Gel with higher stiffness and good young modulus (result of union between water and gel matrix) can be obtained from good cross-linking methods, while hydrogel with strong young modulus does not needed for application of wastewater treatment. Most common equipment for evaluation of youngers modulus for polymer material is called dynamic mechanical analysis (DMA) (Haraguchi, 2008). Viscoelasticity, which is described as the properties of material that show both viscous and elastic attributes when undergoing deformation, is also another mechanical properties of hydrogel. Viscous materials like hydrogel hold out against strain and shear flow and linearly with time when a stress is applied (Oyen, 2014).

2.8.4. Porosity and Permeation

Porosity may be formed in hydrogels by phase separation during synthesis or they may exist as smaller pores within the network. The average pore size, the pore size distribution and the pore interconnections are important factors of a hydrogel matrix that are often difficult to quantify and are usually included together in the parameter. Porosity is a morphological characteristic of a material that can be illustrated as the presence of void cavity inside the bulk. We know that pollutant may enter in to the pore of the adsorbents during removal. Bearing in mind of this, hydrogels with high porosity have high adsorption capacity than non-porous adsorbent materials (Yang et al., 2012).

2.9. Adsorption isotherm

The relation between the amount of the adsorbents and the equilibrium concentration of the adsorbents under constant temperatures is called adsorption isotherms. It is very help full for analyzing the adsorption capacities of the adsorbents and also able to predict the distribution of adsorbent molecules between liquid and solid phase at equilibrium.

Adsorption equilibrium is established when both adsorption and desorption rate are equal, in other word, when adsorbate containing phase has been contact with adsorbent for adequate time (Mustapha et al., 2019). Langmuir and Freundlich models are the most common adsorption isotherm model performed widely (Tran et al., 2018).

2.9.1. Langmuir adsorption isotherm model

The Langmuir model supposes that all the adsorption active sites have the same binding energy and each site is only able to bind a single adsorbate. Langmuir adsorption isotherm model is expressed in its linear form as follows.

$$\frac{C_e}{Q_e} = \frac{1}{q_m . k_L} + \frac{C_e}{q_m} \dots \dots \dots \dots \dots \dots \dots \dots \dots \dots \dots \dots \dots (2.2)$$

Where: Q_e is the equilibrium adsorption capacity of the adsorbent (mg/g), C_e is equilibrium concentration of the adsorbate (mg/L), q_m is the saturated single layer adsorption capacity (mg/g), K_L is Langmuir constant. Affinity between the adsorbent and adsorbate was determined via dimensionless separation factor, R_L as determined using equation below (Zhou et al., 2011).

$$R_L = \frac{1}{(1 + K_L C_o)} \dots \dots \dots \dots \dots \dots \dots \dots \dots \dots \dots \dots \dots (2.3)$$

Where: K_L is the Langmuir adsorption isotherm constant and C_o is the initial concentration of adsorbate.

Dimensionless R_L values promulgate whether the adsorption is irreversible when ($R_L = 0$), if ($0 < R_L < 1$) then the adsorption is favorable, and the adsorption is unfavorable or linear when ($R_L = 1$ or $R_L > 1$) (Bisht & Agarwal, 2016).

2.9.2. Freundlich adsorption isotherm model

The Freundlich isotherm model is another empirical equation which can be used to describe the non-ideal sorption behaviors. The Freundlich model was proven to be consistent with the exponential distribution of active centers, characteristic of heterogeneous surfaces (Farkas, 2019). Unlike the Langmuir model, the Freundlich model is based on the multilayer adsorption and its linear form can be expressed.

Additionally empirical Frendlich isotherms is applied to describe the adsorption of non-uniform (heterogeneous) surface with interconnection between adsorbed solute molecules in the reversible and non-ideal adsorption process (Mustapha et al., 2019).

$$\ln_{Q_e} = \left(\frac{1}{n}\right) \ln C_e + \ln K_F \dots \dots \dots \dots \dots \dots \dots \dots \dots \dots \dots \dots \quad (2.4)$$

Where: q_e is the equilibrium adsorption capacity of the adsorbent (mg/g), Ce is the equilibrium concentration of the adsorbate (mg/g), K_F and n is the Frendlich constant.

2.10. Adsorption kinetics

Adsorption kinetics is important characteristics in evaluation of adsorption efficiency and it's used for intention of developing period of time for adsorption of adsorbate on the hydrogel and also it's important to describe the adsorption process by means of a theoretical model. In batch adsorption process, kinetic studies provide information about optimum conditions, mechanism of sorption, and possible rate controlling step. For this purpose, linear and nonlinear form of pseudo-first- and pseudo-second-order kinetics is applied on adsorption data. These two common kinetic models will be described as follows.

2.10.1. Pseudo- first order model

Describes the proportion of the adsorbate adsorption with time to the concentration of adsorbents (dye adsorption kinetics) and described by formula below (Trane et al., 2018).

$$\frac{d_{q_t}}{dt} = k_1(q_e - q_t) \dots \dots \dots \dots \dots \dots \dots \dots \dots \dots \dots \dots (2.5)$$

Where: k_1 (min^{-1}) is rate constant of pseudo first order adsorption, q_t (mg/g) is the amount of pollutants adsorbed at time (min), q_e (mg/gm) is amount of pollutants adsorbed at equilibrium (determined from the slope and intercept of the plot) and t (min) is the contact time.

2.10.2. Pseudo second order model

Adsorption kinetics can be analyzed by pseudo second order kinetics which is described as follows (Venkatesham et al., 2018).

$$\frac{d_q}{dt} = k_2(q_e - q_t)2 \dots\dots\dots\dots\dots\dots\dots\dots\dots\dots\dots\dots\dots (2.6)$$

Where: $K_2 \, (g/mg \, min)$ is the second-order rate constant of adsorption. The constants can be determined by the plot of t/q_t versus t.

2.11. Factors affecting dye removal efficiency of hydrogels

2.11.1. The pH of the solution

pH affects the extent of adsorption because the distribution of surface charge of the adsorbent can be changed with pH (Mahmoud et al., 2017). In the dye adsorption process, adsorption efficiency is strongly pH-dependent, because pH can change the chemical structure of dye molecules and functional groups on the surface of hydrogels (Van Trane et al., 2018). In the case of cationic dyes the adsorption capacity will increase with increasing pH. in accordance with Peng et al pH range from $4 - 9$ (Peng et al., 2016).

2.11.2. Temperatures

Temperature is the main factor affecting dye removal efficiency of hydrogels which can varies the result on removal efficiency. Literatures reported that there is decreasing in dye removal of adsorbent hydrogel during temperature increment due to decreasing adsorptive force between the dyes and active site on the adsorbent surface which results in high desorption of water; temperatures range from $(29.5 - 55)°C$ is acceptable and (Ramesh et al., 2013).

2.11.3. Contact Time

Contact time is one of the major factors which can affect the removal efficiency of the adsorbent. Increasing contact time may increase or decrease the yield depending on interaction effect of other factors (Dayana et al, 2016). In some literatures, reaction time varies from $(30-180)$ minutes.

2.11.4. Initial concentration of dye and adsorbent dosage

The effects of initial concentration of dye and the adsorbent dose mainly depend on the concentration of adsorbates and the available sites on an adsorbent surface. The increase of adsorbate concentration leads to enhancement in the adsorption capacity but decreases the adsorbate removal efficiency. However, the increase of adsorbent weight showed opposite results which gradually increase the removal ratio of pollutants and decrease the adsorption capacity. These phenomena are explained in the following way: at low adsorbate concentrations, the ratio of the initial number of moles of adsorbate ions to the available surface area of hydrogel is large, whereas at higher concentrations, the available sites of adsorption become fewer, and the percentage removal of pollutants decreases in turn. The higher adsorbent dosage offers a larger number of active sites and a larger surface area for adsorption. Decrease in the total surface area of the adsorbent and the correspondingly high adsorbent concentration results in particle interactions, such as aggregation (Van Tran et al., 2018).

2.12. Sugarcane bagasse

Sugar cane bagasse is the first byproduct of remaining after juice extraction. More than 100 million tons of sugarcane bagasse produced worldwide annually. Bagasse also offers advantage of being low cost, yielding great quantity and eco-friendly. Also it is suitable polysaccharide for synthesis of hydrogel that commonly consists of cellulose, hemicellulose, extractives and lignin composition (Aye et al., 2018a). Alkaline pretreatment can remove the lignin from the biomass, and removing acetyl groups and various uronic acid substitutions on hemicellulose. Dilute NaOH treatment of lignocellulose material causes swelling, leading to an increase of internal surface area, and increased the cellulose level and decreased the hemicellulose content. H_2SO_4 is commonly used acid in the pretreatment of sugar cane bagasse than other (Lavarack and Griffin, 2002; Karp et al., 2013).

2.13. Litrature summery

Textile wastewater has been increasing over years and becoming a major cause of pollution in the world. A considerable amount of dye-bearing wastewater is discharged the environment to without proper treatment, thus, posing severe problems to agriculture-based life-style, aquatic life and aesthetic nature of the environment (Sivri & Toroz, 2007).

Methylene blue dye is one of harmful effluent that was discharged from textile industry. In contrary to its benefits, this stable compound is very toxic and almost non-biodegradable in environment which lasts for many years. Several literatures reported the effect of methylene blue dye on human being like increased heartbeat, cyanosis, vomiting, shocking, headache, tissue neurosis, bluish stained skin, anemia, dyspnea, depression, respiratory stimulation and increased blood pressure and other chronic diseases. It has also been reported to cause bluish discoloration of the urine and stool, Heinz body formation in dogs and cats and conjunctive injury in rabbits (Koch et al., 2013; Sheet et al., 2019). Broadly, three textile wastewater treatment approaches (chemical, physical and biological) have been devised. Chemical treatment method is expensive due to the use of excess chemicals during processing steps and disposal of removed dye as a sludge. The sludge is difficult to be recycled due to breaking down of the dyes into simple pieces and destroying the presence of atom in the color compound (Bhargava, 2016).

Biological treatment method is not widely practiced due to its complex process and difficulty to apply for removal of all type of dyes. Application of adsorption technique which is the most effective physical method, such as activated carbon is limited by virtue of its less efficiency for removal of chemicals that are not attracted to carbon and high cost due to energy intensiveness (Dargo et al., 2014 ; Shendge, 2017). Moreover, all these approaches are inefficient for removal of all type of dye, especially its application toward non-biodegradable dye (eg. methylene blue dye) which has a serious socio-economic and health impacts. Although recent numerous studies have shown improved Methylene blue dye adsorption capability of hydrogel (Hakam et al., 2015; Zendehdel et al., 2010; Zhou et al., 2011). Given its economic feasibility, biocompatibility and adsorption efficiency, a non-conventional adsorption material called hydrogel – a three-dimensional matrix of hydrophilic gel polymer that can able to absorb huge amount of water, swell but does not affect nearby dissolution appeared from cross linking between matrix chains (Okay, 2009) – has got attention nowadays (Van et al., 2018). Hydrogel has demonstrated to be an excellent dye adsorbent material with extremely high level of methylene blue dye adsorption (Garg et al., 2017).

3. MATERIALS AND METHODS

3.1. Material

The raw material for the study: Sugarcane bagasse and wastewater were collected from Didesa sugar factor, Oromiya Region, Ethiopia and Arbaminch textile industry located in sebeta town, Oromiya Region, Ethiopia respectively.

Chemicals and reagents: Good commercial grade of methylene blue dye (Addis Ababa, Ethiopia), Sulfuric acid (H_2SO_4, Delhi India, 99.78% purity), Sodium hydroxide (NaOH, India, 98% purity), Hydrogen peroxide (H_2O_2, Addis Ababa, Ethiopia, 30% purity), Ethanol (Addis Ababa Ethiopia, 97% purity), Citric acid ($C_6H_8O_7$, Mumbai, India 99.5%, extra pure), Poly ethylene glycol (PEG, England) and Phosphoric Acid (H3PO4, Mumbai, India) are main chemicals used in the present study. All laboratory tasks took place by using distilled and deionized water.

Equipment: The main equipment needed for this study were plastic bottle and bag, grinder, sieve, oven, cylinder, beaker, conical flask, magnetic stirrer, electronic balance, petri dish (60 mm), pH meter (Model: JENYWA; 3505 pH meter), water bath, thermometer (digital thermometer tp101 stainless), vacuum filter, reflux condenser, hot plate, round bottom flask, watchman filter pepper, centrifuges, condactometer, Turbidity meter (HACH turbid meter (model 2100N) in NTU)), incubator and COD reactor (HANNA reactor), DR2800 spectrophotometer, AHACH spectrophotometer (Model DR 2500), Fourier transform infrared spectroscopy (FTIR, PERKIN ELMER, L1600300 Spectrum TWO UTA), Scanning Electron Microscopic (SEM, JCM-6000Plus, version 0.2 JEOL/EO), smart coater (DI-29030SCTR smart coater), X-Ray Diffractometer (XRD-7000), furnace, Thermo-Gravimetric Analyzer (TGA-4000, PERKIN ELMER), UV-Visible spectrophotometer (Jenway,6100Z spectrophotometer) and Dynamic light scattering (DLS, ZETASIZER, NANO SERIES HT, ZE3600).

3.2. Methods

3.2.1. Raw material preparation

Sugarcane bagasse was washed using distilled water until impurities and amount of sugar constituent left after removing juice extraction are removed.

The wet bagasse was allowed to dry by exposing it to sunlight for one week and then grounded using traditional mortal as a grinder.

3.2.2. Component characterization of sugar cane bagasse

3.2.2.1. Lignin determination

Lignin content in sugarcane bagasse was determined according ASTM D1106 standard (Campbell, 2016). Two gram of two mm mesh size sugarcane bagasse was well mixed with 25mL of 72% of H_2SO_4 at room temperature for two hours. Then the resulting mixture was transferred to a circular bottom flask and diluted with water to make a 3% acid solution followed by boiling for two hours by using a hot plate and condenser. The hydrolyzed residue was filtered with a vacuum filtration unit and washed until freed from acid by means of hot water. The lignin content is calculated on the basis of the oven-dry sample as follows.

$$\text{Lignin content } (\%) = \frac{W_{DS}}{W_{IS}} \dots \dots \dots \dots \dots \dots \dots \dots \dots (3.1)$$

Where: W_{DS} is weight of dried sample and W_{IS} is initial weight of the sample

3.2.2.2. Determination of extractives

The extractive determination was performed according to ASTM D634 standard ((Vijayanand et al., 2016). For this, Ten gram of bagasse powder with a particle size of 600 µm was taken and mixed in 200 mL of distilled water and kept in a boiling water bath of 80℃ for a period of three hours. Then it was filtered using a vacuum filter. The filtered residue was dried at 105℃ until a constant dry weight was obtained similarly; for the preparation of ethanol extractives, ethanol was diluted to 5% in the 200 mL of distilled water and then extractives were prepared with the same procedure for water extractive preparation. Finally, the extractive percentage was determined as follows.

$$\text{Extractive} (\%) = \frac{W_I - W_e}{W_I} \times 100 \dots \dots \dots \dots \dots \dots \dots \dots \dots \dots (3.2)$$

Where:

W_I = Initial weight of sample

W_e = Weight of extractive

3.2.2.3. Hemicellulose determination

Hemicellulose content in sugarcane bagasse was determined according to ASTM D5896-96 (2012) (Hu & Zhang, 2018). Two gram of sample from dried extractive was taken and 10 mL of 0.5M of NaOH solution was added to it. Then the solution was kept in a boiling water bath for three hours at 80℃. Then it was washed with distilled water until neutral pH. NaOH solution of 0.5M was prepared by dissolving 20 g of NaOH in 1L of distilled water.

Hemicellulose content (%) = $(W_I - W_F) \times 100$ ... ... (3.3)

Where:

W_I = Initial weight of sample

W_F = Final weight of the sample

3.2.2.4. Cellulose determination

The cellulose in sugarcane bagasse was calculated by using the values obtained for their corresponding lignin, hemicelluloses and extractives as follows.

Cellulose = 100 – (Lignin + Hemicellulose + Extractive) ×100%…………………... (3.4)

3.3. Extraction of cellulose from sugarcane bagasse

3.3.1. Delignification process

Delignification of sugarcane bagasse was performed according to a previously described producers (Plermjai et al., 2018). The first procedure was removal of wax from the powder. One gram of sugarcane bagasse powder was added into a conical flask containing 20 mL of distilled water. The mixture was boiled for two hours using the water bath adjusted at 80℃. Then the mixture was kept at room temperature for 30 minutes in order to cool and settle down. Finally, the residue was filtered by using a vacuum filter and washed until the wax was removed. The process was repeated two times to perfectly remove waxes. Next delignification step was performed by using sulfuric acid. The residue was added to 200 mL of 5% H_2SO_4 (v/v) and left under magnetic stirrer for two hours at 60℃. Then the mixture was kept at room temperature for 30 minutes in order to cool and settle down. Then it was filtered via vacuum filter and washed until obtaining neutral pH. The process was repeated four times to partially remove the lignin and hemicellulose.

3.3.2. Isolation of cellulose

After delignification processes were completed, the isolation of cellulose was performed according to procedure described by Karunakaran (Karunakaran, 2016). The residual was added into 200 mL of 4% NaOH (v/v) solution. Then the mixture was left under a magnetic stirrer for two hours at 60℃. Then it was kept at room temperature for 30 minutes in order to cool and settle down. Next the solution was filtered using a vacuum filter and washed until neutral pH. The final oxidation process was performed by using H_2O_2, 200 mL of 24% H_2O_2 (v/v) was added to the residue followed by magnetic stirring at 60℃ for two hours. Finally, the solution with white precipitate was appeared. Then its vacuum filtered, washed until getting neutral pH and oven-dried overnight at 50℃. Figure 3.1 below show flow sheet for extraction of cellulose from sugarcane bagasse.
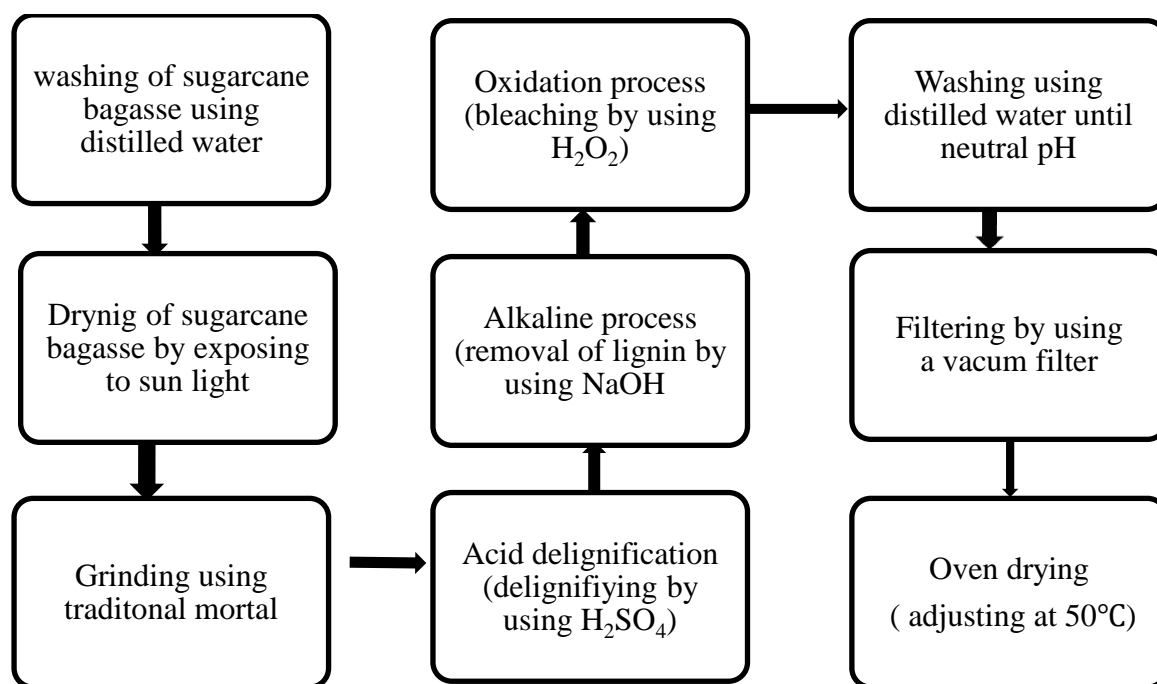
Figure 3.1. Flow sheet for extraction of cellulose from Sugarcane Bagasse

3.3.3. Cellulose yield determinations

After cellulose extraction process, amount of final cellulose product (yield) was obtained according to ASTM D6896- (2020) for yield determination as follows.

$$\text{Yield (\%)} = \frac{\text{Weight of obtained cellulose product(g)}}{\text{Weight of baggase poweder used (g)}} \times 100 \ldots \ldots . . \ldots \ldots \ldots \ldots . (3.5)$$

3.4. Characterization of cellulose product

3.4.1. Uv- Vis Spectrometer analysis

The UV absorbance spectra of cellulose solution is measured from 190 to 700 nm (Plermjai et al., 2018). The intensity absorbance peaks of extracted cellulose corresponding to this range validate presence of cellulose content and product characterization was done at faculty of Material science and engineering, Jimma Institute of Technology, Jimma, Ethiopia.

3.4.2. Fourier Transformed Infrared Spectroscopy (FTIR)

Functional group change between untreated sugarcane bagasse and extracted cellulose product during various treatment methods were analyzed by FTIR spectroscopy using potassium bromide (KBr) as a reference material. The infrared spectra band was recorded by passing a beam of light through the solid sample at a resolution of 4 cm^{-1} in the spectral region between 4500 cm^{-1} and 450 cm^{-1}. The disk was prepared from powered sample of 0.001 g and 0.045 g of cellulose and potassium bromide using 400 Kg/cm^2 for 10 minutes respectively. The infrared spectra band can suggest the absence and presence of lignocellulosic compounds and whether the intensity of the absorption band has changed. Experimental work is done at faculty of Material Science and Engineering, Jimma institute of Technology, Jimma, Ethiopia.

3.4.3. X-ray Diffraction (XRD)

Crystallinity change between untreated sugarcane bagasse and extracted cellulose was examined using XRD-7000 with cu kα radiation at faculty of Material Science and Engineering, Jimma Institute of Technology, Jimma, Ethiopia. The analyses were conducted at an accelerating voltage of 30 KV and the radiation current 25 mA within the choice of diffraction angle $2\theta = (10 - 70)°$. Crystallinity index and crystal size of sugarcane bagasse and extracted cellulose were calculated according to Equation 3.6 below which is described Plermjai.et al (Plermjai et al, 2018).

$$(CI \text{ in } \%) = \frac{\text{Area of crystaline peak}}{\text{total area of all peaks}} \times 100\% \quad (CS) = \frac{k\,\lambda}{\beta cos\theta} \dots \dots \dots \dots \dots \dots . (3.6)$$

Where: CI= is Crystallinity index, K = the correction factor and usually taken to be 0.91, λ = the radiation wavelength, θ is the diffraction angle, and B= the corrected angular width (in radians) at half maximum intensity and CS is crystal size.

3.4.4. Scanning Electron Microscopic (SEM)

Morphological image analysis including bond rigidity, surface shape of the product and structure for extracted cellulose was performed by using Scanning Electron Microscope (JCM-6000Plus, version 0.2 JEOL/EO) at Faculty of Natural Science, Department of Biology, Adama Science and Technology University, Adama, Ethiopia. Cellulose sample was reduced to small size and coated with smart coater (DI-29030SCTR smart coater) for one minute before SEM observation was started for protection of Charge builds up.

3.5. Synthesis of bagasse based cellulose hydrogel

Synthesis of bagasse based cellulose hydrogel from extracted cellulose is performed according to previously described (Haque & Mondal, 2016; Fekete et al., 2017). First, for dissolution of cellulose, one gram of cellulose was added into beaker containing 20 mL of concentrated phosphoric acid in order to break down inter and intra molecular bond of cellulose (HaoLiu et al., 2011). Mixture of cellulose and phosphoric acid was left under a magnetic stirrer for 24 hours until complete dissolution has occurred at room temperatures. Next one gram (w/w) of polyethylene glycol was added to the cellulose mixtures and stirred using mechanical stirrer for 30 minutes until homogeneous solution was obtained. Then 15 mL of 10% of citric acid (w/w) solution was subsequently added to the mixtures under a magnetic stirrer for 30 minutes and the solution is kept at room temperature. Then final solution is kept under room temperature with no string for 24 hours in order to get complete homogeneous solution. Finally the solution was casted in 40 mm of petri dish and oven-dried at 50℃.

3.6. Characterization of bagasse based cellulose hydrogel

3.6.1. Swelling measurement

Swelling measurement for hydrogel was determined according to ASTM D3616 – 95 (2014). To reach swelling equilibrium, 0.5 g of five replicate of hydrogel sample (3mm) was immersed into 100 mL of distilled water at room temperature for 3 days to achieve swelling equilibrium. Degrees of swelling hydrogels were measured after 30 minutes, 2 hours, 6 hours, 1 day, 2 days and 3 days and three times replicates were done for each run and degree of swelling was calculated according Equation (2.1).

3.6.2. Water retention capacity (W$_R$)

Experimental tasks toward Water retention capability for hydrogel were performed according to ASTM D3616 – 95 (2014). Beyond the swelling, the equilibrated hydrogel were removed from the distilled water and weighted initially (W$_o$) and at different time intervals (W$_t$). Water retention capability was determined according to Equation 3.6 below.

$$W_R = \frac{W_t}{W_o} \times 100\% \dots\dots\dots\dots\dots\dots\dots\dots\dots\dots\dots\dots \text{(3.6)}$$

3.6.3. Gel content determination

Determination of gel content was done according to ASTM D2765-01 (2014). For this, One gram of dried hydrogel was immersed in 100 mL of deionized water for 48 hours to completely remove of sol fraction. Then swelled hydrogel was taken out and dried at 50°C by using oven drying technique, finally gel content is determined as follows.

$$\text{Gel Content (\%)} = \frac{\text{Weight of dry gel after swollen}}{\text{Initial weight of dried gel before swelling}} \times 100\% \dots\dots\dots\dots\dots \text{(3.7)}$$

3.6.4. Biodegradability of cellulose hydrogel

Biodegradability of cellulose hydrogel in the soil was performed according to ASTM D5988 (2019). Cellulose hydrogel (5mm) were buried approximately in 10 cm depth from the surface of the soil at room temperature. The degraded hydrogel fragments were taken out one by one after 2 to 30 days and the weight of degraded hydrogel fragments were measured.

3.6.5. Thermogravimetric analysis (TGA)

Thermal stability and temperature decomposition of cellulose hydrogel were determined by using TGA-4000 at faculty of Material Science, Adama Science and Technology University, Adama, Ethiopia. Thermal degradation of hydrogel was undergone starting from $(25 - 450)°C$ with heating rate of 40.00°C/min under inert atmosphere (N$_2$) with flow rate of 20 mL/min to remove all corrosive gases and avoid thermoxidative degradation (Palantöken et al., 2019).

3.6.6. Scanning electron microscopic (SEM)

Porosity of structures and morphological images were analyzed by using SEM-(JCM-6000Plus, version 0.2 JEOL/EO). Cellulose hydrogel was powdered in to 0.25mm mesh size and coated with DI-29030SCTR smart coater for one minute. SEM analysis was done at faculty of Natural Science, Department of Biology, Adama Science and Technology University, Adama, Ethiopia.

3.6.7. X-Ray diffractometer analysis (XRD)

X-ray Diffractometer for crystallinity analysis was carried out to show crystallinity change occurred during esterification reaction. Scanning speed for the process was 0.03 m/s over $2\theta = (10 - 70)°$ using acceleration voltage of 30 KV and current 25 mA. Crystallinity analysis was done at faculty of Material Science, Jimma Inistiute of Thechnology, Jimma, Ethiopia.

3.6.8. Dynamic light scattering analysis (DLS)

Average particle size and Polydispersity index for bagasse based cellulose hydrogel was analyzed by using DLS-Zetasizer Nano instrument (ZE3600) at Addis Ababa Science and Technology University Central Laboratory. Particle size analysis was done when it was in solution form and scan for 30 minutes by using Brownian motion of particle size when light passed through the suspension is scattered of the particles (Bhattacharjee, 2016).

3.6.9. Fourier transformed infrared spectroscopy analysis (FTIR)

Functional group change during synthesis of bagasse based cellulose hydrogel and its chemical structure is determined by using FTIR- PERKIN ELMER –TWO UTA at Biology Department, Addis Ababa Science and Technology University, Addis Ababa, Ethiopia. Dried hydrogel was grinded and mixed with potassium bromide (KBr) for preparation of plates. Potassium bromide plate also prepared to use as a reference material. The peak intensity was recorded between (450-4000) cm^{-1} wavelengths.

3.7. Adsorption experment

Three different batch mode experimental studies were carried out to assess the effect of adsorbent dosage$(2 - 5)$ g/L, initial contact time of $(30 - 60)$minutes and initial dye concentration of $(10 - 20)$ mg/L on removal efficiency of hydrogel.

All adsorption experiments were conducted at room temperature($25°C \pm 5°C$). Finally, mixtures were filtered through watch man filter paper to separate purified water and adsorbent residue with pollutant. Then the adsorbent was removed from a watch man filter pepper and supernatant was analyzed by UV-visible spectrophotometer for the residual concentration of methylene blue dye at maximum wave length of 665 nm and final removal efficiency of hydrogel was determined according to Equation 3.8 (Zhou et al., 2006).

$$\text{Removal Efficency}(\%) = \frac{C_O - C_e}{C_o} \times 100 \dots\dots\dots\dots\dots\dots\dots\dots\dots. (3.8)$$

Where: Co = Initial concentration of dye (mg/L)

Ce = Equilibrium concentration of dye (mg/L)

Adsorption capacity was assessed at different operating condition by using UV visible spectrometer and amount of adsorption capacity calculated as follows:

$$(Q_E) = \frac{C_O - C_{EQ}}{M} V \dots\dots\dots\dots\dots\dots\dots\dots\dots\dots\dots\dots\dots\dots. (3.9)$$

Where: Q_E, C_O, C_{EQ}, V and M were amount of dye adsorbed at equilibrium, initial concentration of dye solution, concentration of dye solution in the equilibrium, mass of the adsorbent and volume of the dye solution respectively.

3.8. Experimental design and statistical analysis

The design expert (version 11) software was used to design the experiments and optimum methylene blue dye removal efficiency of hydrogel. From the response surface methods (RSM), the experiments were designed according to central composite design (CCD) method with selected three important parameters (adsorbent dosage, contact time and initial concentration of methylene blue dye). Central composite design with rotatable feature was selected as a designing tool to investigate effect of each factor, effect of change of variables in dye removal, the interactive effect of process variables and building of mathematical models to describe the overall methylene blue dye adsorption process. The average methylene blue dye concentration in Ethiopian textile industry was reported as it is around 10.4 mg/L (Hayelom Tesfay, 2019). On a basis of figure, initial concentration of methylene blue dye designed in range of $(10 - 20)$ mg/L.

 Based on Zhou et al work (Zhou et al., 2011) adsorbent dosage in range of $(2-5)\,\text{g/L}$ selected in this work. Although it has been reported that reaction time vary from $(30-180)$ minutes, required equilibrium removal efficiency could be achieved at about 50 minutes (Dayana et al., 2016). Based on this, contact time in range of (30–60) minutes was selected in this work. Table 3.1 below shows factors with maximum and minimum range value.

Table 3.2. Factors with Maximum and Minimum Range Value

Factors	Unit	Code	Alpha value = 2 & replication 6 times at center point	
			Low	High
Contact time	Min	B	30	60
Adsorbent dosage	g/L	C	2	5
Initial Concentration of Dye	mg/L	D	10	20

3.9. Reusability of bagasse based cellulose hydrogel

Cellulose hydrogel containing the residue of methylene blue dye was desorbed by washing three times—using 30 mL of HCl solution (0.1M). Then the sample hydrogel was washed with distilled water three times and used for next cycles.

Desorption experiments were repeated five times at optimum process condition that was predicted by response surface method. Removal efficiency of adsorbent at each desorption step was calculated according to Equation 3.3 above.

3.10. Adsorption isotherm and kinetics

Adsorption isotherms were investigated under optimum process variables such as: adsorbent dosage (g/L), contact time (minutes) and initial concentration of dye (mg/L) (Tran et al., 2018). Different batch experiments were conducted under different initial concentration of dye and the reaction was shaken (150 rpm) with optimum adsorbent dosage and contact time at room temperatures. After settling—the residue was separated using watch man filter paper. Then UV-visible spectrometer was used to read adsorption before and after treatment. Then Langmuir isotherm plot Ce/qe versus C_e were calculated according to Equation 2.2 and specific value (Q_m, K_L) were calculated from slop of the plot.

For Empirical Frendlich isotherm plot, (ln Qe versus ln Ce) was calculated according to Equation 2.4 and specific value from Frendlich (n, K_F) was calculated from the slop of the plot. Adsorption kinetics also studied under optimum condition of given variables and different batch experiments were performed at different contact time. The reaction was shaken (150 rpm) with constant optimum adsorbent dosage and initial concentration of dye at room temperatures. After settling—the residue was separated using watch man filter paper. Then UV-visible spectrometer was used to read adsorption before and after treatment. The pseudo-first and second order adsorption kinetics specific values (K, Q_e) were calculated according to Equation 2.5 and 2.6 respectively. Correlation factors (R^2) were calculated by using Equation 2.3 and all results were compared with literatures.

3.11. Wastewater characterization

3.11.1. COD analysis

Reagent used

A. Standard potassium dichromate digestion solution (0.01667M) was prepared. First 500 mL of distilled water was added to 4.903 g of $K_2Cr_2O_7$, primary standard grade, previously dried at 150℃ for two hours. Then 167 mL of H_2SO_4 and 33.3 g of mercuric sulfate powder ($HgSO_4$) added, dissolved, cooled to room temperature, and diluted into 1000 mL were used.

B. Sulfuric acid reagent: Ten gram of silver sulfate powder (Ag_2SO_4) was added into 1000 mL of H_2SO_4 solution (100 mL of H_2SO_4 + distilled water).

C. Standard ferrous ammonium sulfate (0.10M): 39.2 g of $(NH_4)_2Fe(SO_4)_26H_2O$ was added into 200 mL, 20 mL of H_2SO_4 were added, cooled and diluted in to 1000 mL.

D. Ferroin indicator solution: 1.485 g of 1-10 (ortho) phenanthroline monohydrates was dissolved with 0.70 g of iron (II) sulphate ($FeSO_4.7H_2O$) in 100mL of distilled water.

E. Standardization: 200 mL of distilled water, 25 mL of potassium dichromate digestion solution and 20 mL of H_2SO_4 was added together and cooled. Then, it was titrated with 0.10M of ferrous ammonium sulfate with three drop of ferroin indicator.

Experimental producers

COD analysis was done according to ASTM 5220 C. A DR2800 spectrophotometer was used to measure the COD value. Three drop of standardized COD reagent was pipetted into culture tubes containing 10 mL of sample wastewater , then inverting each vial up and down a couple of times, the reagent was mixed with the sample and inserted into a COD reactor. A blank were prepared based on our COD range by mixing equal amount of distilled water (10 mL) with the respective reagent (three drop). In the meantime the COD reactor (HANNA reactor) was warmed up until it reaches up to 150℃ with strong oxidizing agent, potassium dichromate digestion solution, which oxidizes organic matter chemically. Then the sample and the blank was feed in to the reactor and stayed there for two hours at same temperature. After two hours the reactor was off and waiting for some time, until the system cools down to reasonable temperature , the sample and the blank was taken out and put in to a rack until it cools down to room temperature. Finally, DR2800 spectrophotometer as calibrated using the blank, the sample was inserted in the photometer for reading.

3.11.2. Total dissolved solid (TDS), Total solid (TS) and Total suspended solid (TSS) test Procedures

Testing procedures was performed according to 2540 B standards. : For total dissolved solid test, sample of wastewater was filtered using a vacuum filter and the residue retained on the filter was dried in an oven at$(103 - 105)$℃ then, weighted. Finally TDS was calculated according to equation 3.10 below

$$\text{TDS} = \frac{\text{Amount of dried sample(mg)}}{\text{Volume of sample water(L)}} \ldots\ldots\ldots\ldots\ldots\ldots\ldots\ldots\ldots\ldots (3.10)$$

Total solids (TS) are found by evaporating the water at 180℃ and the remaining solid residue was weighted.

TSS is then calculated as follows:

$$\text{TSS = TS-TDS} \ldots\ldots\ldots\ldots\ldots\ldots\ldots\ldots (3.11)$$

3.11.3. pH test, Turbidity test and Temperatures test

In accordance with ASTM D1293 and ASTM D7315-17 Standard pH range, turbidity and temperature were directly measured using pH meter (Model: JENYWA; 3505 pH meter) Turbidity meter (HACH turbid meter (model 2100N) in NTU)) and thermometer (digital thermometer tp101 stainless (℃)) respectively. Before and after test was done; all instrument was properly calibrated before starting the analysis.

3.11.4. Color test

Color test before and after treatment for this work was carried out by using AHACH spectrophotometer (Model DR 2500) which was displayed by Pt-Co unit. First the blank was wiped by using deionized water and placed into the cell holder and touch zero for calibration of the instrument. After instrument displayed zero Pt-Co, 10 mL of prepared wastewater sample was wiped and it into the cell holder then touch read. Finally the result was appeared in Pt-Co unit.

3.11.5. Preparation of methylene blue dye solution

Stock solution was prepared by dissolving 0.1 g of methylene blue dye into distilled water contained in 1000 mL volumetric flask. Different amount of this solution was added to constant volume (100 mL) of distilled water to create different methylene blue dye concentration.

4. RESULTS AND DISCUSSION

4.1. Component characterization for sugarcane bagasse

To synthesize bagasse based cellulose hydrogel for removal of methylene blue dye from textile industry wastewater, we started with determination of the main components of sugarcane bagasse such as lignin, extractive, hemicellulose and cellulose contents. Determination of lignin was performed until obtaining a constant weight (0.37 g) of dried and hydrolyzed sample, resulting in 18.35% of the lignin content as per Equation 3.1. The extractive amount of sugarcane bagasse was found to be 8.5% based on the dry basis (Equation 3.2). The results show that sugarcane bagasse had rigid and strong lignocellulosic component which offers further protection against microbial and chemical attacks (Karp et al., 2013). From the final weight of 1.69 g of sugarcane bagasse, 30.8% of hemicellulose contents was determined (Equation 3.2), showing highly amorphous structure of the bagasse (Garrett et al., 2016). Further, 42.35% cellulose content shows that the sugarcane bagasse has good cellulose contents. Overall, the results of sugarcane bagasse components obtained in this work are comparable to previous studies (Table 4.1). This validates complete removal of the sugarcane bagasse components.

Table 4.1. Comparison of present study with literature value for component characterization

Literatures	Lignin	Hemicellulose	Extractives	Cellulose
(Aye et al., 2018a)	18 -24	25-35	4 -10.41	40-50
(Plermjai et al., 2018)	18.1	33.5	4.8	43.6
(Garrett et al., 2016)	14.1-30.6	22-36	3-14	35-40
(Kullasatri Saelee et al., 2014)	20	30	10	40
(Klemm & Schmauder, 2013	22.5	21.8	No data	44.5
This work	**18.35**	**30.8**	**8.5**	**42.35**

4.2. Extraction of cellulose form sugarcane bagasse

Cellulose was extracted from sugarcane bagasse following a series of processes (dewaxing, acid delignification, Alkalination and bleaching) shown in Figure 4.1. First, boiling of a mixture of bagasse powder and distilled water resulted in a dark black colored solution, which validates removal of wax and other unwanted constituents (Figure 4.1A). Then, stirring of the dewaxed residue with H_2SO_4—acid delignification process; changed the solution to a light brown color (Figure 4.1B), which indicates removal of hemicellulose and other remaining constituents. With immediate addition of NaOH to the residues solution (Alkalination process), a dark green color (loading to black) was obtained—an indicator for presence of lignin in the bagasse (Ameram et al., 2019). To remove the lignin, the solution was stirred with a magnetic stirrer and finally, deep black solution was obtained (Figure 4.1C). The color change from dark green to deep black validates complete removal of lignin from the residue. To avoid residue of NaOH and lignin from the solution, 10 L of distilled water was used. Final oxidation process (bleaching) was performed using H_2O_2 and white precipitated solution was obtained after two hours stirring with magnetic stirrer (Figure 4.1D). Lastly, oven drying of the cellulose product at 50℃ overnight resulted in a dried white powder of cellulose (Figure 4.1E). Several studies employed the same procedure to extract cellulose from sugarcane bagasse in laboratory (Karp et al., 2013; Karunakaran., 2016; Aye et al., 2018; Plermjai, et al., 2018) wich was performed with the same procdueres.

(A) Dewaxing   (B) Acid   C) Alkalination   (D) Bleaching   (E) Cellulose

                      delignification
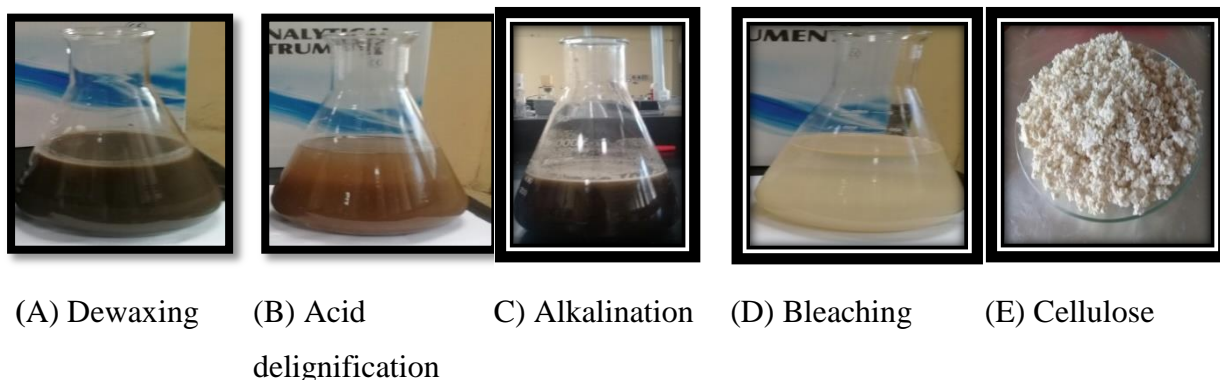
Figure 4.1. Result obtained from cellulose extraction process

4.2.1. Determination of yield

Yield determination for cellulose product was calculated using Equation 3.9, which is ratio of product obtained and total bagasse powder used multiplied by 100%. From 90 g of bagasse powder used in this work and 28.96 g of dried cellulose product obtained, a yield of 32.16% was calculated. Low yield of extracted cellulose was observed; show that there is chemical treatment method affected the yield of the material.

$$\text{Yield (\%)} = \frac{\text{Weight of cellulose(28.95 g)}}{\text{Weight of baggase(90 g)}} \times 100 = \mathbf{32.16\%.}$$

4.3. Characterization of cellulose product

4.3.1. Absorbency analysis

UV absorbance spectra of the cellulose solution were measured from $(190 - 700)$nm and the corresponding result is shown in Figure 4.2. The intensity absorbance peak of the extracted cellulose was observed at 199 nm. In agreement with previous studies (Lina et al., 2018; Plermjai et al., 2018), absorbance spectra between $(190 - 700)$nm show presence of cellulose product.
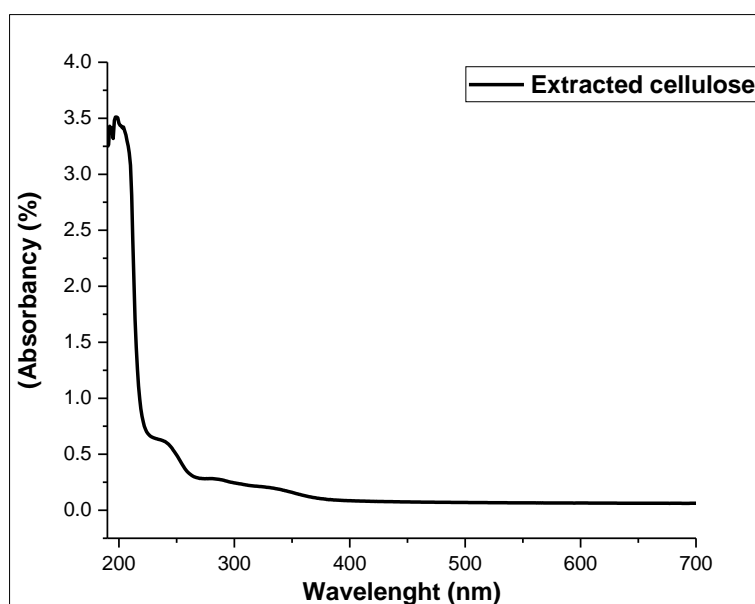
Figure 4.2. UV- Spectrometer analysis for extracted cellulose

4.3.2. Functional group analysis

Functional group analysis for the sugarcane bagasse and extracted cellulose with their respective FTIR spectra is shown in Figure 4.3 and Table 4.2. The FTIR spectra of both samples indicated two main absorbency regions in a range of 800-1800 cm^{-1} and 2700 - 3500 cm^{-1}. In a graph analysis of sugarcane bagasse, 832 cm^{-1} is attributed to bending vibration of arenes C-H bond in lignin, even though wave number containing this peak was not found in graph of extracted cellulose. The result is concordant with a previous report (Rashid et al., 2016). The peak observed at 897 cm^{-1} show presence of $\beta-$ glycosidic linkage between glucose unit in cellulose and hemicellulose. However, this characteristic peak was not found in lignin structure but significantly observed in extracted cellulose (Saeleeh et al., 2018).

The peak at 1042 cm^{-1} is related to C-O stretching in plane due to aromatic C-H deformation of cellulose and lignin (Morán et al., 2008). The peak at 1052 is ascribed to the C-O antisymetric stretching vibration of glucosidic ring in cellulose and hemicellulose but disappears from extracted cellulose (Xing et al., 2012). A peak at 1105 cm^{-1} can be assigned to C-O-C glucosidic ring vibration in cellulose and is compatible with aromatic C-H in plane deformation of lignin. A peak at 1160 cm^{-1} is related to pyranose ring C-O-C asymmetric stretching of cellulose and hemicellulose which is in agreement with a previous report (Ramli et al., 2015). The absorption peaks at 1200 cm^{-1} is O-H deformation vibration mode of cellulose while absorbency peak at 1240 cm^{-1} shows aryl C-O out of plane stretching vibration in lignin, these peaks disappear from extracted cellulose after a treatment process, which is a best suggestion for removal of lignin (Xiong et al., 2013).

A peak at 1320 cm^{-1} represents CH_2 wagging frequency of cellulose which presents in both sugarcane bagasse and extracted cellulose. A peak at 1365 cm^{-1} corresponding to the C-H bending or polysaccharide aromatic C-O vibration and aliphatic C-H stretching mode of cellulose, hemicellulose and lignin A peak observed at 1600 cm^{-1} is due to C=O stretching vibration of lignin, unobservable after alkali treatment (Morán et al., 2008). The absorbance band located at 1634cm^{-1} for both sugarcane bagasse and extracted cellulose are associated with absorbed water in the cellulose and sugarcane bagasse as reported previously (Plermjai et al., 2018).

The peak positioned at 1728cm^{-1} is correlated to C=O stretching vibration of carboxylic group of lignin and hemicellulose. However, this peak didn't appear after chemical treatment method, showing complete removal of polysaccharides from sugarcane bagasse (Hospodarova et al., 2018). The absorbency peak around 2900 cm^{-1} is due to C-H stretching vibration of methyl and methylene group in cellulose and hemicellulose (Hospodarova et al., 2018). The broad peak around 3340 cm^{-1} is attributed to the O-H stretching of intermolecular hydrogen bond of hydroxyl groups (Shi et al., 2012)
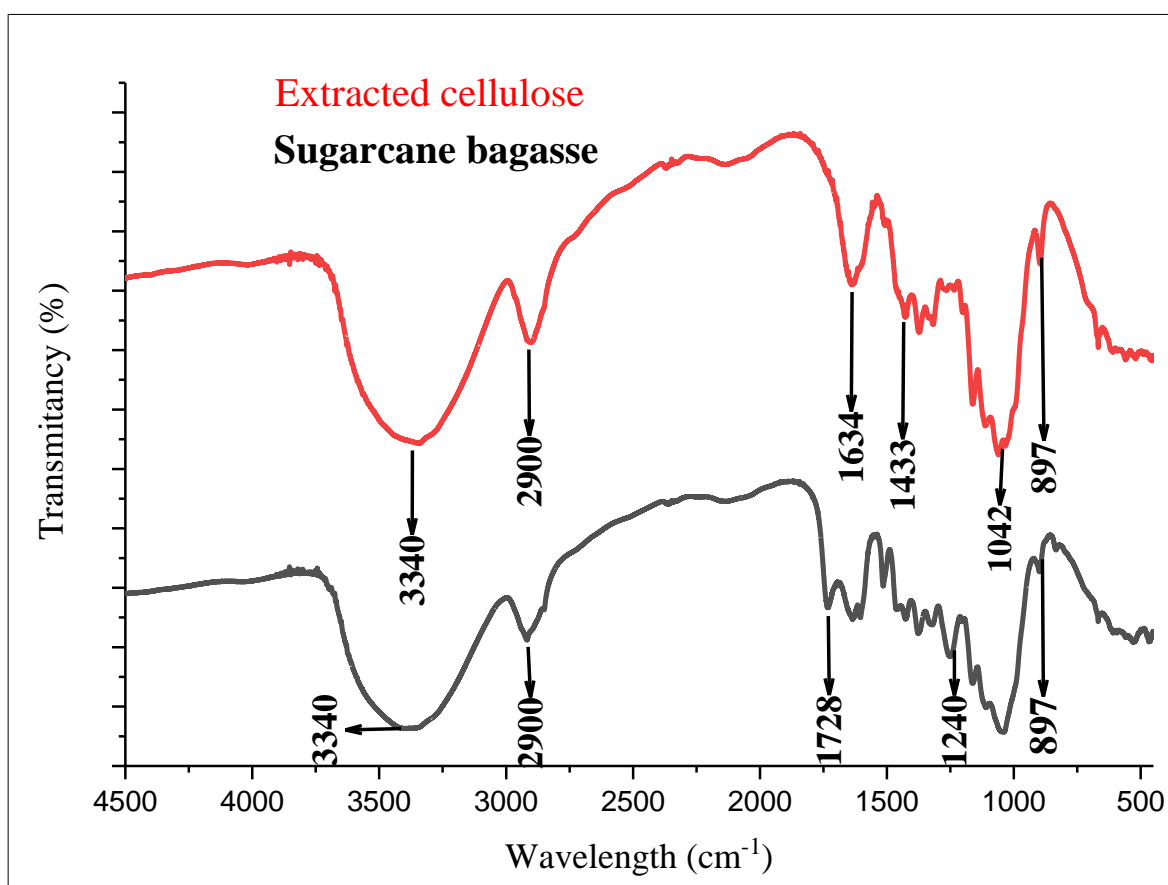
Figure 4.3. FTIR spectra of untreated sugarcane bagasse and extracted cellulose

Table 4.2. Summery on functional group analysis of sugarcane bagasse and cellulose

Wave number (cm^{-1})	Untreated Sugarcane bagasse	Extracted cellulose	Functional group
832	832	Not appeared	bending vibration of arenes C-H bond in lignin
897	897	897	β − glycosidic Linkage between glucose unit in cellulose and hemicellulose.
1042	1042	1042	C-O stretching in plane due to aromatic C-H deformation of cellulose and lignin
1052	1052	Not appeared	C-O antisymetric stretching vibration of glucosidic ring in cellulose and hemicellulose
1105	1105	1105	C-O-C glucosidic ring vibration in cellulose agreeable with aromatic C-H in plane deformation of lignin
1160	1160	1160	Pyranose ring C-C-O asymmetric stretching of cellulose and hemicellulose
1200	1200	1200	O-H deformation vibration mode of cellulose.
1240	1240	Not appeared	C-O out of plane stretching vibrating in lignin
1320	1320	1320	CH$_2$ wagging frequency (of cellulose)
1365	1365	1365	C-H bending/polysaccharide aromatic C-O vibration and aliphatic C-H stretching mode of cellulose, hemicellulose and lignin.
1600	1600	Not appeared	C=O stretching vibration of lignin
1634	1634	1634	Absorbed water in the cellulose and sugar cane bagasse
1728	1728	Not appeared	C=O stretching vibration of carboxylic group of lignin and hemicellulose.
2900	2900	2900	C-H stretching vibration of methyl and methylene group in cellulose and hemicellulose
3340	3340	3340	O-H stretching of intermolecular hydrogen bond of hydroxyl group.

4.3.3. Crstalinity analysis

The Diffractometer peaks analysis observed from XRD analysis scanned over $(10 - 70)°$ with scanning speed of 0.03 s^{-1} was done for sugarcane bagasse and extracted cellulose. Peak corresponding to crystallinity nature of the materials and background corresponds to amorphous nature of materials (Xiaohui et al., 2019). Crystallinity change was clearly observed between sugarcane bagasse and extracted cellulose. Intensity peak located at 22° for extracted cellulose and sugarcane bagasse describes the crystalline nature of the material and the intensity value shows the amount of crystalline structure (2θ value).

High intensity peak observed for extracted cellulose show crystallinity change between cellulose and sugar cane bagasse. Crystallinity index (CI) is a parameter commonly used to quantify the amount of crystalline cellulose present in cellulosic materials and has also been applied to interpret changes in cellulose structures after chemical treatments. We calculated the crystallinity index from area of crystalline peak (4458.14) and total area (9464.79) for sugarcane bagasse; and product cellulose CI was calculated from crystalline area (7488.659) and total area (9648.790). The crystallinity index was found to be 47.11% and 77.62% for the bagasse and extracted cellulose, respectively. The CI changes after treatment was increased by 30.52%, showing the crystal index change between sugarcane bagasse and cellulose which indicates removal of amorphous part of lignin and hemicellulose from sugarcane bagasse. Our result is in line of agreement with previous works (Plermjai et al., 2018; and Xiaohui et al., 2019). Table 4.3 and Fig. 4.4 show summary of crystal index analysis and X-ray diffraction pattern for sugarcane bagasse and extracted cellulose, respectively

Table 4.3. Crystal index analysis for sugarcane bagasse and extracted cellulose

Sample Analyzed	This Work (%)	Literatures (%)	Remark
Sugarcane Bagasse	47.11	44- 49.75	(Xiaohui et al , 2019)
Extracted Cellulose	77.62	71.2	(Plermjai et al , 2018)
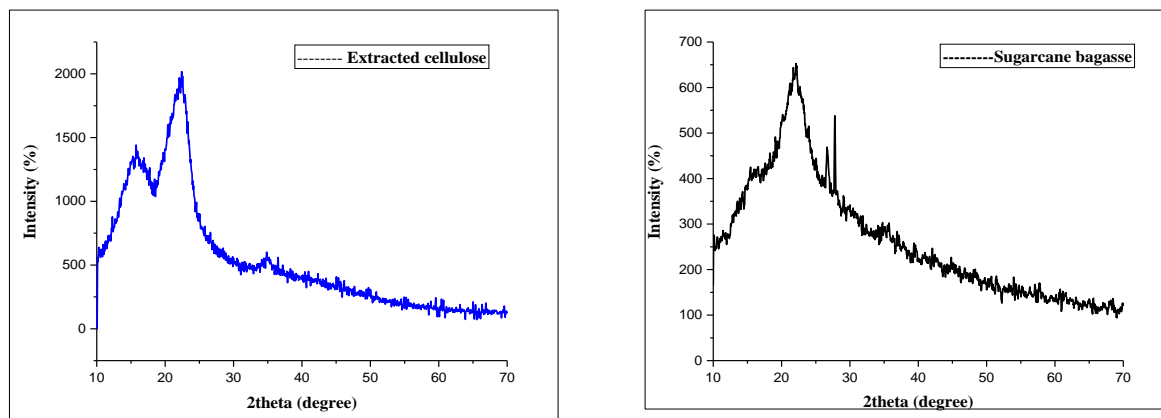
Figure 4.4. X-ray diffraction pattern of extracted cellulose and sugarcane bagasse

Crystal size for sugarcane bagasse and extracted cellulose was also determined from XRD data, 2.51 nm and 1.119 nm crystal size of extracted cellulose and sugarcane bagasse, respectively were obtained. Numerical value for Sherrer equation was derived from XRD data and shown in Table 4.4.

Table 4.4. Crystal size and average size analysis from XRD data

For Extracted Cellulose			For Sugarcane Bagasse		
2Theta	FWHM	Crystallites sizes (nm)	2Theta	FWHM	Crystallites Sizes (nm)
11.68	2.11552	3.774833447	15.82	6.25034	1.283226408
16	4.92	1.631289699	22	6.0184	1.345395472
22	8.97	0.902319367	34.78	11.4258	0.729076034
26.5	1.23	6.639112992			**Average size (nm)= 1.11**
27.85	6.09	1.344240547			
34.93	10.21723	0.815114851			lambda= 0.15406 nm (wavelength of the x-ray source)
		Average size (nm)= 2.58			k= 0.9 (Sherrer constant)
					B= FWHM (radians)
					Theta = peak positions (radians)
					D= (k*Lambda)/ (Beta*cos (Θ)) ,
					Sherrer Equation

4.3.4. Morphological image analysis for cellulose

The scanning electron microscopes (SEM) micrographs of extracted cellulose at different magnifications are depicted in Figure 4.5. The observed surface of the material was clean and a bit rougher, confirming removal of many non-fibrous materials, waxes and pectin scattered over the materials surface. It also confirms efficiency of the dewaxing process of the bagasse fiber via boiling in distilled water and acid hydrolysis using Sulfuric acid. The observed low diameter (maximum of 20 µm) of fibers indicates effectiveness of alkaline treatment method via sodium hydroxide for significant removal of hemicellulose and lignin (Nkosivele et al., 2018). In general, the sugarcane bagasse treatment method achieved removal of non-cellulosic component to promote reduction in diameter, clarity of the surface and uniformity of the shapes. It is well known that complete removal of the non-cellulosic materials promotes hydrogen bonding between adjacent glucose polymers. The hydrogen bonding is observed between third oxygen of one glucose unit and fifth oxygen of preceding glucose unit. Due to this, it has high viscosity in solution and tendency to crystalize than other polysaccharides, leading materials to a rigid bond (Taylor, 2006).
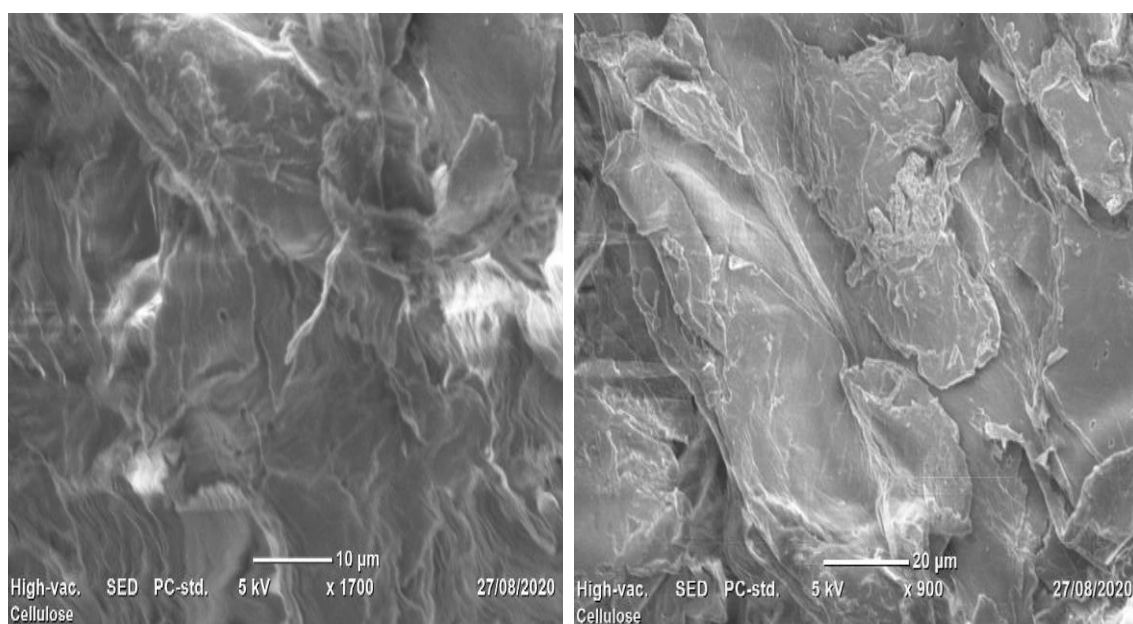

Figure 4.5. Scanning electron microscope image for cellulose at different magnification

4.4. Synthesis of bagasse based cellulose hydrogel

We successfully synthesized bagasse based cellulose hydrogel via multi-step processes for removal of methylene blue dye from wastewater. First, dissolution of cellulose via esterification reaction was performed for 24 hours by using phosphoric acid. A milky suspension of cellulose phosphate solution was appeared (Figure 4.6A), indicating a breakdown of inter- and intra-bonds (Xiong et al., 2013). Then, polyethylene glycol was added to the solution, viscosity of the solution was enhanced. Then, subsequent addition of citric acid resulted in a colorless and porous viscous solution with three dimensional matrixes (Figure 4.6B). This is a confirmation for effective cross-linking of individual polymer chains. The cross-linking promotes for additional bonds between molecules that improve strength of the polymers (Rojas & Azeved., 2011). After 24 hour homogenization of the solution competes gel was formed, (Figure 4.6C). The produced gel was oven dried and grinded as shown in Figure 4.6D & E. Similar procedure was previously reported by others (Aye et al., 2018; Demitri et al., 2008; Haque & Mondal, 2016; Karunakaran, 2016).
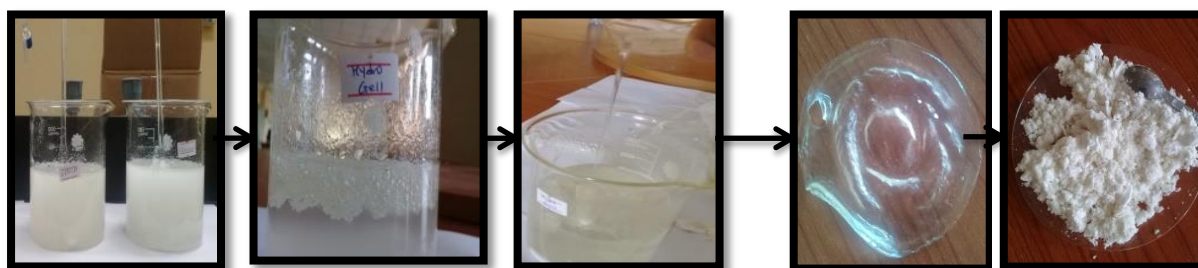
(A) Dissolution   **(B) Crosslinking**   **(C) Gel formation**   **(D) Dried gel**   **(E) Powder gel**

Figure 4.6. Result obtained from synthesis of bagasse based cellulose hydrogel

4.5. Characterazation of bagasse based cellulose hydrogel

4.5.1. Swelling measurement

The swelling ratio was measured as a function of time and the swelling ratio of hydrogel increased gradually with time at room temperatures (Table 4.7). After 3 days, the whole porosity of the hydrogel totally up took water and swelling equilibrium was reached (Table 4.5). The equilibrium swelling ratio of 75.44g/g was gained, showing that bagasse based cellulose hydrogel has high swelling ratio due to expansion of their chain networks in water.

This is achieved during interaction between the polymeric chain networks and water molecules via entanglement of the interpenetrated polymeric hydrogel networks such as capillary, osmotic and hydration force (Jayaramudin et al., 2019). The equilibrium swelling ratio of our study is much higher than that of the previously reported carboxymethyl cellulose based hydrogel (25.68 ± 0.18) g/g (Rahma et al., 2019). This is due to low degree of substitution in carboxymethylene cellulose (lower than degree of substitution of bagasse based cellulose) that affects substitution group added to the cellulose backbone. As degree of substitution increases the substitution group added to the cellulose backbone enhances polymeric chain that will be swollen. The result obtained in this work is in agreement with others (Fekete et al., 2017; Saeed, 2013; Tavera et al., 2018; Yang et al., 2012).

Table 4.5. Swelling study as function of time

Time (hours)	W_{sg} (g)	Swelling ratio (g/g)
0	0.5	1
0.5	11.391	21.78
2	19.628	38.26
6	26.106	51.22
24	30.149	59.29
48	33.673	66.35
72	38.274	75.06
96	38.275	75.55
120	38.277	75.44
144	38.277	75.44

4.5.2. Water retention capacity

The equilibrated hydrogel was removed from the distilled water and de-swelled at room temperature—a reverse of the swelling process known as water retention capacity. Water retention capability of the bagasse based cellulose hydrogel gradually decreased over time. After 24 hours, about 60.19% of water was kept by the hydrogel. The hydrogel retained about 21.56 % and 4.39% of the absorbed water in 72 and 96 hours, respectively (Figure 4.7).

Similar phenomenon has been reported in rice husk ash based super adsorbent hydrogel (Gharekhani et al., 2017). The ability of the hydrogels to retain significant amount of the water inside is related to their well-built network structures (Jayaramudin et al., 2019).
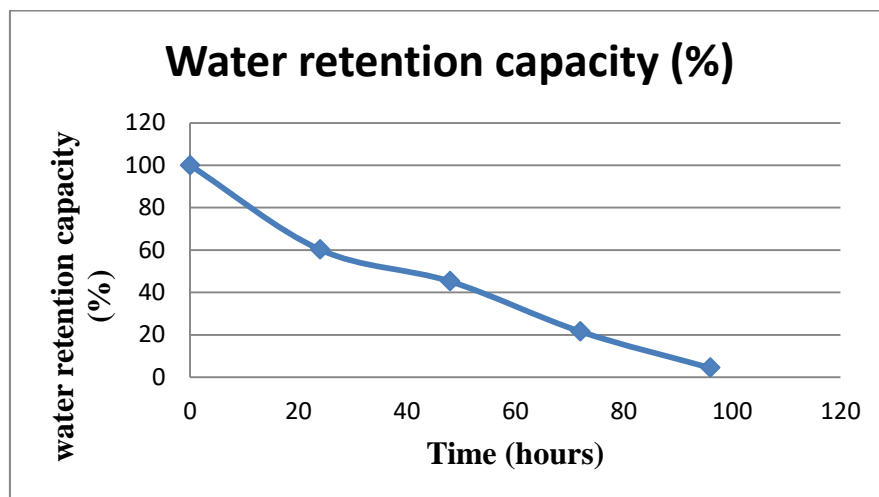
Figure 4.7. Water retention capacity of bagasse based cellulose hydrogel versus time

4.5.3. Biodegradability of hydrogel

The biodegradability of bagasse based cellulose hydrogels was evaluated by the soil test. Three pieces of hydrogel were buried into the soil. The hydrogels lost 40% of their original weight within the initial two days, mainly due to the evaporation of water from the hydrogels (Cui et al., 2019). More than 80% of hydrogels weight was lost after 14 days. After the hydrogels were buried into the soil for 26 days, only small fragments of the hydrogels could be found, and the weight loss reached up to 97%. The hydrogels were observed to be completely degraded after 28 days of burial in the soil. The biodegradation of the hydrogels was caused by the microorganisms in soil without specific enzyme or microorganism.

4.5.4. Gel content determination

After 48 hours of immersion in deionized water, the gel was removed by a metal sieve and constant weight of swollen dry gel was recorded. Oven drying method of the swollen gel was performed four times until gaining the constant weight. Finally, mean value of gel content calculated (Equation 3.12) and about 86.82% of gel content was obtained. This was due to formation of denser hydrogel in the polymer solution. Moreover, addition of polyethylene glycol also enhances the gel content of the hydrogel—a phenomenon reported earlier (Yacob & Hashim, 2015). Table 4.6 show the gel content analysis within four replicates.

Table 4.6. Experimental analysis for gel content determination

Run no	Weight of dry gel (g)	Gel content (%)
1	1.849	92.45
2	1.710	85.50
3	1.699	84.95
4	1.689	84.45
		Average = 86.82%

4.5.5. Thermal stability analysis

Thermogravimetric analysis (TGA) is a process in which materials are decomposed in heat, which cause bonds within the molecules to be broken. The TGA plays important role in determining thermal stability of the material (Astrini et al., 2012). Thermogravimetric curve in Figure 4.8 shows thermal stability of synthesized hydrogel. A thermal degradation of this adsorbent was completed in two stages. The first stage was water loss during heating. As a temperature increased from $(100 - 170)℃$, the sample lost 5% weight indicating loss of moistures present in the samples (via vaporization of water attached to polymer matrix in the sample) (Mohamed et al., 2015). Dehydration starts at temperature higher than $140℃$ (Zaman et al., 2019). The second stage was exothermic degradation of hydrogel polymeric chain. Here, the initial decomposition temperature of cellulose hydrogel was found to be $240.14℃$ (weight loss of 65.57%). Low decomposition temperature shows presence of –COOH groups which may be decomposed to CO_2 gas and crosslinking structure also play important role in thermal decomposition process. The same phenomena has been reported (Mohamed et al., 2015; Astrini et al, 2012). Further, loss of sample weight was monitored during the heating runs from $(280 - 421.31)℃$—sample weight was decreased from $(52 - 36.17)$ %. We also noticed the shifting of peak temperature of the main degradation step to lower temperature, indicating the thermal stability of the cross-linked cellulose hydrogel. This means cross-linking structure formed during esterification reaction play important role. The Polyethylene glycol (PEG) not only increases the total amount of -OH groups available for esterification reaction but also forms thermally stable structure (Costa et al., 2017; Palantöken et al., 2019; Geng, 2018; Kreitschitz & Gorb, 2020).
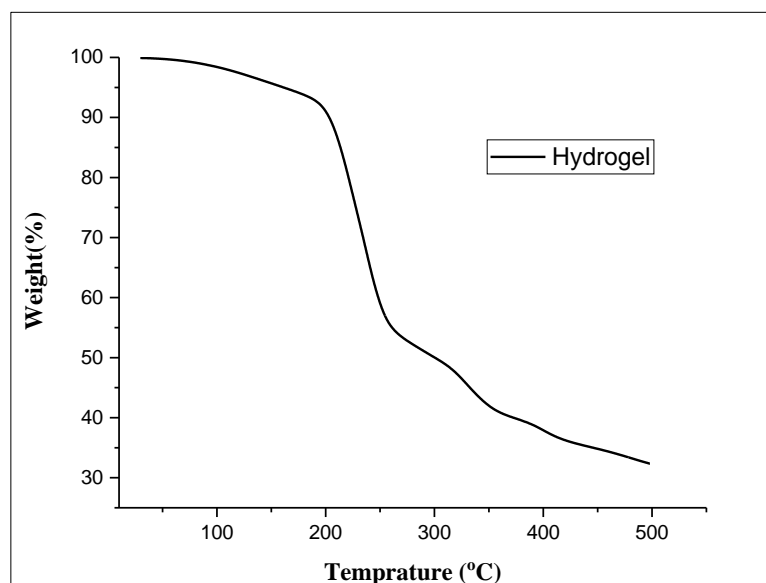
Figure 4.8. Thermogravimetric analysis of hydrogel

4.5.6. Morphological analysis of hydrogel

Morphological properties of hydrogel was analyzed by scanning electron microscopes (SEM) (Sethi, et al., 2020). The SEM reveals the porosity and nature of hydrogel structure (Nomura & Terwilliger, 2020). We observed micropores structures of hydrogel with regular three dimensions (Figure 4.9), confirming theory of hydrogel structure. Because of high water absorption capacity of the hydrogel pores, we noticed that moisture could affect or cover the pores to some extent. Furthermore, surface analysis of the composite hydrogel synthesized in this work also exhibited transparent character at a high magnification(× 1700)(Figure 4.9). The observed regular shape also confirms purity of the synthesized hydrogel (Rahman, 2017). The absence of granular structure of raw cellulose or in other words, totally cross-linked, uniform surface morphology achieved was due to presence of Polyethylene glycol (PEG). Our result agrees with earlier studies (Rodrigues et al., 2016; Lopez-sanchez et al., 2017).
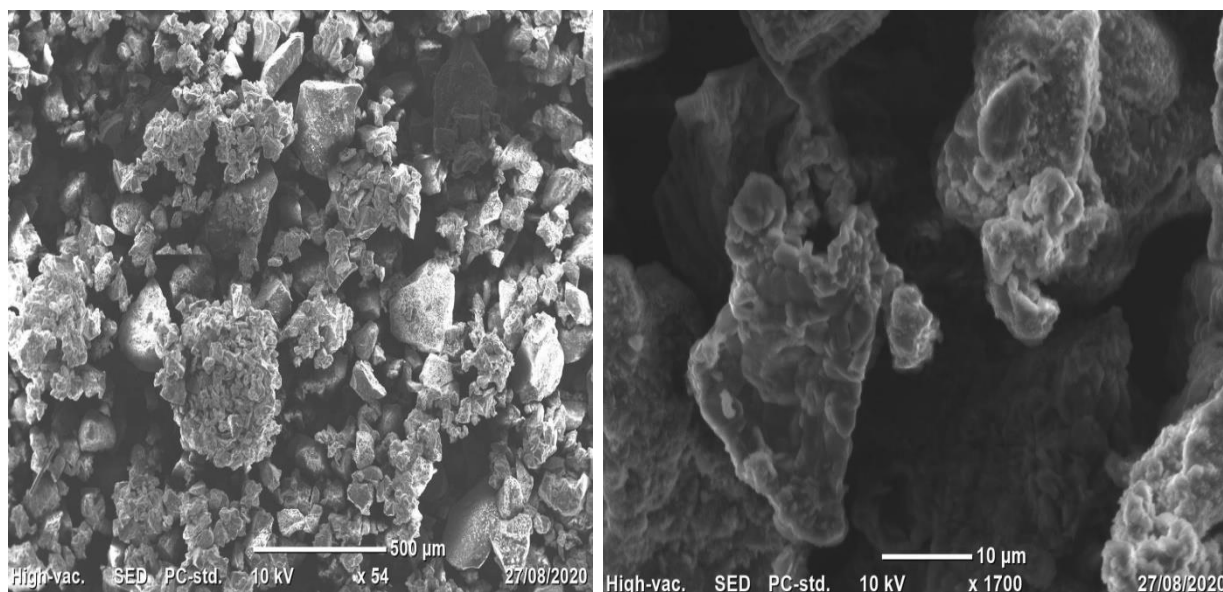
Figure 4.9. Scanning electron microscope image of **c**ellulose hydrogel at different magnification

4.5.7. X-Ray diffractometer analysis of hydrogel

When scanned with XRD, our cellulose hydrogel had one broad diffraction peak between 20°and 30° (Figure 4.10). This merging may be due to the hydrogen bonding between the two cross-linked matrices (Demitri et al., 2008). The crystallinity index (CI) reduction for hydrogel was also observed clearly. Area of crystalline peak (6902.41) and total area (9939.23) were calculated and crystallinity index was reduced from 77.62% (for cellulose) to 69.45 (for the hydrogel). The diffraction peak found around 15℃ in cellulose was totally disappeared, which is a reason behind the CI reduction and removal of cellulose crystallinity peak. This indicates addition of PEG during esterification reaction may affect cellulose crystallinity. Mohamed et al. also observed similar phenomenon (Mohamed et al., 2015). The crystalline regions of cellulose are expected to be less accessible to water molecules than the amorphous regions. Therefore, an enhanced swelling capacity of the hydrogels during crystallinity reduction, which has been described previously (Yang et al., 2020), is also confirmation for the expected good removal efficiency of methylene blue dye.
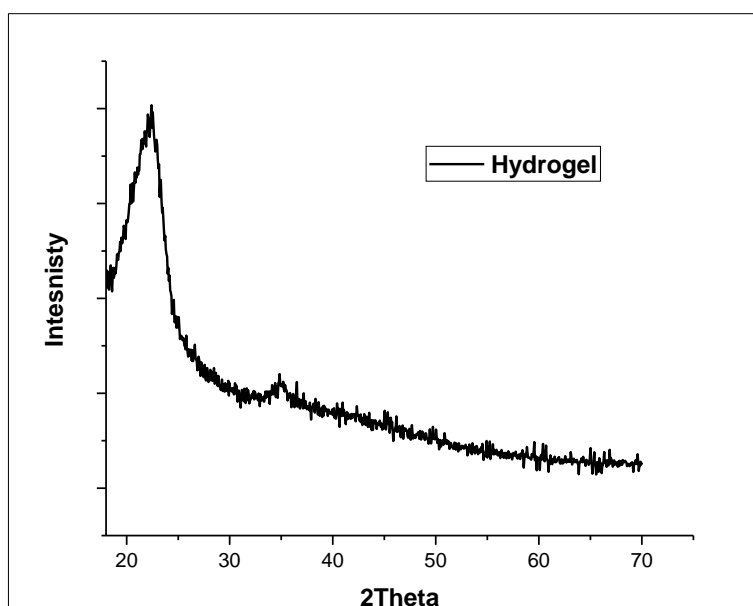
Figure 4.10. X-Ray Diffractometer graph analysis for hydrogel

4.5.8. Dynamic Light Scattering Analysis (Particle Size)

Particle size distribution, average particle size and polydispersity index analysis of the sample for bagasse based cellulose hydrogel was performed by latest particle size analyzer equipment called dynamic light scattering (ZETASIZER, NANO SERIES HT (ZE3600)). As shown in Figure 4.11, particle size of the cellulose hydrogel was fallen in range of (50-150) nm and mode of the variable was observed at one peak point only (i.e. Uni-modal distribution). Uni-modal distribution is indication of single value being particularly dominant among others (Liu et al., 2019). Z-average suggested by instrument was 101.075 nm (Table 4.7). It's obvious that Z-average is an intensity-based overall average size based on specific fit to the raw correlation function data, the fitting is also called cumulant method and can be thought of as force fitting the result to simple Gaussian distribution (Bhattacharjee., 2016). Furthermore, Z-average (101.075 nm) in this work shows smallness of the particle size, a confirmation of a nano-size of the bagasse based cellulose hydrogel.

Table 4.7. DLS term value analysis

Z-average (d.nm); 101.075		Size (d.nm)	Intensity (%)
	Peak 1:	83.4	99.09
PDI: 0.059	Peak 2:	0.00	00.0
Result quality: Good	Peak 3:	0.00	00.00

Small polydispersity index (PDI) suggested by instrument in this work (0.059) (Table 4.7) is an indication of width of the overall distribution, assuming a single mean and perfectly uniform sample. The numerical value of PDI ranging from 0 to 1 is acceptable. Our result is in agreement with literature that material with PDI < 0.1 corresponds to mono-disperse, has uni-modal peak and good uniformity of nanomaterial (Lawler et al., 2013).
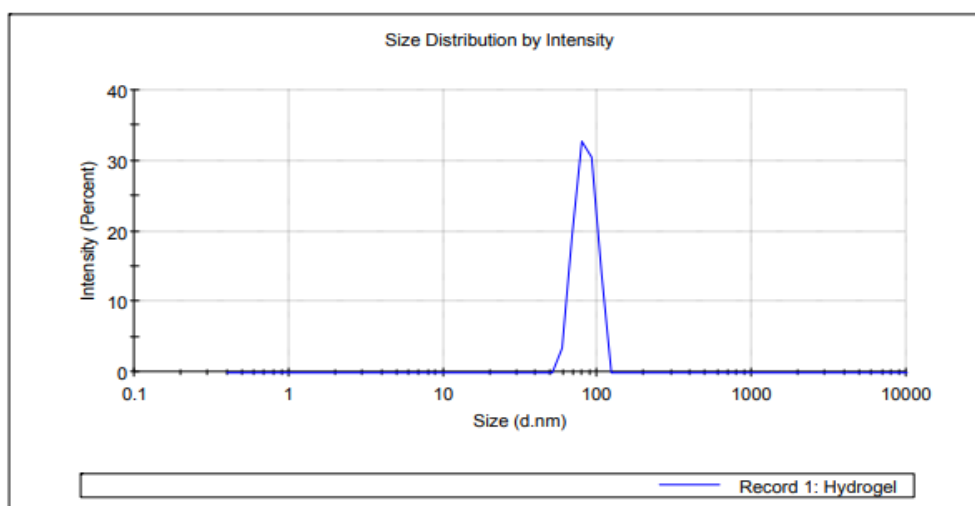
Figure 4.11. Particles size analysis via DLS

4.5.9. Functional group analysis

FTIR spectrum for bagasse based cellulose hydrogel in this studies is given in Figure 4.12 below indicating main absorbency region in the range of (800-3300) cm^{-1}. According to (Zaman et al., 2019) peak between (3300-3500) cm^{-1} displayed for O-H stretching vibration bond. CH_2 stretching vibration bond in methyl, methylene and methane is formed at (2916-2561.15) cm^{-1}. Peak formed at 1727.94 cm^{-1} represents C=O stretching vibration of aldehyde group.

Furthermore, increasing of stretching of vibration band shows ester bond formation during esterification of cellulose and citric acid (Dutta et al., 2019). The peak near 1403.95cm^{-1} was the shear vibration absorption peak of CH_2, which is the characteristics peak of cellulose structures (Deng et al, 2020). Additionally the vibration peak formed at 1218.82 cm^{-1} represents C-O ester bonds. The peak at 1064.54 cm^{-1} is C–O absorption peak, and 894.8234 cm^{-1} is the vibrational frequency of C-H group, i.e. β-glycoside bond. The degradation of hydrogel sample recorded in different peak showed an increase in transmittance (or decreased absorbance) and shifting of some of the peaks in FTIR spectra. The changes in FTIR spectra were observed due to initial cleavage of cross-linked networks between different polymer chains (Química et al., 2015; Mohamed et al., 2015; Damiri et al., 2020 and Jia et al., 2017).
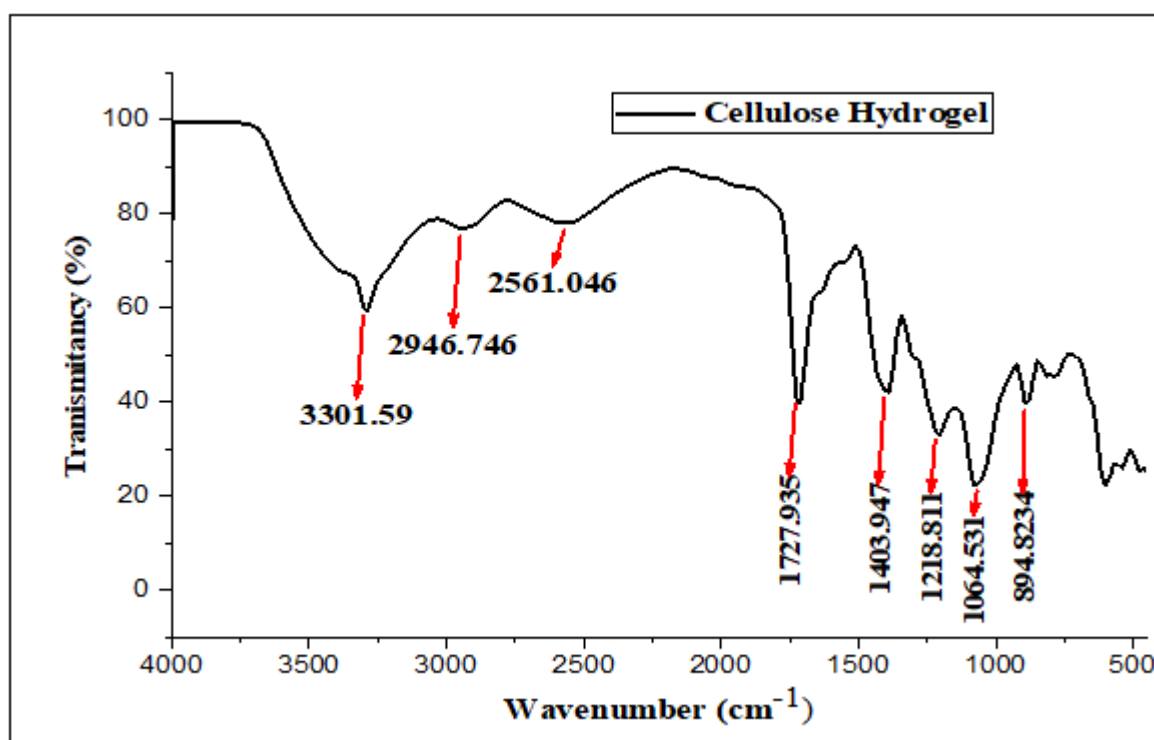
Figure 4.12. Functional group analysis for hydrogel

4.6. Statical analysis of expermental results

4.6.1. Experimental data reports

The correlation between removal efficiency of hydrogel and process variable was analyzed via response surface methodology using central composite design (CCD) modeling technique. Table 4.8 shows the experimental data reports analyzed form design expert software.

Table 4.8. The value of experimental data and predicted data at selected parameter values

Run	Adsorbent Dose (g/L)	Contact Time (minute)	Concentration		Removal Efficiency (%)	
			Initial	Final	Actual	Predicted
1	5	60	10	0.201	97.99	98.48
2	5	60	20	0.602	96.99	96.14
3	3.5	19.7731	15	1.995	86.74	86.16
4	3.5	45	6.59104	0.083	98.75	97.50
5	3.5	45	23.409	2.891	87.61	88.62
6	0.977311	45	15	2.102	85.99	85.68
7	2	30	10	1.310	86.92	87.94
8	3.5	45	15	0.692	95.36	94.57
9	3.5	45	15	0.953	93.97	94.57
10	3.5	70.2269	15	0.689	95.34	95.69
11	6.02269	45	15	0.221	98.78	98.82
12	3.5	45	15	0.533	96.36	94.57
13	2	30	20	3.991	80.01	79.70
14	3.5	45	15	0.719	95.21	94.57
15	5	30	20	1.409	92.92	92.83
16	3.5	45	15	0.945	93.74	94.57
17	5	60	10	0.460	95.41	95.90
18	3.5	45	15	1.093	92.71	94.57
19	2	60	10	0.421	95.72	95.97
20	2	60	20	2.221	88.79	88.47

4.6.2. Fit summery for suggested model

Quadratic model was suggested by design expert software for response removal efficiency and cubic model was aliased in this work. If we select model with more terms than the number of unique points in the design, some terms will be aliased. An aliased model should not be used for prediction of a response. We may be able to find an adequate model without aliased terms. Model analysis in this work suggested adequate quadratic model which confirms with design expert theory. The fit summary analysis of the suggested model is shown in Table 4.9.

Table 4.9. Fit Summery for suggested model

Source	Sequential p-value	Lack of Fit p-value	Adjusted R^2	Predicted R^2	
Linear	< 0.0001	0.0902	0.8165	0.7555	
2FI	0.0934	0.1419	0.8596	0.7512	
Quadratic	**0.0063**	**0.6795**	**0.9441**	**0.8858**	**Suggested**
Cubic	0.5065	0.7883	0.9424	0.9109	Aliased

4.6.3. Analysis of variance (ANOVA)

The significance and adequacy of the model terms were evaluated by p-value, F-value and lack of fit. The obtained F-value of 36.65 ($p<0.0001$) indicates that the quadratic model was significant and the chance the F-value could be due to noise was only $<0.01\%$. According to the theory of ANOVA, a coefficient term with p-value less than 0.0500 indicates statistical significance of model terms. Based on this theory, model with linear terms (A, B, C) and model with interaction terms (AB, AC, A^2 and B^2) were statistically significant, while model terms with p-values greater than 0.05 are statistically insignificant to the response. Lack of fit is also another parameter that confirms the adequacy of model. The p-value and F-value of lack of fit observed from ANOVA were 0.6795 and of 0.6441, indicating statistical insignificance. The lack of fit of (F-value = 0.6441; p=0.6795) implies the lack of fit was not statistically significant relative to pure error (Table 4.10). There is a 67.95 % chance that lack of fit of this large F-value could occur due to noise; meaning signal to noise ratio of 67.95% indicates an adequate signal. Therefore, a non-significant property of lack of fit remarks adequacy of the model.

Table 4.10. Analysis of variance for suggested quadratic model (ANOVA)

Source	Sum of Squares	df	Mean Square	F-value	p-value	
Model	474.27	9	52.70	36.65	< 0.0001	**Significant**
A-Adsorbent Dosage	208.25	1	208.25	144.84	< 0.0001	
B-contact time	109.63	1	109.63	76.25	< 0.0001	
C-Initial Concentration of dye	95.24	1	95.24	66.24	< 0.0001	
AB	14.93	1	14.93	10.39	0.0091	
AC	13.39	1	13.39	9.31	0.0122	
BC	0.2701	1	0.2701	0.1879	0.6739	
A²	9.64	1	9.64	6.71	0.0270	
B²	23.91	1	23.91	16.63	0.0022	
C²	4.07	1	4.07	2.83	0.1233	
Residual	14.38	10	1.44			
Lack of Fit	5.63	5	1.13	0.6441	0.6795	**Not Significant**
Pure Error	8.75	5	1.75			
Cor Total	488.65	19				

4.6.4. Model adequacy analysis

The adequacy of the established model was further supported by high value of coefficient determination terms: R^2 value of 0.9706, predicted R^2 value of 0.8858 and adjusted R^2 value of 0.9441 (Table 4.11), which were quantitatively evaluated the correlation between the actual experimental data and predicted one. This implies that the established quadratic model explained 97.06 % of variations in the experimental results. In other words, actual values from experimental data were much closer to the predicted one. The very small difference (less than 0.2) of adjusted R^2 and predicted R^2 supported the adequacy of the model. Further, the predicted R^2 (0.8858) is in reasonable agreement with the adjusted R^2.

Moreover, regression coefficient (R^2) value between one and zero validates that the regression line perfectly fit the data and high correlation between the actual experimental and predicted data. Adeq precision measures the signal to noise ratio and a ratio greater than 4 is desirable. The obtained ratio of 22.5433 in this analysis (Table 4.11) indicates an adequate signal. This model can be used to navigate the design space. Low values of coefficient of variation demonstrate reliability and good precision of the experiments since it is the error expressed as a percentage of the mean. The lower value of the coefficient of variation (CV = 1.29%) observed in our data (Table 4.11) indicates the better precision and reliability of the experiments. The CV, as a ratio of the standard error of the estimate to the mean value of the observed response, is the measure of reproducibility of the model and as the general rule, a model can be considered reasonably reproducible. Furthermore, the values of standard deviation (SD) offered for the sound predictive ability of the generated quadratic model.

Table 4.11. Fit statics for suggested quadratic model

Standard Deviation	1.20	**R^2**	0.9706
Mean	92.76	**Adjusted R^2**	0.9441
Coefficient Variation (C.V) (%)	1.29	**Predicted R^2**	0.8858
		Adeq Precision	22.5433

4.6.5. Development of model equation

Polynomial regression analysis for suggested model term was good for explaining the interaction between factors with the response variables. Quadratic equation was suggested for interaction explanation in ANOVA and model equation was developed based on this analysis for response methylene blue dye removal. Model development plays a crucial role to predict response change (change in removal efficiency of hydrogel) at a given operating parameter range. The intercept of coded factors is in the center of design space and equation developed in terms of coded factor is also important to analyze relative influence of process variable by comparing the variable coefficient. The final equation of the regression model in terms of coded factors is represented by Equation 4.1.

Removal Efficiency $(\%) = +94.57 + 3.90*A + 2.83*B - 2.64*C - 1.37*AB + 1.29*AC + 0.1837*BC - 0.8179A^2 - 1.29*B^2 - 0.5316*C^2$ ………………..… (4.1)

Where: $A = $ Adsorbent Dosage , $B = $ Contac time, and $C = $ initial concentration of dye

The positive sign in the regression modal indicates that factor mentioned in the model has positive effects on the removal efficiency of the hydrogel, meaning the factor was significantly affecting removal efficiently or increasing response of the design of the factor for an increase in the response of the design and vice versa for negative sign observed in the model (decreasing response of the experimental design removal efficiency of the hydrogel).

4.6.6. Diagnostic plot for response design assessment

A diagnostic plot showing the actual versus predicted efficiency of the hydrogel is depicted in Figure 4.13. A straight linear line observed indicates a closeness of the predicted and actual removal efficiency of the hydrogel, a validation that actual values were fitted on linear straight line which explains fitting of the response surface model to experimental methylene blue dye removal efficiency of the hydrogel. It was further supported by high correlation coefficient value ($R^2 = 0.9706$). In general, the result implies that experimental data was in reasonable agreement with model, hence the model equation developed to assess methylene blue dye removal efficiency of the hydrogel was highly predictive at a given range values of process variables.
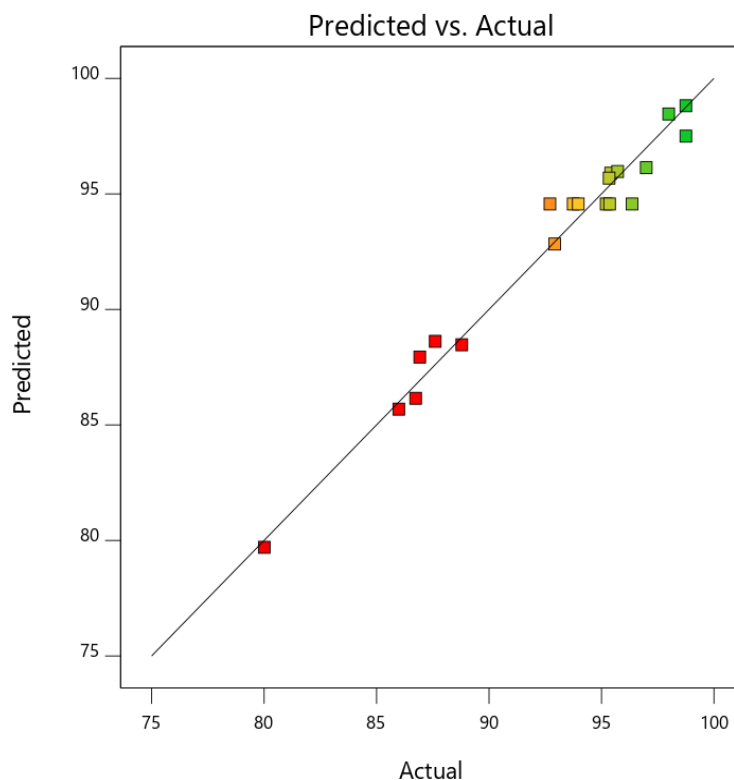
Figure 4.13. Diagnostic plot showing actual verses predicted

Residual, the difference between actual and predicted values, is used to check goodness of data fit on regression line of the developed model and indicates normal probability distribution. In Figure 4.14, all the residuals were fitted on linear line, indicating that normal distribution of residuals of each point were on linear regression line. No abnormality was observed, hence the data was well fitted, it is possible to predict the response variable under a given range of process variables and the quadratic polynomial model satisfied the analysis of the assumptions of variance. Furthermore, normal distribution of the residuals confirmed that the residuals were independent of each other and the error variances are homogeneous.
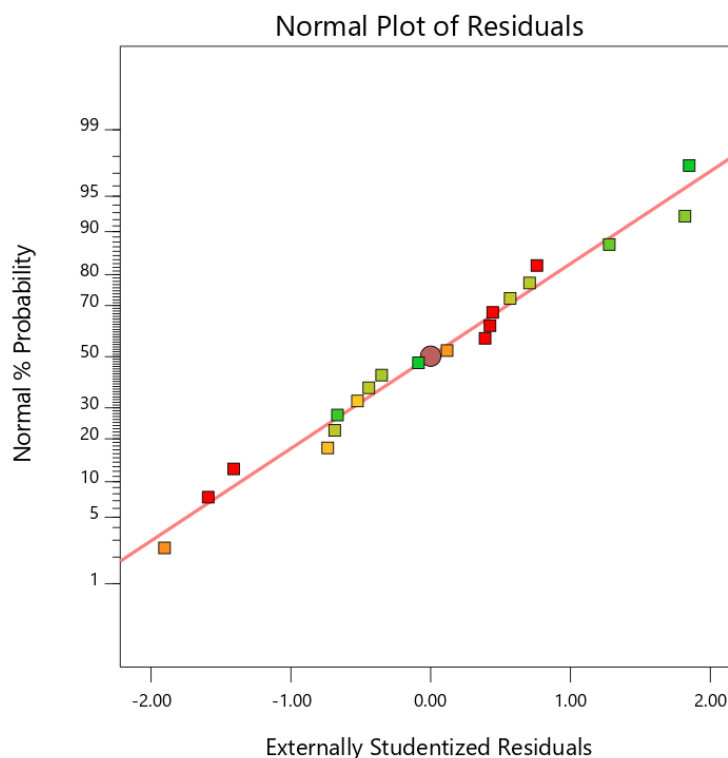
Figure 4.14. Normal plots of residual

All the residuals were fitted to a linear regression line, indicating normal distribution of the residual. Structure less shape residual versus predicted diagnostic plot is a confirmation for correction of model suggested and achievement for assumption satisfaction. Accordingly, we found a scattered structure less shape when the residual values were plotted against predicted values of removal efficiency of the hydrogel (Figure 4.15), justifying the assumption of constant variance testing and no necessity of any alteration to minimize personal error.

Figure 4.15. Plot of predicted versus residuals for the yield

4.7. Effect of model parameteres on removal efficency of hydrogel

4.7.1. Effect of adsorbent dosage

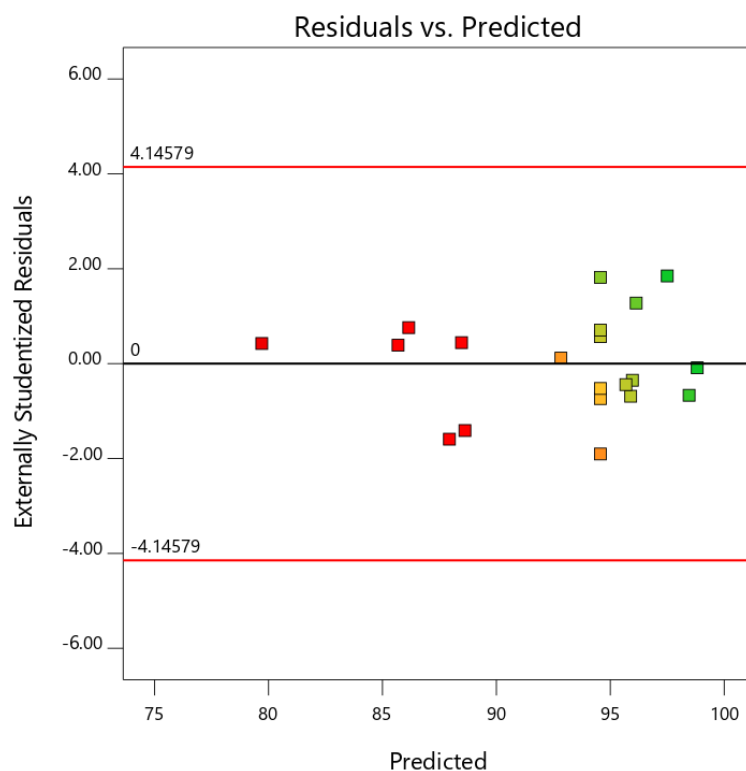The effect of the adsorbent dosage on methylene blue dye removal from wastewater was found to be dependent on the content (Figure 4.16). The content of hydrogel from $(2 - 5)\,\text{g/L}$ significantly affects the color removal of the dye solution. As the content of the hydrogel increases slightly, the removal efficiency also approaches to the maximum point. It's obvious that cellulose based hydrogel absorb preferentially water and later adsorb the solute molecules, which are retained by the electrostatic forces. Accordingly, higher content of hydrogel contents allows absorption of larger water amount to provide a dye-rich environment due to presence of large surface area leading to large active sites (adsorption sites) to uptake solute molecules, methylene blue dye. In agreement with our result, one previous study (Zhou et al., 2006) also reported maximum removal efficiency of hydrogel supported on modified polysaccharide towards the higher adsorbent dosage $(1.5 - 5)\,\text{g/L}$.
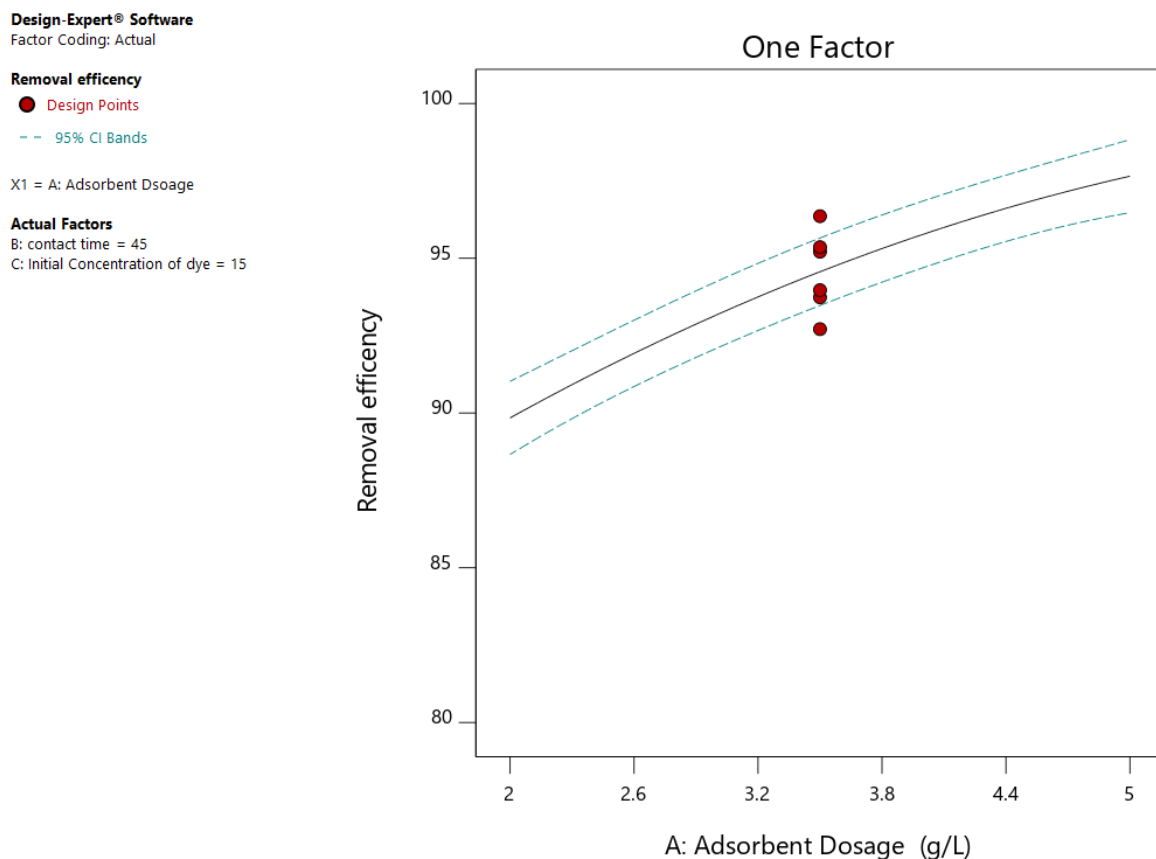
Figure 4.16. Plot expression showing significance effect of adsorbent dosage

4.7.2. Effect of initial concentration of methylene blue

Removal efficiency of bagasse based cellulose hydrogel was also found to be affected by initial concentration of methylene blue dye (Figure 4.17). Decreasing removal efficiency was observed during increments in concentration of the pollutant from $(10 - 20)\,\text{mg/L}$. The reason behind low decolorization effect of hydrogel towards the increasing pollutant concentration is that an increase in adsorbate concentration occupies and reduces adsorption sites available on hydrogel by making saturation phase. Similar phenomenon has been reported (Zhou et al., 2011).
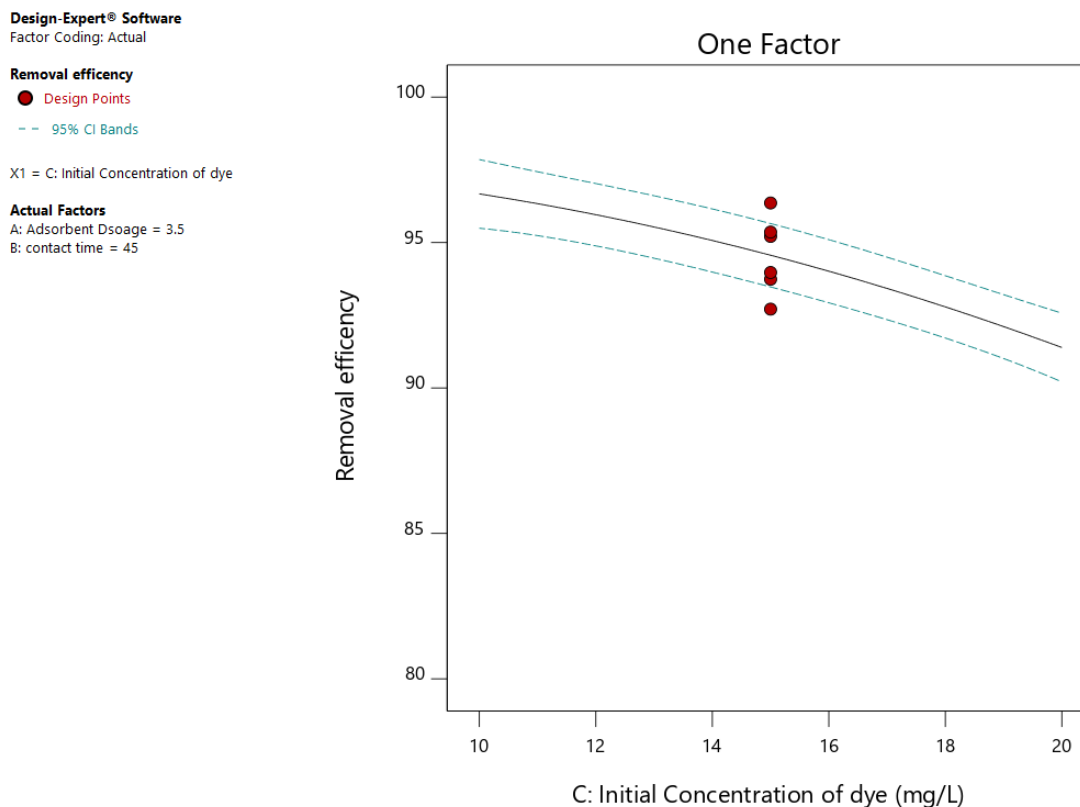
Figure 4.17. Plot expression showing effect of initial concentration of methylene blue dye

4.7.3. Effect of Contact Time

Contact time was another factor that clearly affected methylene blue dye removal efficiency of the hydrogel. Adsorption percentage was increasing with increment of contact time until equilibrium removal efficiency was reached. According to Venkatesham et al. (Venkatesham et al., 2018) the ability of hydrogel to uptake solute molecule as well as attraction force between methylene blue dye and active site of bagasse based cellulose hydrogel increase as contact time increases. Figure 4.18 below show graphical description of significant effect of contact time on the removal efficiency of bagasse based cellulose hydrogel.
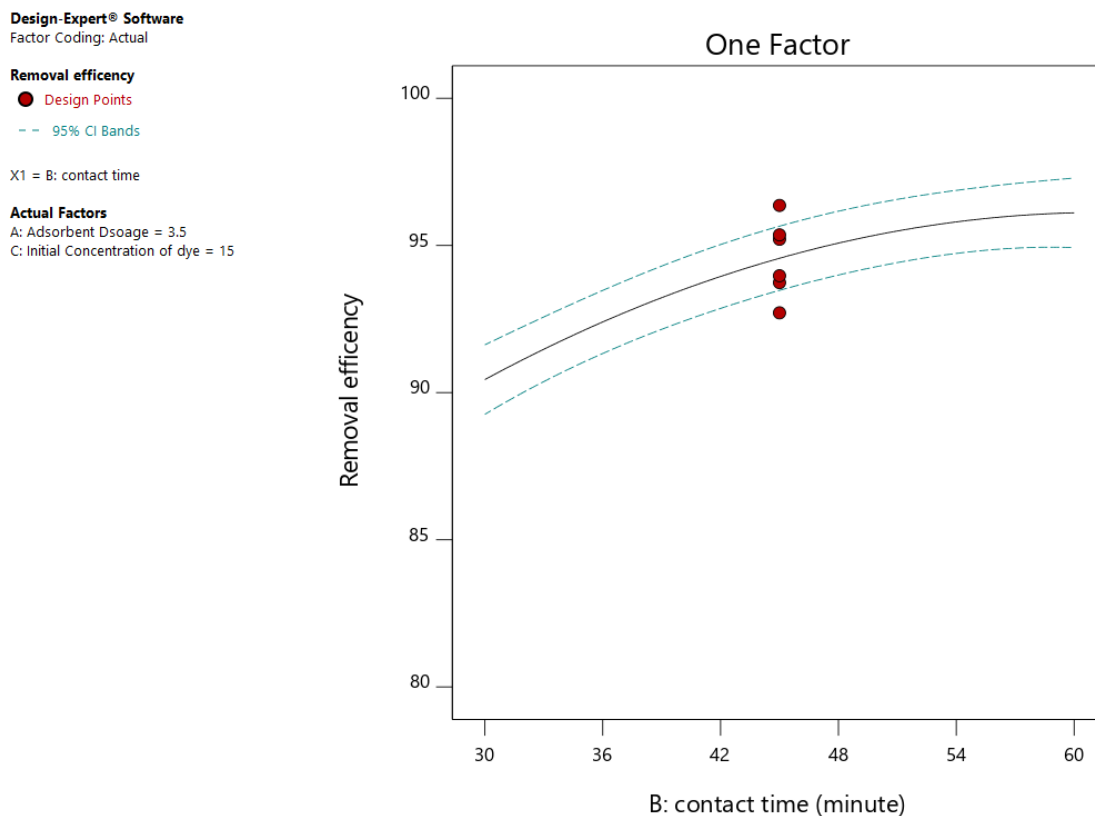
Figure 4.18. Plot expression showing significant effect of contact time

4.8. Interaction effect of process variable in removal efficiency of hydrogel

Operating parameters considered in this work showed highly significant interaction effects on removal efficiency of bagasse cellulose based hydrogel. High significant interaction effect was observed between adsorbent dosage and contact time and initial concentration of methylene blue dye and adsorbent dosage.

4.8.1. Interaction effect of adsorbent dosage and contact time

Interaction effect of adsorbent dosage to contact time is represented by 3D surface plot in Figure 4.19. At a constant adsorbent dosage of 3.5 g/L, contact time of 45 minutes and constant third factor initial methylene blue dye concentration of 15 mg/L, the interaction effect of adsorbent dosage and contact time was observed. The lowest value of adsorbent dosage (2 g/L) to the highest value of contact time (60 minutes) and the lowest value of contact time (30 minutes) to the highest value of adsorbent dosage (5 g/L) resulted in 95.72% and 95.41% removal efficiency, respectively.

The result demonstrated that effect of the lowest value of adsorbent dosage is dependent on the effect of the highest value of contact time and vice versa, validating for significant interaction effect between two independent variables. Further, the lowest value of adsorbent dosage (2 g/L) to contact time (30 minutes) provided 86.92% of removal efficiency and the highest value of adsorbent dosage (5 g/L) to contact time (60 minutes) provided 97.99% of removal efficiency, demonstrating that increasing adsorbent dosage and contact time resulted in increasing removal efficiency of hydrogel. Further, increases from its center point resulted in slightly reduction of removal efficiency of the hydrogel due to overlapping of the two parameters at the center point. This is indicated by negative sign in the model equation, Equation 4.1. Since increasing contact time until (60 minutes) and adsorbent dosage to (5 g/L) lead to high removal efficiency of the hydrogel, the independent factors were demonstrated statistically significant effect on removal efficiency of the hydrogel as supported by p value in the ANOVA ($p < 0.0001$). This is due to increment of adsorption active site during increments of adsorbent dosage and increment of electrostatic force between adsorbent active site and solute molecules when time increasing (Zhou et al., 2011).
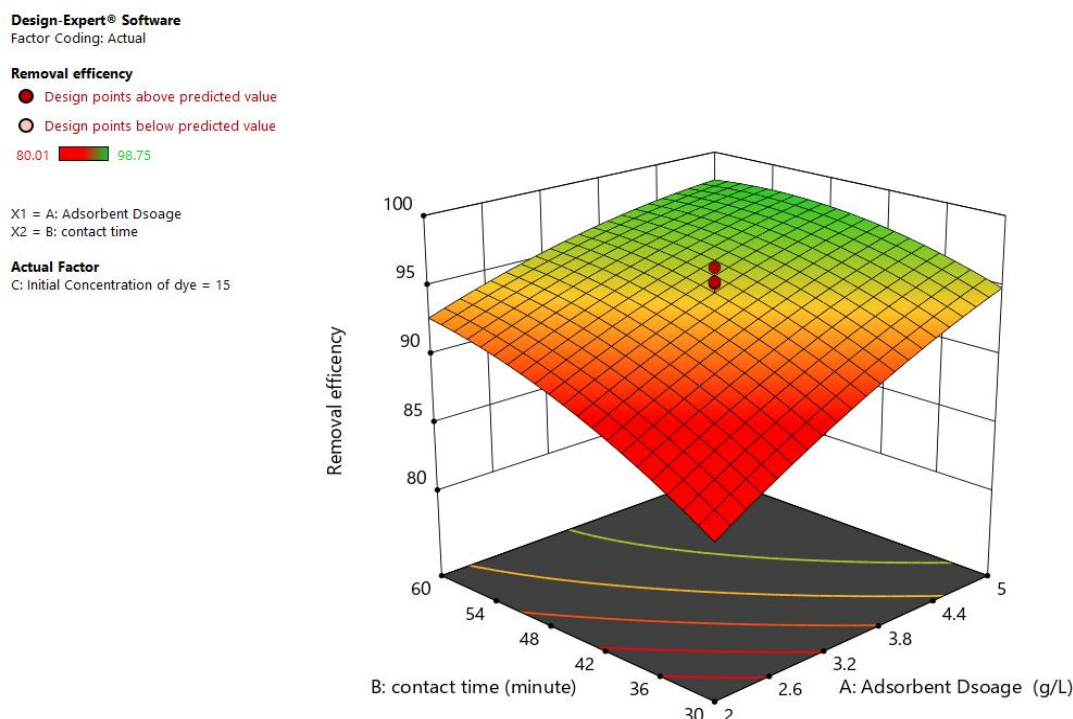

Figure 4.19. 3D surface plot for the interaction effect of adsorbent dosage and contact time

4.8.2. Interaction effect of adsorbent dosage and initial concentration of methylene blue

 Interaction effect of adsorbent dosage to initial concentration of methylene blue dye was represented by 3D surface plot in Figure 4.20. At constant adsorbent dosage of 3.5 g/L, initial methylene blue dye concentration of 15 mg/L and constant third factor contact time of 45 minutes, the interaction effect of the adsorbent dosage and initial concentration of methylene blue dye was observed. The highest value of adsorbent dosage (5 g/L) to lowest value of initial concentration of methylene blue dye (10 mg/L) provide 95.41% of removal efficiency of the hydrogel and the highest value of adsorbent dosage (5 g/L) to highest value of initial concentration of methylene blue dye (20 mg/L) provide 92.99% of removal efficiency of the hydrogel. Further at constant center point of other factors, lowest initial concentrations of methylene blue dye provided 95.36% removal efficiency of the hydrogel. The result demonstrated that increasing adsorbent dosage and decreasing the initial concentration of methylene blue dye resulted in increasing removal efficiency of hydrogel and the interaction of both factor is statically significant as supported by lower P value (p<0.0001).
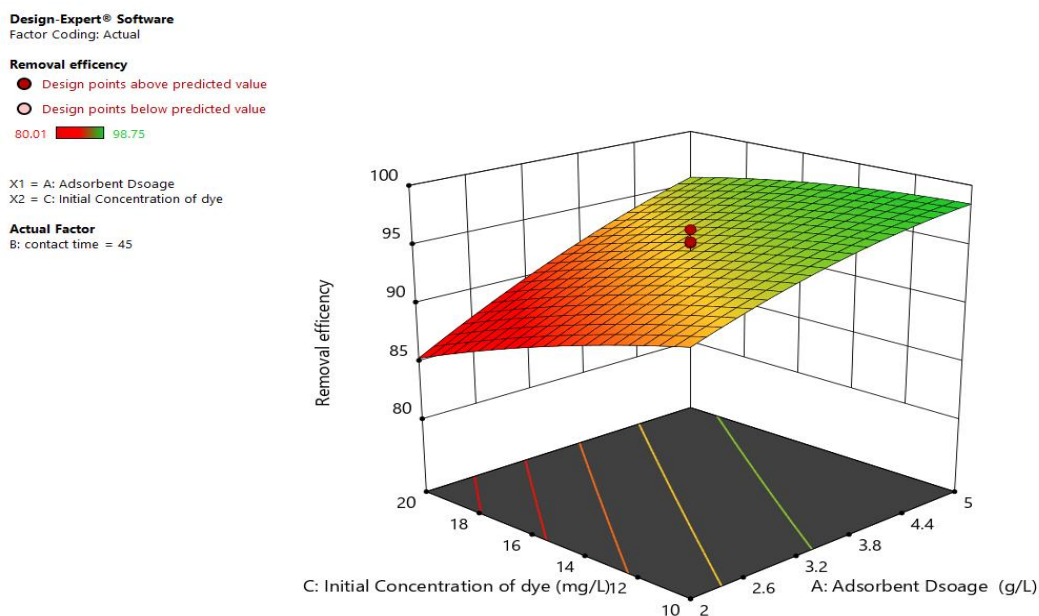

Figure 4.20. 3D surface plot for the interaction effect of adsorbent dosage and initial concentration of methylene blue dye

In general, our ANOVA analysis result explains that optimum methylene blue dye removal efficiency of the hydrogel is obtained at a combination of high amount of hydrogel content, average contact time and low initial concentration of the dye. Further adsorbent dosage had high effect than other model parameter is this work as supported by high F in the value ANOVA (F =144.84).

4.9. Numerical optimization

The targeted objective of this study was to maximize methylene blue dye removal efficiency of bagasse based cellulose hydrogel. The optimum conditions of considered operating parameters were determined by using numerical optimization feature of design expert software. The software utilizes combinations factors that satisfy the requirements for response design space and each of the factors. All the factors and response with their constraints for optimization criteria are listed in Table 4.12 below. The ultimate goal of response was maximizing methylene blue dye removal efficiency of hydrogel within the given range values of process variables. The optimum conditions obtained were then evaluated by the composite desirability, which has a value from 0 to 1.

Table 4.12. Ultimate goal of response and constraints of process variables for optimization

Process variables	Ultimate goal	Lower limit	Upper limit
A-Adsorbent dosage (g/L)	Is in range	2	5
B-Contact Time (minute)	Is in range	30	60
C-initial concentration of methylene blue dye (mg/L)	Is range	10	20
Removal Efficiency (%)	Maximize	80.05	98.76

Optimal process variables and maximum removal efficeny of the hydrogel used for model validation was also selected by design expert software. Table 4.13 shows selected optimum adsorbent dosage (4.97 g/L), contact time (51.97 minutes), and initial concentration of dye (10.32 mg/L) that resulted in 98.76% of removal efficeny. The highest composite desirability of 1.0 at optimized process condition was obtained from design expert software. This indicates that the degree of satisfaction of the optimum conditions for the ultimate goal of response was successfully attained.

Table 4.13. Selected optimum condition by response surface method

Number	Adsorbent Dosage (g/L)	Contact Time (minute)	Initial concentration of methylene blue dye (mg/L)	Removal Efficiency (%)	Desirabi lity (%)	
1	4.97	51.97	10.32	98.76	1.00	Selected
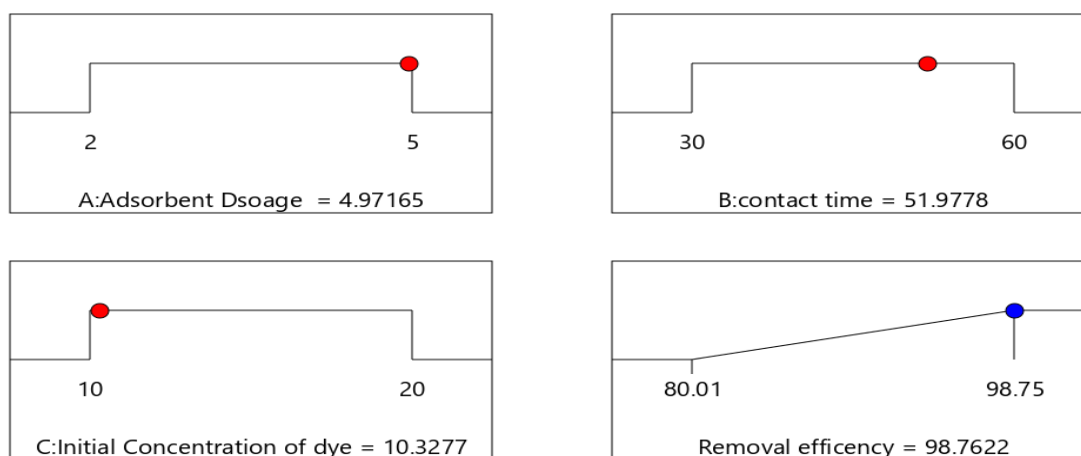
Figure 4.21. Optimum conditions in ramp style

4.9.1. Model Validation

Triplicate experiment for model validation was carried out based on optimum process variables selected by design experiment software (Table 4.13). Three times replication with removal efficiency of 98.63, 98.65, and 98.66 % were recorded. The average value of triplicates of removal efficiency of hydrogel was 98.65%, while the software result was 98.76%. Small deviation (0.1%) in between software and experimental result indicates model is well fitted with experimental data. Therefore, this study shows that bagasse based cellulose hydrogel can definitely enhance methylene blue dye removal efficiency of the hydrogel.

4.9.2. Comparison of hydrogel with other adsorbent

Table 4.14. Comparison of hydrogel with other adsorbent at optimum condition

Adsorbent	Optimum process variables	Efficiency (%)	References
Graphene oxide/hydrogel composite based hydrogel	Dose 5g/L, PH7.41, concentration 20mg/L, time 60 minutes	77.89	(Atyaa1 & Al, 2019)
Chitosan based hydrogel	Dose 2.5g/L, concentration 12mg/L, time 180 minutes	85.09	(Venkatesham et al., 2018)
Activated sawdust and eggshell bio sorbent	Dose 2.5g/L, concentration 20mg/L, time 30 minutes	76.47	(M & Neethu, 2017)
Activated carbon prepared from biowaste precursor	Dose 20g/L, concentration 50mg/L, time, 90 minutes	84.00	(Singh, Sidhu, & Singh, 2017)
Cotton cellulose based hydrogel	Dose 5g/L, PH7.41, concentration 20mg/L, time 60 minutes Dose 3.99g/L, PH8,concentration 5mg/L, time 180 minutes	98.00 96.47	(Zhou et al., 2011)
Super adsorbent hydrogel supported on modified polysaccharide	Dose 20g/L, concentration 50mg/L, time, 50 minutes	98.00	(Zhou et al., 2006)
Bagasse based cellulose hydrogel	**Dose 4.97 g/L, concentration 10.89 mg/L, time, 51.97 minutes.**	**98.76**	**This work**

4.10. Reusability of bagasse based cellulose hydrogel

To verify the reusability of the bagasse cellulose based hydrogel, the adsorbent was recycled five times by using optimum process variable suggested by design expert software.

Over the five rounds of recycling, the removal efficiency of the hydrogel showed declining tendency. After five successive cycles, the efficiency was declined from 98.76% to 70.63% (Figure 4.22). This is due to active site occupation by methylene blue dye ion and blockage by additional pollutants
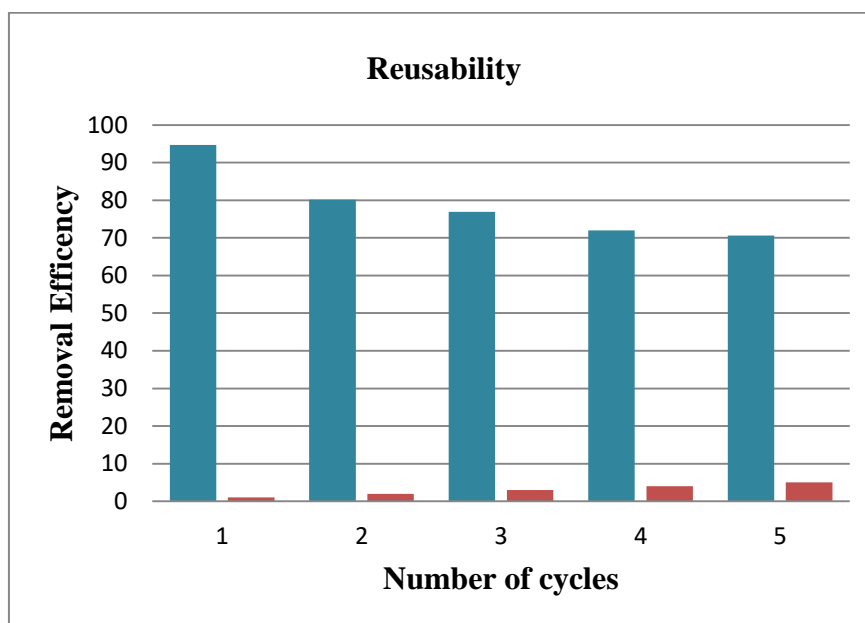

Figure 4.22. Desorption behavior of hydrogel at five cycles

4.11. Adsorption Isotherm

The relation between amount of methylene blue dye adsorbed at a constant optimum time, adsorbent dosage, and its concentration from (5–25) mg/L in the equilibrium solution is called adsorption isotherm. Adsorption isotherm is expressed by specific value which is coherent with the surface properties and affinity of adsorbent hydrogel, and used to find maximum adsorption capacity. Data gathered from adsorption isotherm models were used to obtain information about capacity of hydrogel or amount of hydrogel required for removing a unit mass of pollutant under the system concentrations.

Two most common adsorption isotherm models called Langmuir adsorption isotherm model and Frendlich adsorption isotherm model were used for analysis as follows. The parameters obtained from these different models provide important information on hydrogel mechanisms, the surface properties and affinities. Linear regression was subsequently used to determine the best-fitting isotherm, and the applicability of isotherm equations is compared by judging the correlation coefficients (R^2).

4.11.1. Langmuir Adsorption Isotherm Model

Langmuir plot, Ce/qe (equilibrium concentration versus equilibrium adsorption capacity) was calculated according to Equation 2.2. Q_m (one divided by intercept) and K_L (ratio between intercept and slope) value were calculated from y-intercept and slope of the Langmuir plot. From a plot shown in Figure 4.23, regressing constant ($R^2 = 0.9967$) were determined. R_L value also determined as Equation 2.3. All the specific values were listed in Table 4.15. According to (Atyaa1 & Al., 2019) value of R_L is between 0 and 1, indicating that methylene blue dye adsorption in bagasse based cellulose hydrogel is favorable.

Table 4.15. Parameter and correlation coefficient of Langmuir isotherm model

Langmuir isotherm model parameters				
	Parameters			
Adsorbent	Q_m (mg/g)	K_L (L/mg)	R_L	R^2
Hydrogel	13.21	5.29	0.39	0.9967

We determined high correlation values (R^2) and (K_L), which confirm that Langmuir isotherm model fits the experimental data and high value of Langmuir constant shows that there is strong binding (affinity) between adsorbent hydrogel and adsorbed methylene blue dye.
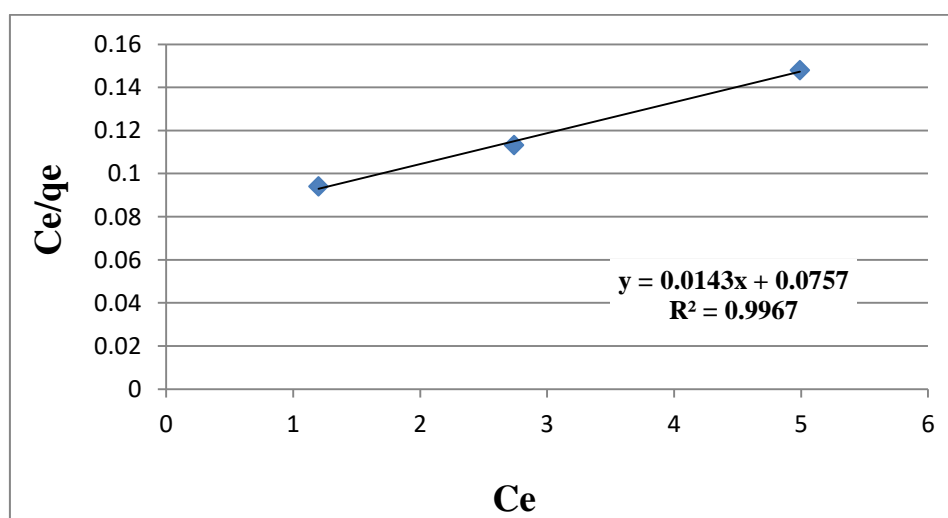

Figure 4.23. Langmuir isotherm plot for removal of methylene blue dye using bagasse based cellulose hydrogel

4.11.2. Frendlich adsorption isotherm model

Empirical Frendlich isotherms is applied to describe the adsorption of non-uniform (heterogeneous) surface with interconnection between adsorbed solute molecules in the reversible and non-ideal adsorption process (Mustapha et al., 2019). Specific value from Frendlich adsorption isotherm was calculated (Table 4.16).

Table 4.16. Parameter and correlation coefficient of Frendlich adsorption isotherm model

	Frendlich Adsorption Isotherm Model		
	Parameters		
Adsorbent	**n**	$\mathbf{K_F=(mg/g)(L/mg/)^{1/n}}$	$\mathbf{R^2}$
Hydrogel	1.5297	8.389	0.9662

As indicated in Table 4.16, n value is 1.5297 (1/n=0.6537). A value of 1/n less than 1 or n is between 1 and 10 indicate a favorable adsorption process. Frendlich constant (K_F) is an indicator of adsorption capacity of adsorbent (Ren et al., 2014).
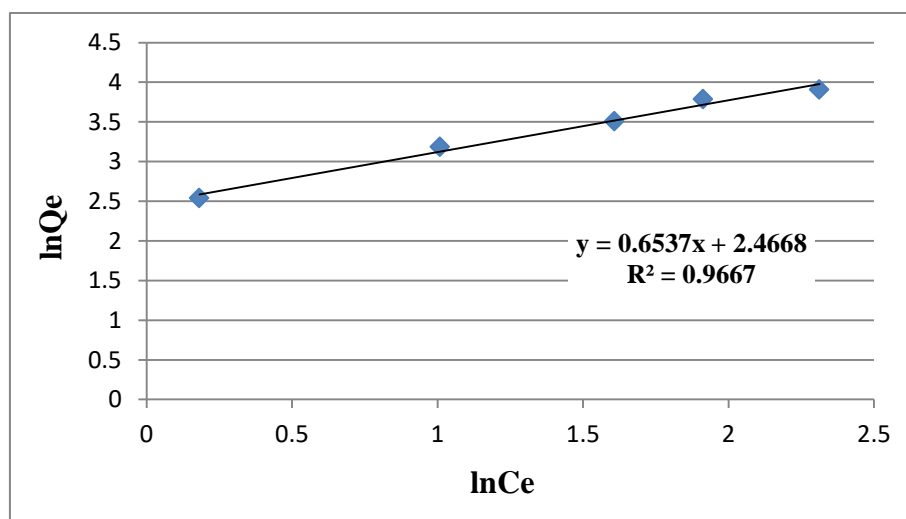

Figure 4.24. Frendlich isotherm plot for removal of methylene blue dye using bagasse based cellulose hydrogel

From the two adsorption isotherm models discussed above, Frendlich adsorption isotherm correlation factor ($R^2 = 0.9667$) (Figure 4.24) was less than correlation factor for Langmuir adsorption isotherm ($R^2 = 0.9967$).

Therefore, Langmuir adsorption isotherm fit the experimental data and indicates enthalpy of adsorption is independent of amount of adsorbed methylene blue dye. Langmuir equation assumes that the surface of active sites of the adsorbent is homogenous. Furthermore, inability of Frendlich adsorption isotherm not fitting experimental data in this work is a confirmation for homogeneity of adsorbent hydrogel active sites.

4.12. Adsorption kinetics

Adsorption kinetics models were common parameter in order to describe mechanism of sorption and possible controlling step as well as for providing optimum condition for full-scale of batch process. The kinetic in variables analyzed via pseudo first and second order are valuable for prediction of adsorption rate as well as giving full information for designing and modeling the adsorption process. High value of correlation factor (R^2) is acceptable for fitting of kinetic model which is confirmation between experimental data and predicted values (Lin et al., 2018).

4.12.1. Pseudo-first-order kinetic model

Linear graph of log (Qe-Qt) versus contact time for pseudo first order kinetic model was plotted according to calculation done using Equation 2.5 and rate constant was calculated form slope and intercept of the plot. Correlation factor ($R^2 = 0.9998$) was obtained from the plot. Linear graph for pseudo first order kinetic model and rate constant value are shown in Figure 4.25 and Table 4.17.
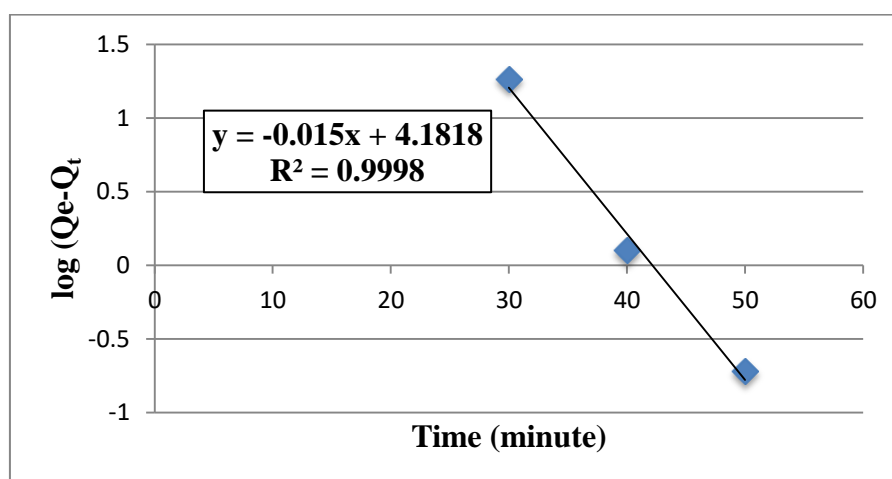

Figure 4.25. Pseudo first order adsorption kinetics of methylene blue dye on bagasse based cellulose hydrogel

4.12.3. Pseudo second order kinetic model

A straight line plot of t/Qt versus contact time for pseudo-second order kinetics was shown in Figure 4.26. High correlation factor (R^2=0.9810) and rate constant was obtained from the plot. According to theory of kinetics model, adsorption kinetics model with high value of correlation factor is in favorable for the adsorption of adsorbate, which is a confirmation for agreement of experimental Q_e and Qe calculated for kinetic model (Asuero et al., 2006). Rate constant for pseudo-second order is shown in Table 4.17.
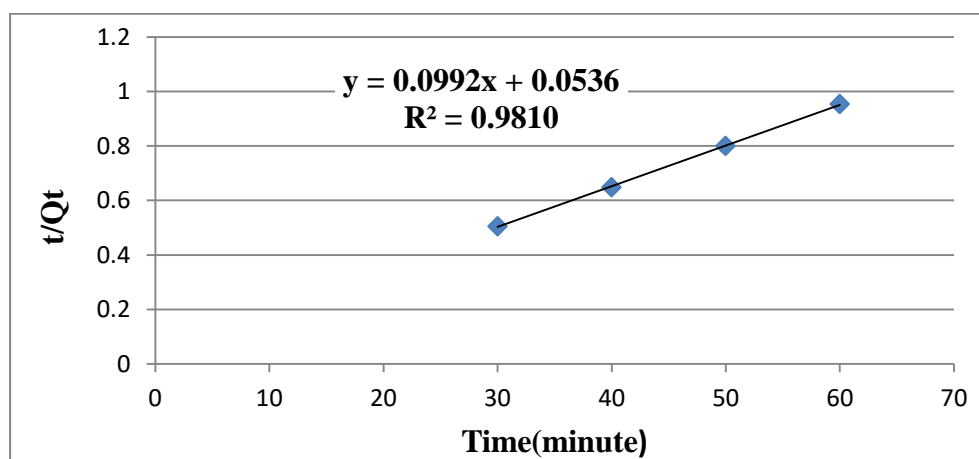
Figure 4.26. Pseudo Second order adsorption kinetics of methylene blue dye on bagasse based cellulose hydrogel

Generally, the adsorption kinetics analysis done in the present study showed that pseudo first order with R^2 = 0.9998 was more applicable than pseudo second order (R^2 =0.9810), the calculated Qe value did not much with experiment in pseudo second order and vice versa for pseudo first order. This pointed that the adsorption of methylene dye does not obey the second order kinetic model (confirmation for physisorption process) and is not used to calculate first order kinetic model but Qe value of pseudo-first order with linear regression coefficient perfectly fit the experimental data.

Table 4.17. Pseudo first and second order for adsorption of methylene blue dye on hydrogel

Adsorbent	Q_e (exp) (mg/g)	Pseudo first order			Pseud second order		
		K_1 (min^{-1})	Qe (mg/g) (calc)	R^2	Q_e (mg/g) (cal)	K_2 (min^{-1})	R^2
Hydrogel	68.97	0.229	66.66	0.9998	10.080	0.0345	0.9801

4.13. Characterization of arbaminch textile industry wastewater

Table 4.18. Characterization of textile wastewater before and after treatment

Parameter	Recorded result in this work		Previous work (mg/L)	References
	Before treatment	After treatment		
COD (mg/L)	1216.05	1193.74	1115–12,000	(Yaseen & Scholz., 2019)
TDS (mg/L)	1240.65	1209.02	900–3100	(Asuero et al., 2006)
TS (mg/L)	1710.49	1400.99	910–2300	(Palani, et al., 2015)
TSS (mg/L)	469.84	454.97	130–1740	*Tamil Nadu*, 2019)
pH	10.241	7.47	6-8	(Panhwar et al., 2019)
Temperature (^{O}C)	39.67	37.90	35–45	(Mehta., 2013)
Turbidity (NTU)	165.91	133.25	103–930	(Fenta., 2014)
Color (Pt-Co)	2459	1044	2300 ±200	(Hayelom tesfay., 2019)

As shown in Table 4.18, other contaminants have huge impact on removal efficiency of hydrogel in real textile industry. Our hydrogel removed the color down to 1044 (Pt-Co), about 52.45%, from real textile industry wastewater. The reduced efficiency observed here compared to treatment of synthetic wastewater (98.76%) is due to presence of other contaminants that could interfere with the adsorption capacity of the hydrogel.

Figure 4.27 shows difference between textile effluent and synthetic waste before and after treatment. However, it still efficiently removed the color below the set safety standard. Moreover, our hydrogel also showed suitability and efficiency to remove other pollutants including those mentioned in Table 4.18.

(A) Wastewater before and after treatment

(B) Synthetic wastewater before and after treatment

Figure 4.27. Real and synthetic wastewater before and after treatment

5. CONCLUSIONS AND RECOMMENDATION

Textile industry has become a key component for a daily life and is on a continuous growth. The sector consumes various chemicals, dyes and huge amount of water at multi-steps product processing and generates hazardous effluents including dyes as byproducts. The inevitable impact of such pollutants necessitates removal/treatment before being released to the environment. Although many researchers have devised several wastewater treatment approaches, removal of cation dyes like methylene blue dye remained challenging. Here, we described a highly efficient sugarcane bagasse based cellulose hydrogel for removal of methylene blue dye from textile industry wastewater. The hydrogel was synthesized from sugarcane bagasse based cellulose, an abundantly available at low cost and a renewable agricultural byproduct. A reusable hydrogel with a good swelling ratio and gel contents was successfully produced. The hydrogel showed good thermal stability, porosity, less crystalline index, good uniformity and uni-modal graph of nanomaterial.

Ester bond formation during esterification reaction between cellulose and crosslinking citric acid observed contributed for thermal stability of the hydrogel. Methylene blue dye removal efficiency was found to be determined by interaction of experimental variables (interaction among adsorbent dosage, initial concentration of methylene blue and contact time). Design Expert software predicted and actual experimental removal efficiency (98.76% and 98.65%, respectively) showed good concordance, indicating well fitness of the model for the experimental data. Finally, the hydrogel has efficiently removed the dye below the set safety standard when applied onto wastewater collected from Arbaminch textile industry and even showed further suitability and efficiency to remove other pollutants. However, wastewater characterization in this study was performed only on limited parameters. Hence; further studies should address the limitations of the current study as follow:

❖ Large scale wastewater characterization should be conducted to characterize wastewater contaminants, removal efficiency and feasibility of the hydrogel on the contaminants (including methylene blue dye), and effects of the contaminants on the removal efficiency.

❖ Further works on thermodynamic parameter, surface area and effect of parameter on swelling ratio of the hydrogel and extraction of cellulose related to optimum yield determination would help to characterize the hydrogel in detail.

REFERENCES

Ahmed, E. M. (2015). Hydrogel : Preparation , characterization , and applications : A review. *Journal of Advanced Research*, https://doi.org/10.1016/j.jare.2013.07.006

Ameram, N., Muhammad, S., Ainur, N., Nik, A., Ishak, S., Fazliani, N., & Pao, T. (2019). *Chemical composition in sugarcane bagasse : Delignification with sodium hydroxide.*

Assefa, T., & Sahu, O. (2016). Performance Analysis of Textile Industry Wastewater Treatment Plant with Physicochemical Characterizations. *Journal of Environmental Treatment Techniques*,.

Astrini, N et al, 2012. (2012). *Crosslinking Parameter on the Preparation of Cellulose Based Hydrogel with Divynilsulfone*. *4*, 275–281. https://doi.org/10.1016/j.proche.2012.06.038

Asuero, A. G., Sayago, A., & González, A. G. (2006). The correlation coefficient: An overview. *Critical Reviews in Analytical Chemistry*, *36*(1), 41–59. https://doi.org/10.1080/10408340500526766

Atyaa1, A. I., & Al, et al. (2019). *Synthesis and Characterization of Graphene Oxide / Hydrogel Composites and Their Applications to Adsorptive Removal Congo Red from Aqueous Solution Synthesis and Characterization of Graphene Oxide / Hydrogel Composites and Their Applications to Adsorptive*. https://doi.org/10.1088/1742-6596/1234/1/012095

Aye, T., Nu, T., & Cho, C. (2018a). *Preparation of cellulose hydrogel films*. *xvi*(1).

Aye, T., Nu, T., & Cho, C. (2018b). *Preparation of cellulose hydrogel films*. *020005*(41636),

Bahram, M., Mohseni, N., & Moghtader, M. (2016). *An Introduction to Hydrogels and Some Recent Applications World ' s largest Science , Technology & Medicine Open Access book publisher*. (April 2018). https://doi.org/10.5772/64301

Bhargava, D. akshey. (2016). *Physico-Chemical Waste Water Treatment Technologies : An Overview Physico-Chemical Waste Water Treatment Technologies : An Overview*. (September). https://doi.org/10.18535/ijsre/v4i05.05

Bhattacharjee, S. (2016). Review article DLS and zeta potential – *Journal of Controlled Release*, *235*, 337–351. https://doi.org/10.1016/j.jconrel.2016.06.017

Bisht, R., & Agarwal, M. (2016). *Heavy metal removal from wastewater using various adsorbents : a review adsorbents : a review*. (October 2017). https://doi.org/10.2166/wrd.2016.104

Catoira, M. C., Fusaro, L., Di Francesco, D., Ramella, M., & Boccafoschi, F. (2019). Overview of natural hydrogels for regenerative medicine applications. *Journal of Materials Science: Materials in Medicine*, *30*(10). https://doi.org/10.1007/s10856-019

Chang, C., & Zhang, L. (2011). Cellulose-based hydrogels : Present status and application prospects. *Carbohydrate Polymers*, https://doi.org/10.1016/j.carbpol.2010.12.023

Chieng, B. W., Ibrahim, N. A., Yunus, W. M. Z. W., & Hussein, M. Z. (2014). Poly(lactic acid)/poly(ethylene glycol) polymer nanocomposites: Effects of graphene nanoplatelets. *Polymers*, *6*(1), 93–104. https://doi.org/10.3390/polym6010093

Chirani, N., Yahia, L. H., Gritsch, L., Motta, F. L., & Natta, C. G. (2015). *iMedPub Journals History and Applications of Hydrogels Abstract*. 1–23. https://doi.org/10.4172/2254

Costa, A. F. S., Almeida, F. C. G., Vinhas, G. M., & Sarubbo, L. A. (2017). *Production of Bacterial Cellulose by Gluconacetobacter hansenii Using Corn Steep Liquor As Nutrient Sources*. 8(October), 1–12. https://doi.org/10.3389/fmicb.2017.02027

Crini, G., & Lichtfouse, E. (2019). Advantages and disadvantages of techniques used for wastewater treatment. *Environmental Chemistry Letters*, *17*(1), 145–155. https://doi.org/10.1007/s10311-018-0785-9

Cui, X., Lee, J. J. L., & Chen, W. N. (2019). Eco-friendly and biodegradable cellulose hydrogels produced from low cost okara: towards non-toxic flexible electronics. *Scientific Reports*, *9*(1), 1–9. https://doi.org/10.1038/s41598-019-54638-5

Damiri, F., Bachra, Y., Bounacir, C., Laaraibi, A., & Berrada, M. (2020). *Synthesis and Characterization of Lyophilized Chitosan-Based Hydrogels Cross-Linked with Benzaldehyde for Controlled Drug Release*. 2020.

Dargo, H., Gabbiye, N., & Ayalew, A. (2014). *Removal of Methylene Blue Dye from Textile Wastewater using Activated Carbon Prepared from Rice Husk Removal of Methylene Blue Dye from Textile Wastewater using Activated Carbon Prepared from Rice Husk*. (January 2019).

Das, N. (2013). *Preparation methods and properties of hydrogel : a review*. 5(3).

Dayana, S., Sharuddin, A., Abnisa, F., Mohd, W., & Wan, A. (2016). A review on pyrolysis of plastic wastes. *Energy Conversion and Management*, *115*, 308–326. https://doi.org/10.1016/j.enconman.2016.02.037

Demitri, C., Sole, R. Del, Scalera, F., Sannino, A., Vasapollo, G., Maffezzoli, A., … Nicolais, L. (2008). *Novel Superabsorbent Cellulose-Based Hydrogels Crosslinked with Citric Acid*. https://doi.org/10.1002/app

Deng, Y., Chen, J., Huang, J., Yang, X., & Zhang, X. (2020). Preparation and characterization of cellulose / flaxseed gum composite hydrogel and its hemostatic and wound healing functions evaluation. *Cellulose*, *3*. https://doi.org/10.1007/s10570-020

Dutta, S. D., Patel, D. K., & Lim, K. (2019). *Functional cellulose-based hydrogels as extracellular matrices for tissue engineering*. 0, 1–19.

Farkas, R. (2019). *Methylene Blue Adsorption Study on Microcline Particles in the Function of Particle Size Range*.

Fekete, T., Borsa, J., Takács, E., & Wojnárovits, L. (2017). Synthesis of carboxymethylcellulose / starch superabsorbent hydrogels by gamma - irradiation. *Chemistry Central Journal*, 1–10. https://doi.org/10.1186/s13065-017-0273-5

Fenta, M. M. (2014). Heavy Metals Concentration in Effluents of Textile Industry, Tikur Wuha River and Milk of Cows Watering on this Water Source, Hawassa, Southern Ethiopia. *Research Journal of Environmental Sciences*, *8*(8), 422–434. https://doi.org/10.3923/rjes.2014.422.434

Ganji, F., Farahani, S. V., Manufacturing, C. B., States, U., & Vasheghani-farahani, E. (2010). *Theoretical Description of Hydrogel Swelling: A Review*. (April).

Garg, S., Garg, A., & Vishwavidyalaya, R. D. (2017). *Hydrogel : Classification , Properties , Preparation and Technical Features*. (August).

Garrett, E., Riley, L., & Figueiredo, F. C. De. (2016). *Sugarcane b agasse h emicellulose p roperties , e xtraction t echnologies and*.

Geng, H. (2018a). A one-step approach to make cellulose-based hydrogels of various transparency and swelling degrees. *Carbohydrate Polymers*, *186*(October 2017), 208–216. https://doi.org/10.1016/j.carbpol.2018.01.031

Geng, H. (2018b). SC. *Carbohydrate Polymers*. https://doi.org/10.1016/j.carbpol.2018.01.031

Hakam, A., Rahman, I. A., Jamil, M. S. M., Othaman, R., Amin, M. C. I. M., & Lazim, A. M. (2015). Removal of methylene blue dye in aqueous solution by sorption on a bacterial-g-poly-(acrylic acid) polymer network hydrogel. *Sains Malaysiana*, *44*(6), 827–834. https://doi.org/10.17576/jsm-2015-4406-08

Haque, O., & Mondal, I. H. (2016). *Synthesis and Characterization of Cellulose-based. hydrogel*

Haraguchi, K. (2008). *Nanocomposite hydrogels*. *11*(2007), 47–54. https://doi.org/10.1016/j.cossms.2008.05.001

Henze, M., & Comeau, Y. (2008). *Wastewater Characterization*.

Hospodarova, V., Singovszka, E., & Stevulova, N. (2018). Characterization of Cellulosic Fibers by FTIR Spectroscopy for Their Further Implementation to Building Materials. *American Journal of Analytical Chemistry*, *09*(06), 303–310. https://doi.org/10.4236/ajac.2018.96023

Hu, L., Du, M., & Zhang, J. (2018). *Hemicellulose-Based Hydrogels Present Status and Application Prospects : A Brief Review*. 15–28. https://doi.org/10.4236/ojf.2018.81002

Jayaramudu, T., Ko, H., Kim, H. C., Kim, J. W., & Kim, J. (2019). *Swelling Behavior of Polyacrylamide – Cellulose Temperature , and pH E ff ects*.

Jia, Y., Wang, X., Huo, M., Zhai, X., Li, F., & Zhong, C. (2017). *Preparation and characterization of a novel bacterial cellulose / chitosan bio-hydrogel*. 7, 1–8. https://doi.org/10.1177/1847980417707172

Joshi, M., Bansal, R., & Purwar, R. (2004). *Colour removal from textile effluents*. *29*(June), 239–259.

Kabir, S. M. F., Sikdar, P. P., Rahman, B. H. M. A., & Ali, B. A. (2018). Cellulose - based hydrogel materials : chemistry , properties and their prospective applications. *Progress in Biomaterials*, *7*(3), 153–174. https://doi.org/10.1007/s40204-018-0095-0

Kaczmarek, B., Nadolna, K., & Owczarek, A. (2019). The physical and chemical properties of hydrogels based on natural polymers. In *Hydrogels Based on Natural Polymers*. https://doi.org/10.1016/B978-0-12-816421-1.00006-9

Kanafi, N. M., Rahman, N. A., & Rosdi, N. H. (2019). ScienceDirect Citric acid cross-linking of highly porous carboxymethyl cellulose / poly (ethylene oxide) composite hydrogel films for controlled release applications. *Materials Today: Proceedings*, *7*, 721–731.

https://doi.org/10.1016/j.matpr.2018.12.067

Karp, S. G., Woiciechowski, A. L., Soccol, V. T., & Soccol, R. (2013). *Pretreatment Strategies for Delignification of Sugarcane Bagasse : A Review*. *56*(August), 679–689.

Karunakaran, K. (2016). *Preparation and Characterisation of Cellulose-Based Hydrogel Derived From Sugarcane Bagasse •*. (41636).

Katheresan, V., Kansedo, J., & Lau, S. Y. (2018). *Journal of Environmental Chemical Engineering E ffi ciency of various recent wastewater dye removal methods : A review*. *6*(February), 4676–4697. https://doi.org/10.1016/j.jece.2018.06.060

Koch, R. (2013). *Methylene blue 1*. 85.

Kreitschitz, A., & Gorb, S. N. (2020). *The micro- and nanoscale spatial architecture of the seed mucilage — Comparative study of selected plant species*. *1*, 1–15.

Kullasatri Saelee et al, 2018. *Extraction and characterization of cellulose from sugarcane bagasse by using environmental friendly method*.

Lawler, D. F., Mikelonis, A. M., Kim, I., & Lau, B. L. T. (2013). *Silver nanoparticle removal from drinking water : Flocculation / sedimentation or filtration*. (September 2015). https://doi.org/10.2166/ws.2013.125

Li, Q., Yang, D., Ma, G., Xu, Q., Chen, X., Lu, F., & Nie, J. (2009). *International Journal of Biological Macromolecules Synthesis and characterization of chitosan-based hydrogels*. *44*, 121–127. https://doi.org/10.1016/j.ijbiomac.2008.11.001

Lin, Y., Fang, G., Deng, Y., Shen, K., Wu, T., & Li, M. (2018). Highly Effective Removal of Methylene Blue Using a Chemi-Mechanical Pretreated Cellulose-based Superabsorbent Hydrogel. *BioResources*, *13*(4), 8709–8722. https://doi.org/10.15376/biores.13.4.8709-8722

Liu, K., Abebe, D. G., Wiley, E. R., & Fujiwara, T. (2019). *Characterization and Optimization of PLA Stereocomplexed Hydrogels for Local Gene Delivery Systems*.

Lopez-sanchez, A. P., Martinez-sanz, M., Bonilla, M. R., Wang, D., Gilbert, E. P., Stokes, R., & Gidley, M. J. (2017). Cellulose-pectin composite hydrogels: intermolecular interactions and material properties depend on order of assembly. *Carbohydrate Polymers*. https://doi.org/10.1016/j.carbpol.2017.01.049

M, R. R., & Neethu, M. K. (2017). *Degradation of methylene blue in textile waste water using activated sawdust and eggshell biosorbent*. (4), 7–16.

Mahmoud, G. A., Abdel-aal, S. E., El-kelesh, N. A., & Alshafei, E. A. (2017). *Effective Removal of Hazardous Dyes from Aqueous Solutions Using Starch Based Hydrogel and Gamma Radiation*. *5*(7), 480–488. https://doi.org/10.13189/eer.2017.050703

Maitra, J., & Shukla, V. K. (2014). Cross-linking in Hydrogels - A Review. *American Journal of Polymer Science*, *4*(2), 25–31. https://doi.org/10.5923/j.ajps.20140402.01

Maitra, J., & Shukla, V. K. (2019). *Cross-linking in Hydrogels - A Review*. (June). https://doi.org/10.5923/j.ajps.20140402.01

Mane, S., Ponrathnam, S., & Chavan, N. (2016). Effect of Chemical Crosslinking on

Properties of Polymer Microbeads: A Review. *Canadian Chemical Transactions*, *3*(4), 473–485. https://doi.org/10.13179/canchemtrans.2015.03.04.0245

Mehta, P. (2013). Chemical Treatment of Textile Effluents Using Ferric Chloride As Coagulant : an Analysis. *International Journal of Basic and Applied Chemical Sciences*, *3*(3), 49–55. Retrieved from http://www.cibtech.org/jcs.htm

Mohamed et al, 2015. (2015). *Synthesis and Characterization of Cross-linked Polyethylene Glycol/Carboxymethyl Chitosan Hydrogels*. *34*(1), 1–6. https://doi.org/10.1002/adv.21479

Morán, J. I., Alvarez, V. A., Cyras, V. P., & Vázquez, A. (2008). Extraction of cellulose and preparation of nanocellulose from sisal fibers. *Cellulose*, *15*(1), 149–159. https://doi.org/10.1007/s10570-007-9145-9

Mustapha, S., Ndamitso, D. T. S. M. M., & Sumaila, M. B. E. A. (2019). Adsorption isotherm , kinetic and thermodynamic studies for the removal of Pb (II), Cd (II), Zn (II) and Cu (II) ions from aqueous solutions using Albizia lebbeck pods. *Applied Water Science*, *9*(6), 1–11. https://doi.org/10.1007/s13201-019-1021-x

Nakasone, K., Ikematsu, S., Kobayashi, T., & Accepted, J. (2015). *Biocompatibility Evaluation of Cellulose Hydrogel Film Regenerated from Sugarcane Bagasse Waste and Its in vivo Behavior in Mice*. https://doi.org/10.1021/acs.iecr.5b03926

Nkosivele, Z., Mzimela, T., Linganiso, L. Z., Revaprasadu, N., & Motaung, T. E. (2018). *Comparison of Cellulose Extraction from Sugarcane Bagasse Through Alkali 3 . Results and Discussion*. *21*(6), 1–7.

Nomura, K., & Terwilliger, P. (2020). *Self-dual Leonard pairs Preparation and properties of hydrogel based on sawdust cellulose for environmentally friendly*. 139–152.

Okay, O. (n.d.). *General Properties of Hydrogels*. 1–15. https://doi.org/10.1007/978-3-540-75645-3

Oyen, M. L. (2014). *Mechanical characterisation of hydrogel materials*. *59*(1). https://doi.org/10.1179/1743280413Y.0000000022

Palani, M., Rajoo, B., Periyasamy, S., & Sharmila, S. (2015). Physico Chemical Analysis of Textile Industrial Effluents from Tirupur City , Tn, India. *International Journal of Advance Research In Science And Engineering*, *4*(02), 93–104. Retrieved from https://www.researchgate.net/publication/273321403%0APhysico

Palantöken, S., Bethke, K., Zivanovic, V., Kalinka, G., Kneipp, J., & Rademann, K. (2019). *Cellulose hydrogels physically crosslinked by glycine : Synthesis , characterization , thermal and mechanical properties*. *48380*(July 2018), 23–25. https://doi.org/10.1002/app.48380

Plermjai, K., Boonyarattanakalin, K., & Mekprasart, W. (2018). *Extraction and characterization of nanocellulose from sugarcane bagasse by ball-milling-assisted acid hydrolysis Extraction and Characterization of Nanocellulose from Sugarcane Bagasse by Ball-milling-assisted Acid Hydrolysis*. *020005*(September).

Química, I. De, Estadual, U., Júlio, P., & Filho, D. M. (2015). *Synthesis and Characterization of Methylcellulose Produced from Bacterial Cellulose under Heterogeneous Condition*.

Rahman, M. (2017). *Preparation and characterization of bijoypur clay- crystalline cellulose composite for application as an adsorbent*. *2*(3), 1–7. https://doi.org/10.15761/AMS.1000126

Ramesh, K. S. B. S. T. (2013). *Removal of dyes using agricultural waste as low-cost adsorbents : a review*. 773–790. https://doi.org/10.1007/s13201-013-0117-y

Ramli, R., Junadi, N., Beg, M. D. H., & Yunus, R. M. (2015). *Microcrystalline Cellulose (MCC) From Oil Palm Empty Fruit Bunch (EFB) Fiber via Simultaneous Ultrasonic and Alkali Treatment*. *9*(1), 8–11.

Rashid, T., Kait, C. F., & Murugesan, T. (2016). A "fourier Transformed Infrared" Compound Study of Lignin Recovered from a Formic Acid Process. *Procedia Engineering*, *148*, 1312–1319. https://doi.org/10.1016/j.proeng.2016.06.547

Ren, J., Kong, W., & Sun, R. (2014). *com Preparation of Sugarcane Bagasse/Poly(Acrylic Acid- co - Acrylamide) Hydrogels and their Application*. *9*(2), 3290–3303.

Rodrigues, P., Sousa, F. De, Saska, S., Barud, H., Maria, A., Plepis, D. G., … Schimidt, A. (2016). *Bacterial Cellulose / Collagen Hydrogel for Wound Healing*. *19*(1), 106–116.

Rojas, J., & Azevedo, E. (2011). *Review Article Functionalization and crosslinking of microcrystalline cellulose in aqueous media :* *8*(1).

Saeed, A. M. (2013). *Temperature effect on swelling properties of commercial polyacrylic acid hydrogel beads .* *1*(12), 1614–1627.

Sannino, A., Demitri, C., & Madaghiele, M. (2009). *Biodegradable Cellulose-based Hydrogels: Design and Applications*. 353–373. https://doi.org/10.3390/ma2020353

Saruchi, Kaith, B. S., Kumar, V., & Jindal, R. (2016). Biodegradation study of enzymatically catalyzed interpenetrating polymer network: Evaluation of agrochemical release and impact on soil fertility. *Biotechnology Reports*, *9*, 74–81. https://doi.org/10.1016/j.btre.2015.12.004

Scholz, D. A. Y. M. (2018). Textile dye wastewater characteristics and constituents of synthetic effluents : a critical review. In *International Journal of Environmental Science and Technology*. https://doi.org/10.1007/s13762-018-2130-z

Sethi, S., Kaith, B. S., Kaur, M., Sharma, N., & Khullar, S. (2020). A hydrogel based on dialdehyde carboxymethyl cellulose – gelatin and its utilization as a bio adsorbent. *Journal of Chemical Sciences*, *0123456789*. https://doi.org/10.1007/s12039-019-1700-z

Shendge, M. A. B. S. V. S. M. R. (2017). *Waste Water Treatment of Textile Industry : Review Waste Water Treatment of Textile Industry : Review*. (April).

Shi, J., Xing, D., & Li, J. (2012). FTIR studies of the changes in wood chemistry from wood forming tissue under inclined treatment. *Energy Procedia*, *16*(PART B), 758–762. https://doi.org/10.1016/j.egypro.2012.01.122

Siddique, K., Rizwan, M., Shahid, M. J., & Ali, S. (2017). *Textile Wastewater Treatment Options : A Critical Review Textile Wastewater Treatment Options : A Critical Review*. (October). https://doi.org/10.1007/978-3-319-55423-5

Singh, S., Sidhu, G. K., & Singh, H. (2017). Removal of methylene blue dye using activated

carbon prepared from biowaste precursor. *Indian Chemical Engineer*, *00*(0), 1–12. https://doi.org/10.1080/00194506.2017.1408431

Sivri, N., & Toroz, İ. (2007). *Pollutants of Textile Industry Wastewater and Assessment of its Discharge Limits by Water Quality Standards*. *103*, 97–103.

State, O. R., Dadi, D., Stellmacher, T., & Senbeta, F. (2017). *Environmental and health impacts of effluents from textile industries in Environmental and health impacts of effluents from textile industries in Ethiopia : the case of Gelan and Dukem , Oromia Regional State*. (January). https://doi.org/10.1007/s10661-016-5694-4

Tavera-quiroz, M. J., Jairo, J., Díaz, F., & Pinotti, A. (2018). *Characterization of Methylcellulose Based Hydrogels by Using Citric Acid as a Crosslinking Agent*. *13*(17), 13302–13307.

Taylor, et al. (2006). *Relationship Between Bond Strength and Relationship Between Bond Strength and Crystallinity of High Polymers-Polyethylene , Polyethyleneterep htha late , and Nylon ?* (November 2014), 37–41. https://doi.org/10.1080/00218467208072215

Terefe Gemeda, F., Diriba Guta, D., Senbeta Wakjira, F., & Gebresenbet, G. (2020). Physicochemical characterization of effluents from industries in Sabata town of Ethiopia. *Heliyon*, *6*(8), e04624. https://doi.org/10.1016/j.heliyon.2020.e04624

Thakur, G., & Singh, K. (2018). *Crosslinking Biopolymers for Advanced Drug Delivery and Tissue Engineering Applications*. (January). https://doi.org/10.1007/978-981-13-0950-2

Tran, V. Van, Park, D., & Lee, Y. (2018). *Hydrogel applications for adsorption of contaminants in water and wastewater treatment*.

Van Tran, V., Park, D., & Lee, Y. C. (2018). Hydrogel applications for adsorption of contaminants in water and wastewater treatment. *Environmental Science and Pollution Research*, *25*(25), 24569–24599. https://doi.org/10.1007/s11356-018-2605-y

Venkatesham, V., Khan, M., Shrikanth, Y. N., B, S. K. M., & Manjunath, B. V. (2018). *Removal of Heavy Metals and Dyes from Wastewater using Hydrogels*. *2*(2), 1046–1065.

Vijayanand, C., Kamaraj, S., Karthikeyan, S., & Sriramajayam, S. (2016). Characterization of Indigenous Biomass. *International Journal of Agriculture Sciences*, *8*(50), 2124–2127.

Vuono, D. (2014). *Synthesis Methods of Carbon Nanotubes and Related Materials*. (May 2010). https://doi.org/10.3390/ma3053092

Xiaohui et al , 2019. (2019). (509), 1–21.

Xiong, R., Li, F., Yu, J., Hu, P., Liu, Z., & Hsieh, Y. Lo. (2013). Investigations on solution of cellulose in complex phosphoric acid solvent and its stability. *Cellulose Chemistry and Technology*, *47*(3–4), 153–163.

Yacob, N., & Hashim, K. (2015). *Morphological effect on swelling behaviour of hydrogel Morphological Effect on Swelling Behaviour of Hydrogel*. *153*(February). https://doi.org/10.1063/1.4866123

Yang, J., Medronho, B., Lindman, B., & Norgren, M. (2020). *Simple One Pot Preparation of Chemical Hydrogels from Cellulose Dissolved in Cold LiOH / Urea*.

Yang, T. (2012). *M echanical and s welling*.

Yang, Z., Peng, H., Wang, W., & Liu, T. (2010). Crystallization behavior of poly(ε-caprolactone)/layered double hydroxide nanocomposites. *Journal of Applied Polymer Science*, *116*(5), 2658–2667. https://doi.org/10.1002/app

Yaseen, D. A., & Scholz, M. (2019). Textile dye wastewater characteristics and constituents of synthetic effluents: a critical review. In *International Journal of Environmental Science and Technology* (Vol. 16). https://doi.org/10.1007/s13762-018-2130-z

Zaman, A., Ahmed, T., Biswas, S., & Sharmeen, S. (2019). *Morphological Characterization of Hydrogels*.

Zendehdel, M., Barati, A., Alikhani, H., & Hekmat, A. (2010). *Removal of methylene blue dye from wastewater by adsorption onto semi-inpenetrating polymer network hydrogels composed of acrylamide and acrylic acid copolymer and polyvinyl alcohol*. *7*(5), 423–428.

Zhou, Y., Fu, S., Liu, H., Yang, S., & Zhan, H. (2011). *Removal of Methylene Blue Dyes From Wastewater Using Cellulose-Based Removal of Methylene Blue Dyes From Wastewater Using Cellulose-Based Superadsorbent Hydrogels*. (December). https://doi.org/10.1002/pen.22020

Zhou, Y., Guilherme, M. R., Reis, A. V, Campese, G. M., Muniz, E. C., & Nozaki, J. (2006). *Removal of Methylene Blue Dye from an Aqueous Media Using Removal of methylene blue dye from an aqueous media using superabsorbent hydrogel supported on modified polysaccharide*. (October). https://doi.org/10.1016/j.jcis.2006.04.036

APPENDIX

Appendix A: Adsorption isotherm and kinetics analysis

Table A.1. Adsorption isotherm analysis

Conc. Of MBD	Abs After	C_e	q_e	Ce/qe	ln C_e	ln qe
5	0.1362	1.199	12.67	0.094	0.1814	2.539
10	0.323	2.741	24.196	0.113	1.0083	3.186
15	0.497	4.821	33.363	0.148	1.6076	3.507
20	0.645	6.769	44.103	0.153	1.9123	3.786
25	1.019	10.096	49.68	0.203	2.3121	3.905

Table A.2. Adsorption kinetics analyses

Run	Time	Absorb. After	C_t	Q_t	Q_e-Q_t	Log(Qe-Qt)	t/Qt
1	30	0.272	2.180	59.4	3.54	1.264	0.505
2	40	0.209	1.491	61.68	1.26	0.10037	0.6485
3	50	0.177	1.264	62.453	0.487	-0.7194	0.800
4	60	0.088	1.124	62.94			0.953

Appendix B: Graph from design experts
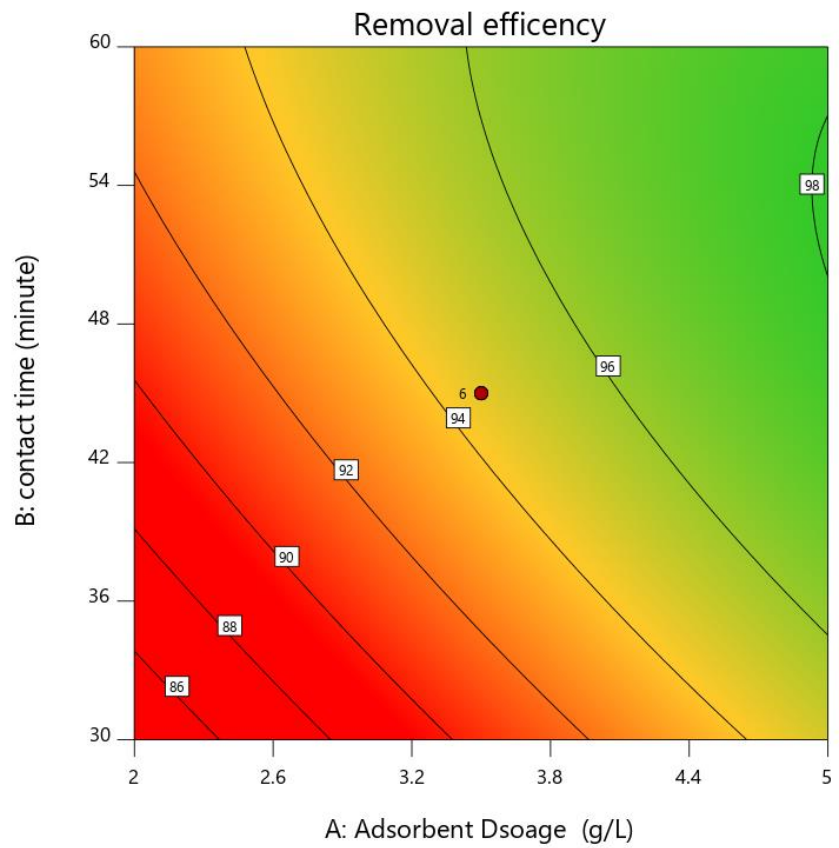
Figure B-1: Contour plot of adsorbent dosage and contact time
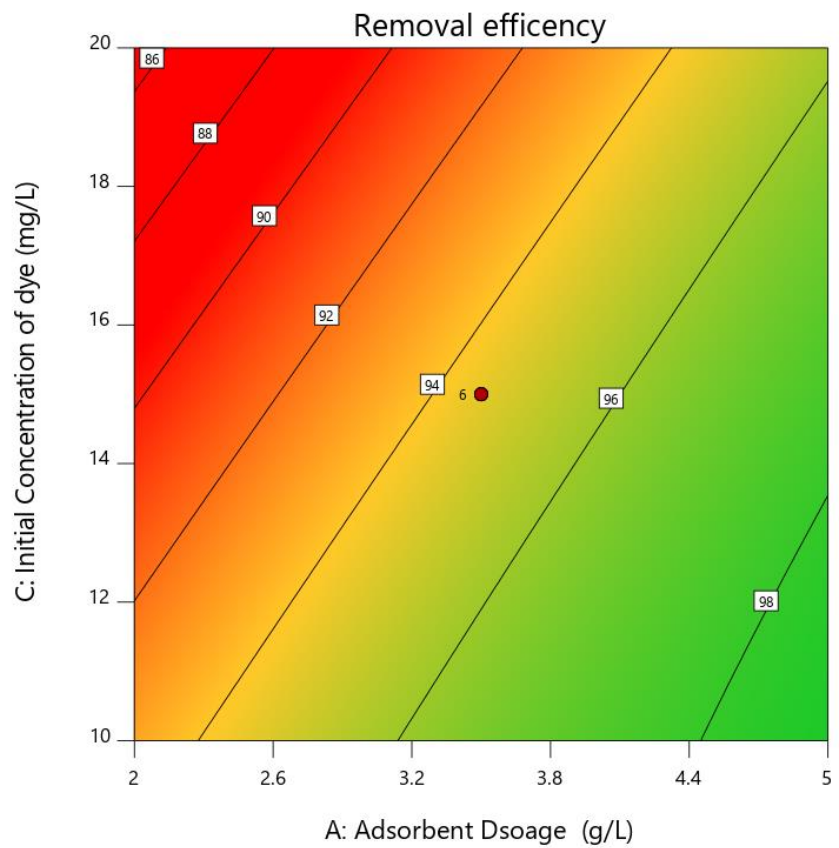
Figure B-2: Contour plot for initial concentration of methylene blue dye and adsorbent dosage
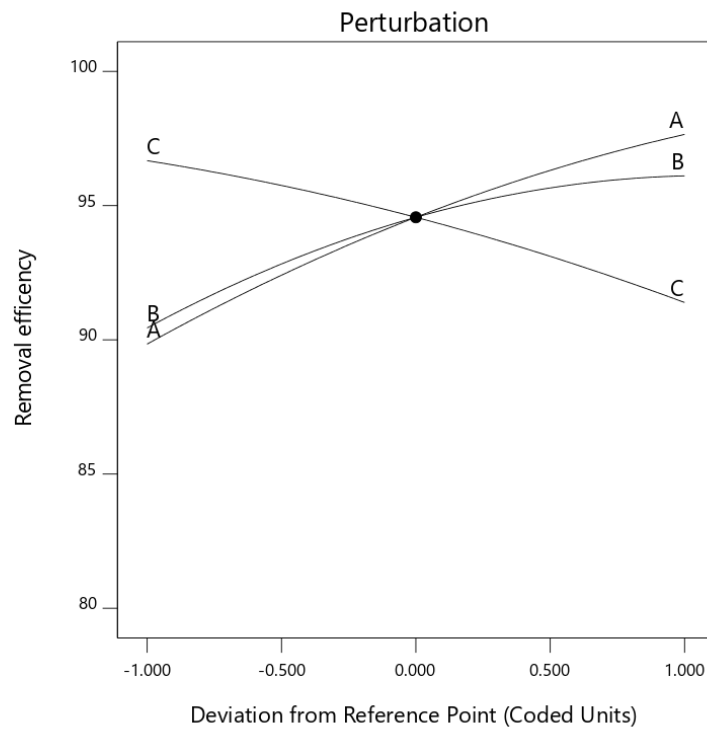
Figure B-3: Perturbation curve of the dependent and independent variable

Appendix C: Some pictures from lab work

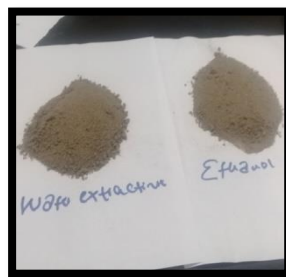Collecting of sugarcane bagasse from factory

Washing of sgarcane bagasse

Dried and grinded of sugarcane bagasse

Lignin product

Extractive product

Hemicellulose

Dewaxing process

Acid deligfinication

Alkalination

Bleaching

Washing and vacum filter

Wet cellulose

Oven drying

Dierd cellulose

Dissolution of cellulose

Cross-linking with citric acid

Complete gel

Gel with porosity formed

Oven drying of hydrogel

Dried gel

Powdered gel

Untreted real wastewater

Synthetic wastewater

Shaking

Treated real wastewater

Treated synthetic wastewater

Residue of hydrogel